

# **Mechanistic Investigation of Peptide Sorption and Acylation in Poly(lactic-co-glycolic acid)**

by

**Andreas M. Sopohcleous**

A dissertation submitted in partial fulfillment  
of the requirements for the degree of  
Doctor of Philosophy  
(Chemical Engineering)  
in The University of Michigan  
2009

Doctoral Committee:

Professor Steven P. Schwendeman, Chair  
Professor Nicholas A. Kotov  
Professor Henry Y. Wang  
Associate Professor Joerg Lahann

© Andreas M. Sopotcleous

---

All Rights Reserved

2009

To my parents, Marios and Thelma,  
who have nurtured the passion, curiosity, and love of learning  
that made this accomplishment possible.

# Acknowledgments

I would like to thank my advisor, Dr. Steven P. Schwendeman, for his wisdom, advice, and patience. I will always be indebted to him for the rigorous approach to science and courage to seek insight into challenging questions that I have obtained during my time in his laboratory.

I would also like to thank the other members of my committee. I thank Dr. Henry Wang, who has been a mentor to me and through his Pharmaceutical Engineering program, first excited my interest in the biotechnology and pharmaceutical industries. I thank Dr. Nick Kotov and Dr. Joerg Lahann for always keeping a door open and providing a valuable viewpoint.

I need to thank all of my lab-mates and post-doctoral researchers who have helped me thought my time in Dr. Schwendeman's lab: Dr. Jichao Kang, Dr. Chegju Cui, Dr. Amy Ding, Dr. Lei Li, Dr. David Gu, Dr. Sam Reinhold, Dr. Li Zhang, Dr. Christian Wischke, Dr. Kashappa Goud Desai, Dr. Ying Zhang, and Gesine Heuck. Dr. Ying Zhang and Gesine Heuck helped support this project directly.

Additionally, many former faculty, students, and post-doctoral resarchers from other labs have helped me in my research, including Dr. John Carpenter, and the rest of the Carpenter Lab, especially Dr. Tia Estey, Dr. Vincent Pecoraro, Dr. Mark Meyerhoff, Dr. Mariusz Pietrak, Dr. Ryan Hartman, Dr. Ben Gould, Dr. Chris Iacovella, Dr. Pat Marsac, Parag Desai, and Ryan Welch.

Several technicians at various analytical facilities at the University have been instrumen-

tal in supporting me during my research, including Jim Windak (EPR), Antek Wong-Foy ( $N_2$  adsorption), Carol Carter (ICP), Dr. Kai Sun at the North Campus EMAL (XPS), Dr. Pilar Herrera-Fierro (XPS analysis), Carl Henderson at the Central Campus EMAL (SEM), the entire staff of the Microscopy and Image Analysis Laboratory, Harald Eberhart (glass cutting), and Kent Pruss at the Automotive machining shop.

Numerous staff members in the Department of Chemical Engineering and College of Pharmacy have assisted along the way, including Susan Hamlin, Christine Moellering, Clair O'Connor, Ruby Sowards, Pablo Lavalle, in the Department of Chemical Engineering, Pat Greeley and L.D. Heiber, Vickie McMartin, Barbara Johnson, Dawn Coy, and the staff of the ITS group in the College of Pharmacy.

I would like to thank various sources of funding, including the Department of Chemical Engineering, Rackham Graduate School, the National Institutes of Health (Grant R01 HL68345-03), and Novartis AG.

My scientific training began fairly recently, but my life training began a long time ago. Accordingly, I owe an immense debt of gratitude to my wonderful parents, Marios and Thelma Sophocleous, my sisters Melissa and Tonya, and the rest of my extended family. They have encouraged and supported me always, and have inspired me to reach to maximize my potential. Without them, I clearly would not be where I am today.

# Table of Contents

<b>Dedication</b> . . . . .	ii
<b>Acknowledgments</b> . . . . .	iii
<b>List of Tables</b> . . . . .	ix
<b>List of Figures</b> . . . . .	xi
<b>Abstract</b> . . . . .	xv
<b>Chapter 1 Introduction</b> . . . . .	1
1.1 Motivation . . . . .	1
1.2 Overview . . . . .	2
<b>Chapter 2 Background: Therapeutic delivery of peptides and proteins</b> . . . . .	4
2.1 Oral Delivery . . . . .	6
2.2 Pulmonary Delivery . . . . .	7
2.3 Transdermal Delivery . . . . .	8
2.4 Controlled Release Depots . . . . .	9
2.4.1 Physical and Chemical Properties of PLGA . . . . .	10
2.4.2 Preparation of PLGA Microparticles . . . . .	12
2.4.3 Polypeptide Instabilities in PLGA Controlled Release Systems . . . . .	15
<b>Chapter 3 Methodology</b> . . . . .	26
3.1 Selection of polymers for investigation . . . . .	26

3.1.1	Characterization of PLGA particles . . . . .	27
3.1.2	PLGA film preparation and characterization . . . . .	28
3.2	Model peptides . . . . .	29
3.3	General Methodology . . . . .	30
3.4	Uncertainty and Error Analysis . . . . .	31
<b>Chapter 4</b>	<b>A new class of inhibitors of peptide sorption and acylation in PLGA</b>	<b>35</b>
4.1	Introduction . . . . .	35
4.2	Materials and Methods . . . . .	37
4.2.1	Materials . . . . .	37
4.2.2	Analysis of octreotide by HPLC . . . . .	38
4.2.3	Analysis of octreotide by HPLC-MS . . . . .	38
4.2.4	Analysis of divalent cations by ICP-OES . . . . .	39
4.2.5	Preparation and Characterization of PLGA Nanoparticles in the Presence of Divalent Cations . . . . .	40
4.2.6	Electron paramagnetic resonance (EPR) spectroscopy of Mn in the presence of octreotide acetate and PLGA . . . . .	40
4.2.7	Recovery of octreotide and divalent cation from PLGA via two-phase extraction . . . . .	41
4.2.8	Octreotide sorption studies . . . . .	41
4.2.9	Preparation of PLGA millicylinders . . . . .	42
4.2.10	Purification of PLGA by precipitation method . . . . .	43
4.2.11	Purification of PLGA by two-phase extraction method . . . . .	43
4.2.12	Octreotide release from PLGA millicylinders . . . . .	44
4.3	Results and Discussion . . . . .	44
4.3.1	Effect of divalent cations on nanoparticle zeta-potential . . . . .	44
4.3.2	Kinetics of octreotide sorption to PLGA . . . . .	45
4.3.3	Effect of divalent cations on octreotide sorption . . . . .	45
4.3.4	Long-term interaction of octreotide with PLGA . . . . .	48
4.3.5	Effect of salts on peptide acylation when encapsulated in PLGA . . . . .	49
4.4	Conclusions . . . . .	51

4.5	Appendix . . . . .	53
4.5.1	Preliminary investigation into the effect of excipients on octreotide sorption to PLGA . . . . .	53
4.5.2	Polycations as inhibitors of octreotide sorption to PLGA . . . . .	54
<b>Chapter 5 Kinetics of Peptide Sorption to PLGA . . . . .</b>		<b>61</b>
5.1	Introduction . . . . .	61
5.2	Materials and Methods . . . . .	63
5.2.1	Materials . . . . .	63
5.2.2	Investigation of octreotide sorption kinetics . . . . .	63
5.2.3	Analysis of octreotide by HPLC . . . . .	64
5.2.4	Model of peptide sorption to PLGA and estimation of kinetic parameters . . . . .	64
5.3	Results and Discussion . . . . .	65
5.3.1	Effect of Octreotide Concentration on Octreotide Sorption Kinetics . . . . .	65
5.3.2	Effect of Ionic Strength on Octreotide Sorption Kinetics . . . . .	66
5.3.3	Comparison of Leuprolide and Octreotide Sorption Kinetics . . . . .	67
5.3.4	Temperature Dependence of Octreotide Sorption . . . . .	68
5.4	Conclusions . . . . .	69
<b>Chapter 6 Sorption Behavior of Peptides to PLGA . . . . .</b>		<b>73</b>
6.1	Introduction . . . . .	73
6.2	Materials and Methods . . . . .	74
6.2.1	Materials . . . . .	74
6.2.2	Analysis of octreotide by HPLC . . . . .	75
6.2.3	Octreotide sorption studies . . . . .	75
6.2.4	Desorption of octreotide from PLGA 50:50 . . . . .	75
6.2.5	Two-phase extraction of octreotide sorbed to PLGA 50:50 . . . . .	76
6.3	Results and Discussion . . . . .	76
6.3.1	Investigation of peptide sorption mechanism to PLGA from 24-hr isotherms. . . . .	76



6.3.2	Quantification of the maximal amount of peptide sorbed using a modified Langmuir model . . . . .	78
6.3.3	Effect of solution conditions on desorption of octreotide from PLGA . . . . .	81
6.4	Conclusions . . . . .	83
<b>Chapter 7</b>	<b>Octreotide Localization Upon Sorption to PLGA . . . . .</b>	<b>86</b>
7.1	Introduction . . . . .	86
7.2	Materials and methods . . . . .	87
7.2.1	Materials . . . . .	87
7.2.2	PLGA film preparation and characterization . . . . .	87
7.2.3	Analysis of octreotide solution concentration by HPLC . . . . .	88
7.2.4	Sorption of octreotide to PLGA films . . . . .	88
7.2.5	<sup>1</sup> H Nuclear magnetic resonance of sorbed octreotide . . . . .	89
7.2.6	Sectioning and analysis of PLGA films sorbed with octreotide . . . . .	89
7.2.7	Surface analysis by x-ray photoelectron spectroscopy . . . . .	90
7.3	Results and Discussion . . . . .	90
7.3.1	<sup>1</sup> H-NMR of octreotide-PLGA ion-pair dissolved in <i>d</i> <sub>3</sub> -acetonitrile . . . . .	90
7.3.2	Peptide sorption to PLGA films . . . . .	91
7.3.3	Localization of sorbed octreotide within PLGA . . . . .	94
7.3.4	Surface analysis by X-ray Photoelectron Spectroscopy . . . . .	95
7.4	Conclusions . . . . .	96
<b>Chapter 8</b>	<b>Contributions . . . . .</b>	<b>102</b>
<b>Bibliography</b>	<b>. . . . .</b>	<b>105</b>

# List of Tables

## Table

2.1	Mechanisms and characterization methods of physical and chemical instabilities of peptides and proteins [48, 51, 56]. . . . .	16
3.1	Characteristics of Boehringer-Ingelheim Resomer <sup>®</sup> PLGAs. Molecular weight polydispersity (Mw/Mn) is ~1.7. . . . .	27
3.2	Characteristics and manufacturing conditions of PLGA films. . . . .	28
4.1	LC-MS identification octreotide acylation products. . . . .	39
4.2	Octreotide recovery via two-phase extraction with time after incubation in pH 7.4 buffers at 37°C (unless otherwise noted). Initial octreotide concentration ~0.42 mM. . . . .	42
4.3	Summary of encapsulation of octreotide and salt in PLGA millicylinder formulations. . . . .	43
4.4	Zeta-potential of PLGA 50:50 nanoparticles (diameter = 250 nm) in the absence and presence of divalent cations at 37°C in 20 mM HEPES buffer with 0.1% poly(vinyl alcohol), pH 7.4. . . . .	45
4.5	Effect of PLGA composition and excipients on octreotide acylation during millicylinder production. Theoretical octreotide and excipient loading were both 5 wt%. . . . .	49
4.6	Long-term stability of octreotide extracted from PLGA millicylinders. . . .	52
4.7	Long-term release of native and acylated octreotide from PLGA millicylinders.	52
4.8	Effect of sodium salts of weak acids, trifluoroacetic acid, and Polysorbate 80 on octreotide adsorption to PLGA 50:50 in 0.1M phosphate buffer, pH 7.4. Standard error of the means in parentheses (n=3). . . . .	53

5.1	Parameters of biexponential kinetic model for data shown in 5.1(a), at various initial concentrations of octreotide. $k_f = 1.38 \text{ hr}^{-1}$ ; $k_s = 3.10 \times 10^{-3} \text{ hr}^{-1}$ . . . . .	65
5.2	Parameters of biexponential kinetic model fit for data shown in Figure 5.2, with ionic strength modulated by buffer concentration and type. Initial octreotide concentration was 0.4 mM. $k_f = 1.15 \text{ hr}^{-1}$ ; $k_s = 2.56 \times 10^{-3} \text{ hr}^{-1}$ . . . . .	66
5.3	Parameters of biexponential kinetic model fit for peptides sorbed to PLGA from solutions of 0.4 mM <b>(A)</b> octreotide in 0.1 M HEPES, pH 7.4 at 25°C (data shown in Fig. 5.5), <b>(B)</b> leuprolide in 0.1 M HEPES, pH 7.4 at 37°C (data shown in Fig. 5.4), and <b>(C)</b> octreotide in 0.1 M HEPES, pH 7.4 at 37°C (fit singularly for comparison). . . . .	67
6.1	Langmuir model fitted parameters and estimated fraction of acids occupied at maximal sorption, calculated using Equation 6.1. . . . .	79
7.1	Effect of zeta-potential on solution concentration at the surface in [mM], calculated using Equation 7.2, for a bulk concentration of 1 mM. . . . .	93
7.2	Octreotide recovery from sectioned PLGA films incubated in the presence of 1 mM octreotide acetate solution. . . . .	95
7.3	Atomic compositions of PLGA films determined from XPS spectra shown in Figures 7.5 – 7.7. Trace amounts of sodium were not included. . . . .	96

# List of Figures

## Figure

2.1	The structure of the PLGA family of polyesters. . . . .	11
3.1	Boehringer-Ingelheim Resomer <sup>®</sup> RG502H particles before ( <b>top</b> ) and after ( <b>bottom</b> ) 24 hour incubation at 37°C in 0.1M HEPES buffer, pH 7.4 . . . .	32
3.2	Surface area determination via multi-point BET analysis of N <sub>2</sub> sorption to RG502H particles. . . . .	33
3.3	Scanning electron micrograph of a cross section of a PLGA 50:50 film prepared according to E conditions (see Table 3.2) on a glass substrate. . . .	33
3.4	Structure of octreotide, D-Phe-c(Cys-Phe-D-Trp-Lys-Thr-Cys)-Thr-ol ( <b>left</b> ). Structure of leuprolide, pGlu-His-Trp-Ser-Tyr-D-Leu-Leu-Arg-Pro-NH <sub>2</sub> ( <b>right</b> ). . . . .	34
4.1	( <b>A</b> ) Sample chromatogram of reference sample of acylated octreotide products. ( <b>b</b> ) Sample chromatogram of acylated octreotide products in solution after 21 days incubation in the presence of PLGA 50:50 at 37°C. . . . .	55
4.2	Kinetics of octreotide acetate sorption to PLGA 50:50 in the presence of 15 mM CaCl <sub>2</sub> (◆), MnCl <sub>2</sub> (▲), no salt (●), and kinetics of Ca <sup>2+</sup> (○) sorption to PLGA during 24 h incubation in peptide-free 0.1M HEPES buffer solution, pH 7.4 at 37°C. PLGA was 10 mg in 1 mL of buffer solution. Initial octreotide and calcium chloride concentrations were 0.8 and 15 mM, respectively. Dotted trendlines shown for clarity. . . . .	56
4.3	Effect of ( <b>A</b> ) MgCl <sub>2</sub> and ( <b>B</b> ) CaCl <sub>2</sub> on octreotide acetate sorption to PLGA 50:50 at 0 (○), 1 (●), 15 (▲), and 50 (◆) mM salt concentrations after 24 hr incubation in 0.1M HEPES buffer solution, pH 7.4 at 37°C. PLGA was 10 mg in 1 mL of buffer solution. . . . .	57

4.4	Effect of 15 mM Mg <sup>2+</sup> (■), Ca <sup>2+</sup> (△), Sr <sup>2+</sup> (▲), Ni <sup>2+</sup> (○), and Mn <sup>2+</sup> (●) chloride and 50 mM NaCl (□) on octreotide sorption to PLGA 50:50 after 24 hr incubation in 0.1M HEPES buffer solution, pH 7.4 at 37°C. PLGA was 10 mg in 1 mL of buffer solution. . . . .	58
4.5	EPR spectra of (A) unincubated MnCl <sub>2</sub> , (B) MnCl <sub>2</sub> and octreotide incubated without PLGA, and (C) MnCl <sub>2</sub> and octreotide incubated with PLGA. . . . .	58
4.6	Octreotide sorption and formation of acylated products, native (●), acylated (○), and total (▼) octreotide, during incubation of PLGA at 37°C in 0.1M HEPES buffer solution, pH 7.4 containing (A) no additional salt, (B) 15 mM CaCl <sub>2</sub> , and (C) 15 mM MnCl <sub>2</sub> . Initial octreotide concentration was 0.2 mM and PLGA was 10 mg in 1 mL of buffer solution. . . . .	59
4.7	Effect of 0.24 mg/mL poly(arginine) (▲) 0.2 (○), 1.0 (●), and 2.0 (■) mg/mL poly(ethyleneimine) on octreotide acetate sorption to PLGA 50:50 after 24 hr incubation in 0.1M HEPES buffer solution, pH 7.4 at 37°C. PLGA was 10 mg in 1 mL of buffer solution. . . . .	60
5.1	(A) Kinetics of octreotide sorption to PLGA 50:50 from solutions of 0.26 (▲), 0.39 (△), 0.54 (●), 0.87 (○), 1.80 (■) mM octreotide in 0.1 M HEPES, pH 7.4 at 37°C and fits to biexponential model (solid lines). (B) Normalized kinetic data (same symbols). Model fits for 0.26 and 0.54 mM omitted for clarity. . . . .	70
5.2	Effect of ionic strength on octreotide sorption kinetics to PLGA 50:50 (Boehringer-Ingelheim RG502H) at 37°C in solutions of pH 7.4. The ionic strength was adjusted using buffer type and concentration: 10mM HEPES buffer (I = 4 mM, ▲), 10 mM phosphate buffer (23 mM, ○), 0.1M HEPES buffer (49 mM, △), 0.1 M phosphate buffer (236 mM, ●). Initial octreotide concentration was 0.4 mM. . . . .	71
5.3	Effect of buffer type and concentration (pH 7.4) on octreotide sorption to 10 mg PLGA 50:50 (Boehringer-Ingelheim RG502H) from 300 mM ionic strength solutions (adjusted by NaCl) at 37°C. Amount sorbed: shaded area; amount remaining in solution: white area. . . . .	71
5.4	Comparison of leuprolide (●) and octreotide (△) sorption to PLGA 50:50 (Boehringer-Ingelheim RG502H) at 37°C in solutions of 0.1 M HEPES buffer, pH 7.4. Initial peptide concentration was 0.4 mM. . . . .	72
5.5	Effect of temperature on octreotide sorption to PLGA 50:50 (Boehringer-Ingelheim RG502H) in solutions of 0.1 M HEPES buffer, pH 7.4. Initial octreotide concentration was 0.4 mM. . . . .	72

6.1	24-hour sorption isotherms of leuprolide (○) and octreotide (●) on PLGA 50:50 (Boehringer-Ingelheim RG 502H) in 0.1 M HEPES buffer, pH 7.4 at 37°C. . . . .	84
6.2	Effect of pH on octreotide sorption to PLGA 50:50 (Boehringer-Ingelheim RG502H) in solutions of 0.1 M HEPES buffer, pH 7.4 (▲), 0.1 M MES buffer, pH 5.5 (■), and 0.05 M DEPP buffer, pH 4.0 (●) after 24 hours incubation at 37°C. . . . .	84
6.3	Effect of PLGA 50:50 molecular weight on 24-hr octreotide sorption isotherms at 37°C from solutions of 0.1 M HEPES buffer, pH 7.4. Boehringer-Ingelheim Resomer <sup>®</sup> (●) RG 502H, (▲) RG 503H, and (■) RG 504H. . . . .	85
6.4	Desorption of octreotide from PLGA 50:50 particles and films (FH7) after 24 hr incubation at 37°C with 1 mM octreotide acetate in 0.1 M HEPES buffer, pH 7.4 (~650 nmol octreotide sorbed to RG502H particles (10 mg), ~360 nmol to RG503H particles (10 mg), and ~300 nmol to RG502H Film D (30 mg)). Desorption solutions: 5 wt% SDS in water ( <b>SDS</b> ); 50 vol% methanol in water ( <b>MeOH</b> ); 1 mg/mL PEI in 0.1 M acetate buffer, pH 4.0 ( <b>AP4</b> ); 0.1 M HEPES, pH 7.4 ( <b>3H7</b> ); 0.1% TFA in 0.1 M HEPES, pH 7.0 ( <b>TFAH7</b> ); 0.1 M DEPP, pH 4.0 ( <b>D4</b> ); 0.1 M HEPES, pH 7.4 ( <b>2H7</b> : particles and <b>FH7</b> : films); 2 M CaCl <sub>2</sub> in HEPES ( <b>HCa</b> ); 0.1 M HEPES, pH 7.4 ( <b>H4C</b> ). All desorptions were at 37°C, except H4C, which was at 4°C. PLGA RG502H was used in all cases, except 3H7, which used RG503H. SDS desorption was assessed by recovering sorbed octreotide via two-phase extraction. . . . .	85
7.1	<sup>1</sup> H-NMR of PLGA 50:50 in <i>d</i> <sub>6</sub> -dimethylsulfoxide (top), sorbed octreotide-PLGA 50:50 in <i>d</i> <sub>3</sub> -acetonitrile (middle), and octreotide acetate in <i>d</i> <sub>6</sub> -dimethylsulfoxide (bottom). . . . .	97
7.2	Scanning electron micrograph of the surface of a PLGA 50:50 film prepared according to A conditions (see Table 3.2) after 24 h incubation in 0.1M HEPES buffer, pH 7.4 <b>A</b> without and <b>B</b> with 1 mM octreotide acetate at 37°C. . . . .	98
7.3	Scanning electron micrograph of the surface of a PLGA 50:50 film prepared according to C conditions (see Table 3.2) after 24 h incubation with 1 mM octreotide acetate in 0.1 M HEPES buffer, pH 7.4 at 37°C. . . . .	99
7.4	Effect of mass/thickness on peptide sorption to PLGA 50:50 (Boehringer-Ingelheim RG502H) films in 0.1 M HEPES buffer, pH 7.4 at 22°C (octreotide: ●), 30°C (octreotide: ▲), and 37°C (octreotide: △, leuprolide: ■). Initial peptide concentration was 1.0 mM. . . . .	99
7.5	The XPS survey spectra of a PLGA 50:50 film prepared according to D conditions (see Table 3.2). . . . .	100

7.6	The XPS survey spectra of octreotide acetate powder. . . . .	100
7.7	The XPS survey spectra of a PLGA 50:50 film prepared according to D conditions (see Table 3.2) after 24 hr incubation at 37°C with 1mM octreotide acetate in 0.1 mM HEPES, pH 7.4. . . . .	101

# Abstract

The aim of this dissertation is to understand peptide sorption to PLGA, with the goal of stabilizing octreotide against acylation within PLGA. These studies describe the first detailed investigations of peptide sorption to low  $M_w$  free-acid PLGA. A new class of inhibitors of the sorption and acylation of a model peptide, octreotide, has been described. Long-term sorption studies indicated that  $\text{CaCl}_2$  and  $\text{MnCl}_2$  disrupt peptide sorption to PLGA with the inorganic divalent cation inhibitors translates to inhibition of peptide acylation. The octreotide-PLGA interactions are mostly irreversible in aqueous solution and strongly increase solubility of octreotide in acetonitrile. Only the addition of solvent or 5% SDS resulted in a substantial desorption from PLGA, strongly suggesting the irreversibility is due to hydrophobic interactions or hydrogen-bonding between the peptide and PLGA.

The kinetics of peptide sorption to PLGA was studied and well described using a biexponential model. Sorption is reduced at low octreotide concentrations, high ionic strength and low temperature, suggesting polymer mobility plays a critical role in the sorption interaction. Although irreversible, peptide sorption follows Langmuir behavior. Sorption of octreotide decreased as the pH of the solutions tested was decreased toward the  $\text{pK}_a$  of PLGA carboxylates. Reducing the number of total acid end-groups by increasing the PLGA molecular weight also decreased octreotide sorption. These results indicate the critical role of ionized PLGA acid end-groups during the peptide sorption pathway. Quantification of the maximal amount of peptide sorbed at high solution concentration showed this value to be similar to the total number of PLGA acid end-groups for RG502H and RG503H.



The low amount of sorption to the higher molecular-weight RG504H is also consistent with peptide partitioning into the polymer phase. Film sectioning after peptide sorption showed a proportional decrease in peptide remaining in the polymer with fraction of film removed. Hence, these results suggest both multilayer adsorption and absorption of peptide to free-acid PLGA.

# Chapter 1

## Introduction

### 1.1 Motivation

Biodegradable controlled-release systems for the delivery of biological therapeutics provides the opportunity to enhance patient acceptability, compliance, and outcomes relative to parenteral formulations typically used currently. The stability of peptides and proteins within poly(lactic-co-glycolic acid) (PLGA) microspheres and implants has been identified as a major challenge for the successful development of PLGA controlled release systems. Significant resources have been committed to gaining a mechanistic understanding of the physical and chemical instabilities of peptides and proteins in the solution- and solid-states, as well as at phase interfaces.

The acylation of amine-containing molecules with PLGA is a deleterious chemical reaction that could compromise drug purity, efficacy, and safety. Compared to other instability pathways, such as aggregation or deamidation, which have been investigated for decades by a large number of research groups, significant contributions towards a complete understanding of the peptide acylation pathway with PLGA have only recently been developed by a few research groups. Although progress has been made to clearly demonstrate acylation of peptides in PLGA, there remain significant mechanistic questions unanswered. For examples, it is still unclear what role primary or higher order structure plays on the rate and extent of peptide acylation. It is also unclear in which phase acylation occurs— whether

at the interface between the aqueous solution and the polymer or whether the peptide has limited solubility in the bulk. Is it possible that the low molecular weight polymer has some solubility for the peptide? There appears to be a relationship between octreotide sorption and acylation in PLGA. What factors govern peptide sorption to PLGA? If the questions previously described were answered, there is a reasonable possibility of significantly inhibiting the acylation reaction in PLGA.

## **1.2 Overview**

In this dissertation, peptide acylation with PLGA is investigated in detail, with an emphasis on understanding the reaction mechanistically and utilizing this understanding to develop a rational inhibition strategy. Our specific aims are to evaluate excipients and conditions that inhibit acylation, investigate how peptide or PLGA properties effect sorption and acylation, and ascertain whether the peptide interacts with PLGA by via multilayer formation or by absorbing into the bulk polymer phase.

Chapter 1 provides motivation for carrying out the research described within this thesis. Chapter 2 provides background on the therapeutic delivery of peptides and proteins, including an overview of several non-parenteral delivery technologies, with a focus on PLGA controlled release systems. The stability of peptides and proteins in PLGA, one of the key challenges in controlled release systems, is also reviewed. The the acylation reaction and literature reports of peptide acylation are reviewed in detail.

A general introduction to the experimental system and methodology is presented in Chapter 3. More detailed experimental protocols can be found in the relevant individual chapters.

Chapters 4, 5, 6, and 7, containing the bulk of the experimental data of this dissertation have been written an a manner that allows them to be read individually as 'stand-alone' doc-

uments, to the extent that it was possible. As a result, there is a small amount of redundancy in certain sections.

Chapter 4 presents a new method to inhibit acylation involving disruptors of peptide sorption, namely, water-soluble inorganic divalent cations salts. The effect of divalent cations on the kinetics of sorption and 24-hr sorption isotherms of a model peptide, octreotide acetate, to free-acid end-group PLGA was monitored to determine their order and absolute effectiveness on inhibition of acylation.

In Chapter 5, we study the effect of initial concentration and ionic strength on the kinetics of peptide sorption to PLGA, investigate the rate-limiting step, compare the sorption kinetics of two model peptides, octreotide and leuprolide, which have different structures, net charge, and conformational flexibility, and present a biexponential kinetic model that describes the sorption process well.

In Chapter 6, the characteristics of peptide sorption to PLGA, such as the stoichiometry, binding affinity, and maximal amount of peptide sorbed, 24-hour sorption isotherms were obtained for two model peptides, octreotide and leuprolide. Although octreotide sorption to PLGA is found to be essentially kinetically irreversible in aqueous solutions, the data follows Langmuir-like behavior; a modified Langmuir isotherm is used to estimate the maximum amount of peptide sorbed and show that this value is roughly equal to the total acid content of the polymer.

Chapter 7 investigates the localization of octreotide sorbed to PLGA. Several studies are performed to learn whether octreotide sorption is primarily surface-associated or whether partitioning into the bulk polymer phase occurs.

Chapter 8 summarizes the important results and contributions of this work.

# Chapter 2

## Background: Therapeutic delivery of peptides and proteins

The development of recombinant DNA technology in the 1970s and the success of the human genome project in the 1990s have made discovery and large-scale production of biological therapeutics possible. More than 325 million people worldwide have been helped by the more than 155 biotechnology drugs and vaccines approved by the U.S. Food and Drug Administration (FDA) [1]. Numerous peptide and protein therapeutics are now indicated for treatment of life-threatening diseases previously untreatable with low-molecular weight drugs—insulin for diabetes, erythropoietin for anemia, growth hormone for dwarfism, interleukins and interferons for cancer and multiple sclerosis, vaccines, and monoclonal antibodies for cancer, Crohns disease, immunosuppression, etc. There are also more than 400 biotechnology drug products and vaccines currently in clinical trials targeting more than 200 diseases, including various cancers, Alzheimer’s disease, heart disease, diabetes, multiple sclerosis, AIDS and arthritis [1]. The biotechnology industry has grown rapidly since 1992, with revenues increasing from \$8 billion in 1992 to \$58.8 billion in 2006 [1]. The successes of the biotechnology industry, however, have not been matched by progress in the formulation and development of peptide and protein therapeutics [2, 3, 4, 5, 6]. In many cases, the successful development of formulation and delivery methods has been the bottleneck for their wide spread use. As the number of biotechnology drug products moving through the pipeline increases, the significance of the development of a generic formulation and delivery strategy has become paramount.

Oral delivery is the preferred method for most patients because it is simple, convenient, and familiar. Unlike traditional small molecule therapeutics, proteins are large, hydrophilic molecules with many labile bonds and side chains as well as a higher order structure that if perturbed can lead to reduced activity or immunogenicity [7]. The development of a successful oral polypeptide formulation has been limited by several factors: chemical instability due to extreme pHs in the digestive tract, susceptibility to enzymatic degradation by proteases, low permeability across the intestinal epithelial membrane as a result of proteins charge, hydrophilicity, and high molecular weight, and rapid post-absorptive clearance [7, 8]. For these reasons, most biological therapeutics currently on the market are formulated for parenteral administration.

Parenteral administration of proteins can be painful and inconvenient for patients. Furthermore, plasma half-life of proteins and peptides can vary dramatically. Many, for example cytokines, have half-lives on the order of minutes [9], requiring multiple injections per day or an infusion to obtain therapeutically effective drug levels. The use of other, more non-invasive delivery routes could increase ease of use and patient compliance, especially in an out-patient setting, as well as offer delivery options such as site-specific delivery and/or controlled release. Potential minimally invasive protein delivery methods that have received substantial interest include oral, nasal, transdermal, pulmonary, and buccal routes. Unfortunately, success in these areas has been limited and a general method has not yet been developed. The advantages and disadvantages of three of the more widely researched potential delivery routes will be discussed, followed by a description of controlled release technology and its clinical applications.

## 2.1 Oral Delivery

The development of an oral protein formulation has been hindered by several factors, namely low epithelial permeability and instability in the GI tract. Due to the potential benefits of successful oral formulations, substantial research has been aimed at developing methods to overcome the barriers to oral delivery of biopharmaceuticals. Two major approaches have been to increase permeability of either the epithelium or the protein drug or to protect the protein from the extreme pH and proteolytic enzymes in the stomach and duodenum.

Several types of penetration enhancers have been studied, such as bile salts, fatty acids, and surfactants [9]. The use of these molecules to enhance the permeability of epithelium suffer many drawbacks, particularly damage to the epithelium, the unacceptably high concentrations necessary, the potential for increasing absorption of toxins, and the dilution of the permeability enhancer in the GI tract when localized delivery of the entire formulation is needed at epithelium surface [8].

Enhancing the permeability of the polypeptide can be done using carrier molecules that are either covalently attached or interact non-covalently. Covalently linked molecules, such as vitamin B12, can target proteins to membrane transporters, where the protein is absorbed via active transport (transcytosis) [10]. The permeability of proteins can also be increased by covalently linking a lipophilic molecule. An example of this is hexyl-insulin monoconjugate-2 (HIM2), developed by Nobex [11]. The former method is limited by the density of receptors, while both methods result in increased complexity and cost of manufacturing due to the difficulty in linking the attachment to the protein without altering its activity. Furthermore, the covalent attachment must be labile, so that it is easily removed from the peptide upon absorption. Another approach to increase permeability, developed by Emisphere, uses small amphiphilic carriers that interact non-covalently with proteins, reversibly altering their conformation to a molten globule state with exposed hydrophobic residues [12].

## 2.2 Pulmonary Delivery

The pulmonary route of administration is attractive because it is non-invasive, it has been successfully utilized for the delivery of several traditional small molecule drugs, and it has received encouraging results for the delivery of some proteins. Pulmonary delivery is particularly advantageous in cases where the lungs are the intended site of drug delivery, for example the use Pulmozyme<sup>®</sup> (recombinant human deoxyribonuclease (rhDNase)) to treat cystic fibrosis. However, the potential for local toxicity must be considered in cases where systemic delivery via the lungs is desired [13]. The large contact area with blood vessels in the alveoli of the lungs leads to rapid, bolus-like drug absorption. This is desirable for drugs like insulin, where the rapid onset of a peak serum level is necessary prior to meals, but may not be acceptable for other peptides or proteins with a narrow therapeutic index and short serum half-life.

Unfortunately, the bioavailability of inhaled protein formulations varies substantially, between 0-60% [13, 14]. Pulmonary bioavailability depends on the efficiency of the inhalation device, the fraction of drug that is deposited in the lung, and the fraction of drug that is absorbed from the alveoli. Current aerosol devices deliver drugs into the lungs at efficiencies on the order of 20% with significant dose to dose variability [15]. For example, Cipolla et al. evaluated four types of jet nebulizers for the pulmonary delivery of Pulmozyme<sup>®</sup>, and found an average delivery of rhDNase of 25% to the mouth-piece [16]. Only a fraction of the dose delivered to the mouth actually enters the lungs. Furthermore, the efficiency of alveolar absorption is low and can vary from protein to protein [14] as well as among individuals for several reasons, such as differences in breathing patterns or due to smoking. Such variations are unacceptable for proteins with a narrow therapeutic index.



## 2.3 Transdermal Delivery

Another potential route of administration is the transdermal delivery of biological molecules. Successful transdermal delivery would avoid inconveniences of parenteral therapy, permit continuous drug delivery at a controlled rate, useful for drugs with a short half-life and/or a narrow therapeutic index, and permit rapid termination of delivery [17]. Human skin, however, is an excellent barrier to the outside, severely limiting transdermal delivery, especially for proteins, which have high molecular weights and are hydrophilic. An ideal candidate for transdermal delivery is potent, has low molecular weight, and is slightly lipophilic [18]. However, considering the hundreds of approved drugs, many with all three characteristics, only about ten small molecules are currently marketed for transdermal delivery [19].

The key to overcoming the skins barrier function for drug delivery is to disrupt the stratum corneum, the outermost layer of the skin consisting of dead cells surrounded by lipids. Several methods exist to permeate the skin by disrupting the stratum corneum, such as iontophoresis (small electric current), electroportation (short, high-voltage pulses), and sonophoresis (ultrasound) [19]. Mitragotri et al. have shown that insulin (~6000 kDa), interferon- $\alpha$  (~17000 kDa), and erythropoietin (~48000 kDa) can be transported across the epidermis in vitro at rates that are therapeutically useful using low frequency ultrasound, although variations in the data were significant (22-40%) [20]. Nevertheless, the safety of skin permeation methods such as low-frequency ultrasound has not been validated. Methods such as iontophoresis can denature proteins and irritate the skin, sometimes leaving a rash and eliciting a harmful immune response [21]. Another disadvantage of transdermal delivery is the large number of enzymes and macrophages in the epidermis that can degrade peptides prior to their absorption, further decreasing bioavailability.

## 2.4 Controlled Release Depots

Traditional delivery systems for biological therapeutics administer the entire dose of drug in one bolus resulting in high, sometimes near-toxic, plasma levels. Since most therapeutic proteins, such as hGH [22] and cytokines [9], have short half-lives, repeated administration of large doses is often necessary to maintain therapeutically effective levels. Depot delivery systems offer the advantage of a continuous, zero-order release profile similar to that of an infusion. This could eliminate side-effects from repeated injections of large doses such as fever, diarrhea, anorexia that is observed with some proteins, for example IL-1 $\alpha$  [9]. Furthermore, controlled release of vaccine antigens could eliminate the need for repeated immunizations, resulting in increased patient compliance an important issue in many underdeveloped countries [23, 24]. Currently, several peptide controlled release formulations, including Lupron Depot<sup>®</sup> (leuprolide acetate), Sandostatin<sup>®</sup> (octreotide acetate), and Zoladex<sup>®</sup> (goserelin acetate). These formulations can deliver peptide therapeutics continuously over a period up to six months [25], eliminating the need for daily injections.

Controlled release systems can also be used to deliver proteins in a site-specific manner. This is advantageous for proteins such as cytokines (IL-2, TNF- $\alpha$ ) or growth factors (bFGF, VEGF [26], BMP [27]), where systemic toxicity occurs at the high levels necessary for local efficacy [28]. Polymeric microparticles have uses in many different site-specific applications. For example, they can be implanted in discreet locations of the brain using stereotaxy [29] to deliver neurotrophins (NGF, BDNF, CNTF) for the treatment of neurological degeneration and Alzheimers [30]. Microspheres can also be surface modified with a ligand to target them to specific receptors on cells [31]. Biodegradable nanoparticles have been utilized for oral delivery of antigens. These nanoparticles are taken into the lymphatic system by M cells in Peyer's patches, inducing immune response [31]. Recently, drugs have been loaded onto stents using degradable polymeric coatings to prevent restenosis [32]. Biodegradable microspheres containing growth factors have also been incorporated into scaffolds to facilitate

growth and vascularization of new tissues to replace damaged or diseased tissues [33, 34].

Controlled release has been achieved with both non-degradable and degradable delivery systems. The use of non-degradable polymers in implantable applications, such as poly(ethylene-co-vinyl acetate) (EVA) and silicone rubber, often has been limited to use for long term delivery (several years) because these materials should be surgically removed. On the other hand, biodegradable polymers, such as polyesters and polyanhydrides, are much more desirable since they are naturally degraded and eliminated by the body. Furthermore, drug release from degradable polymers is erosion-controlled, resulting in slower release than for diffusion-controlled non-degradable polymers. Many degradable homo-polymers, copolymers, and polymer blends have been studied for potential use in controlled release depots. Among them, the homo- and co-polymers of lactic and glycolic acid (PLA, PGA, and PLGA, respectively) have been the most widely studied. PLGAs are biocompatible and their degradation end products, lactic and glycolic acid, are incorporated into the TCA cycle or eliminated in the urine [35]. PLGA has a long history of surgical use, having been used as a resorbable suture material for over 30 years [36] and is the only biodegradable polymer approved by the FDA for use in humans.

### **2.4.1 Physical and Chemical Properties of PLGA**

The structures of poly(glycolic acid), poly(L-lactic acid), and poly(D,L-lactic-co-glycolic acid) are shown in Figure 2.1. The  $pK_a$  of LA and GA are 3.86 and 3.83, respectively, at 25°C. Lactic acid differs from glycolic acid by an additional methyl group. Because of this, lactic acid contains an asymmetric carbon and has two stereoisomeric forms. Due to the stereochemistry of lactic acid, several types of PLGAs can be fabricated: poly(L-lactic acid), poly(D,L-lactic acid), poly(glycolic acid), poly(L-lactic-co-glycolic acid), and poly(D,L-lactic-co-glycolic acid). PLGAs with racemic mixtures of lactic acid are generally referred to as PLA or PLGA, while those containing only one isomer of lactic acid will

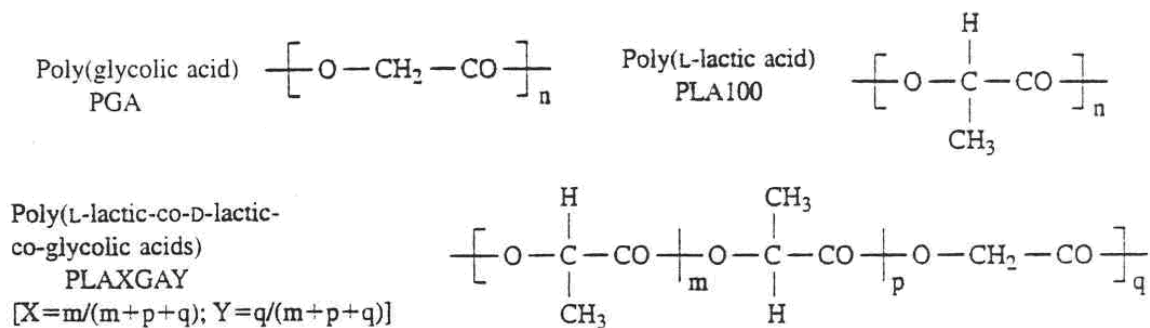


**Figure 2.1** The structure of the PLGA family of polyesters.

contain an additional L or D in its abbreviation to specify the stereochemistry (e.g. PLLA, PDLA, PLLGA).

PLGA can be synthesized from LA and GA monomers by step-growth polymerization or by condensation using cyclic dimers. The former process is not frequently used because the production of PLGA with  $M_w$  larger than 10,000 Da is impractical due to the difficulty of removing water [37]. Condensation from cyclic dimers, however, can easily produce PLGA with molecular weights of 100,000 Da using organometallic catalysts such as stannous octoate [37].

PLGA characteristics can be modified by adjusting the monomer stereochemistry, monomer ratio, molecular weight, polymer chain linearity, and end-capping. Monomer stereochemistry affects the crystallinity, melting point, and solubility of PLGA. The stereoregular homopolymers PLLA and PGA are crystalline, have a high melting point, and are only soluble in more aggressive solvents. Racemic mixtures of lactic acid (PLA) and PLGA are amorphous, do not have a true melting point, and are soluble in less aggressive solvents. The hydrophobicity, glass transition temperature ( $T_g$ ), and degradation half-life increase as the LA:GA ratio increases. Lactic acid is more hydrophobic than glycolic acid because of its additional methyl group. Thus, water uptake is decreased for PLGAs with higher LA:GA ratios, resulting in lower rates of hydrolysis. The  $T_g$  of PLA and PGA are

55-60°C and 35-40°C, respectively, while the  $T_g$  of PLGAs is intermediate between the two, increasing with increasing LA. The  $T_g$  of LA is higher than that of GA because the additional methyl group decreases the free volume and chain flexibility [38]. Similarly, the  $T_g$  also increases with molecular weight due to decreased chain flexibility. At physiological temperature, PLGA microspheres with a typical  $T_g \sim 45^\circ\text{C}$  will be in the glassy state in the absence of solvent (water). Upon incubation in an aqueous environment, the  $T_g$  of the microspheres with sufficiently low molecular weight will decrease and they will become rubbery at physiological temperature (37°C) due to the plasticization effect of water [39, 40]. Park [39] has shown that the  $T_g$  of PLA microspheres with  $M_w = 17$  and 41 kDa decreases from 41.7 and 47.0°C, respectively, to 34.2 and 39.4°C, respectively after two days incubation at 37°C. Subsequently, Blasi et al. [40] found that the  $T_g$  of RG503H decreases from 45  $\rightarrow$  27°C after one day incubation at 37°C. In most cases, microspheres in the rubbery state are preferred because the increased permeability of water and water soluble species is desirable.

PLGA  $M_w$  and polydispersity ( $M_w/M_n$ ) also affect degradation rate and intrinsic viscosity, which are important for release from, and manufacture of, microspheres, respectively. As PLGA  $M_w$  decreases and polydispersity increases, the number of acids chain ends decreases, affecting the pH inside microparticle pores. PLGA carboxylic acid chain ends may be modified by end-capping. Common end groups include lauryl or methyl esters. The addition of end groups affects PLGA hydrophilicity, solubility, and increases the  $T_g$ , decreasing the degradation rate at a given  $M_w$  [41].

## 2.4.2 Preparation of PLGA Microparticles

Microspheres are spherical, drug containing particles, typically between 1–100  $\mu\text{m}$  in diameter; millicylinders are cylindrical, drug containing particles, typically between 0.5–2 mm in diameter and 1–10 mm in length. Several methods have been developed to encapsulate drugs into polymer microspheres. A successful encapsulation method produces microspheres with

a) unaltered structure and activity of the encapsulated drug, b) high drug encapsulation efficiency and microsphere yield, c) reproducible physical characteristics and release profiles, and d) low residual solvent. Three of the most commonly used methods to produce microspheres are emulsion-solvent evaporation, coacervation, and spray drying. Millicylinders are produced using an extrusion process. Since emulsion-solvent evaporation is typically used to prepare microspheres at the bench scale, it will be described in detail below, followed by a brief description of extrusion, coacervation and spray-drying techniques.

The emulsion-solvent evaporation methods can be subdivided into four categories: oil-in-water (O/W), (water-in-oil)-in-water (W/O/W), (solid-in-oil)-in-water (S/O/W), and oil-in-oil (O/O). The suitability of each technique is determined by the solubility and stability of the drug to be encapsulated. In the O/W method, the polymer and drug are dissolved in a volatile, water-immiscible organic solvent and emulsified into an aqueous phase containing surfactant. As the volatile organic solvent diffuses into the continuous phase and evaporates, the microspheres harden and precipitate. This is commonly referred to as in-liquid drying. The O/W method is only useful for hydrophobic drugs, since they can dissolve in the organic solvent and won't leach into the aqueous continuous phase.

Water soluble drugs, such as peptides and proteins must be encapsulated using a multiple emulsion technique. The W/O/W is the most commonly used multiple emulsion method to encapsulate proteins. First, a buffered protein solution is emulsified into a volatile, water-immiscible organic solvent containing polymer using a sonicator, homogenizer, or vortex (W/O). The resulting primary emulsion is then added to a second aqueous phase containing surfactant and a second emulsion is formed (W/O/W). The organic solvent then diffuses into the continuous aqueous phase and is evaporated, precipitating the microspheres. Finally, the microspheres are filtered, rinsed, and lyophilized.

The S/O/W method is similar to the O/W method, except the former consists of lyophilized drug/excipient particles dispersed into a polymer containing organic phase,

rather than a dissolved hydrophobic drug. The S/O/W method may be preferred when structural perturbations occurring during the formation of the primary emulsion using the W/O/W technique lead to significant protein inactivation.

In the O/O method, the drug and polymer are first dispersed and dissolved, respectively, in an organic solvent, typically acetonitrile. The dispersion is then emulsified into an oil phase containing surfactant, typically a Span surfactant in cottonseed oil. After extraction of the organic solvent, the microspheres are washed with a solvent such as petroleum ether. Microspheres prepared by the O/O method are typically larger than those prepared by the W/O/W due to the coalescence of particles during the long evaporation process [42], although lower interfacial tension between the two oil phases relative to the O/W interface can result in smaller particles if evaporation is sufficiently rapid [43]. The O/O technique is useful when use of water is undesirable due to stability issues or when low encapsulation efficiency is obtained using W/O/W due to the leaching of a highly water soluble drug to the aqueous hardening bath [43].

For millicylinder preparation, a suspension of sieved drug/excipient particles ( $<90 \mu\text{m}$ ) in acetone-PLGA solution (50% wt/wt) is loaded in a syringe and extruded into silicone rubber tubing (0.8 mm i.d.) at approximately 0.1 ml/min [44]. The solvent-extruded suspension is then dried at room temperature for 24 hours and then under vacuum at 37–45°C for another 24 hours.

Coacervation, or phase separation, is a process where microspheres are precipitated by adding a cosolvent to decrease the solubility of the polymer. Similar to the O/O method, the drug and polymer are first dispersed and dissolved, respectively, in an organic solvent. Next, a miscible cosolvent is added, resulting in phase separation of microspheres into a coacervate phase. There are two main disadvantages of the coacervation method: a) it typically produces agglomerated particles, since no surfactant is used to stabilize the emulsion and b) it requires large amounts of solvents that are difficult to remove from the

microspheres after drying [45].

In spray drying methods, lyophilized peptide or protein is dispersed in a polymer containing solvent and atomized by a nozzle into fine particles. These particles can then be sprayed into heated air to remove the solvent [45] or into frozen ethanol (the extraction agent) with liquid nitrogen overlaid [46]. Spray drying involves milder conditions than double emulsion solvent evaporation techniques, is rapid, easy to scale up, and can be done aseptically [47]. For these reasons, spray drying is often used for industrial scale manufacturing of microspheres.

### **2.4.3 Polypeptide Instabilities in PLGA Controlled Release Systems**

Protein instabilities fall under two major categories: physical and chemical. Physical and chemical instabilities often result in a protein that is inactive, immunogenic, or toxic. Physical instabilities such as denaturation, aggregation, adsorption, or precipitation result in a change of conformation or state. On the other hand, chemical instabilities such as hydrolysis, deamidation, oxidation, disulfide exchange, cross-linking, or racemization result in a change in the amino acid composition of a peptide or protein. Physical and chemical instabilities are not mutually exclusive—a physical instability may lead to a chemical instability and vice versa. A common example is covalent aggregation resulting from  $\beta$ -elimination or disulfide interchange. Detailed descriptions of physical and chemical instabilities have been reviewed elsewhere [48, 49, 50, 51, 52, 53, 54, 55] and are summarized in Table 2.1.

Incomplete release of native protein from PLGA microparticles is often a result of physical and chemical instabilities. Almost all reported cases of incomplete release of native protein from PLGA microspheres have been a result of physical instabilities, for example aggregation incurred during manufacture [57, 58, 59] or as a result of low microclimate pH ( $\mu$ pH) [60, 61]. Recently, methods have been developed to stabilize proteins against



**Table 2.1** Mechanisms and characterization methods of physical and chemical instabilities of peptides and proteins [48, 51, 56].

<b>Inactivation Process</b>	<b>Mechanism</b>	<b>Characterization Method</b>
<i>Chemical Instabilities</i>		
Hydrolysis	Acid-catalyzed peptide bond cleavage at X-Asp or Asp-X linkage especially for Asp-Gly and Asp-Pro.	Determine $M_w$ by SDS-PAGE or MS.
Oxidation	Oxidation occurs typically at Met, Trp, His, Cys, and Tyr in the presence of oxidants such as air, peroxides, metal ions and DMSO.	Monitor MS changes by LC-MS, amino acid analysis, RP-HPLC, or by using chemical reactions, e.g. CNBr reacts with nonoxidized Met only.
Deamidation	Acid- or base-catalyzed hydrolysis of Asn residues to cleave the amide bond of the side chain via a cyclic imide intermediate. Occurs most often at Asn-Gly linkages. Can also occur at Gln but at a much slower rate.	Measure the amount of ammonia liberated, isoelectric focusing, or ion-exchange chromatography.
$\beta$ -elimination and thiol-disulfide interchange	Base-catalyzed reaction of cystein residues with Lys and thiocystein to generate dehydroalanine, lysinoAla, and thols.	Determine free thiol groups by Ellmans reagent, dehydroalanine by amino acid analysis, and measure isoelectric point change.
Racemization	L-amino acids transform to D-enantiomers, especially for Asp.	Monitor conformational changes by fluorescence, circular dichroism, or amino acid analysis using chiral chromatography.
Acylation	Nucleophilic primary amines interact with solid PLGA and/or PLGA degradation products, resulting in the addition of amide-linked LA or GA	HPLC-MS
<i>Physical Instabilities</i>		
Aggregation	Intermolecular interactions by noncovalent forces or covalent linkage. Severe aggregation can cause precipitation. Covalent aggregation results from $\beta$ -elimination, thiol-disulfide interchange, lysinoalanine cross-linking, isopeptide bond formation, and formaldehyde-mediated aggregation.	Measure CD and fluorescence spectra or determine secondary structure by FTIR.
Denaturation	Disruption of secondary structure by denaturants such as extremes of pH, heat, organic solvents, or detergents.	Characterize the aggregates by SDS-PAGE or size exclusion chromatography. Dissolve precipitates in denaturing solvents such as 6 M GuHCl or urea.
Adsorption	Adhesion of proteins to surfaces by surface interaction due to relatively high interfacial activity of proteins.	Detect structural changes using FTIR, CD, or fluorescence spectra.

physical instabilities during manufacture and release, for example by using the S/O/W encapsulation method [57, 58, 59] or coencapsulating a basic excipient [60, 61]. As large structural perturbations resulting from physical instabilities can now be circumvented for many proteins, there is now a need to investigate the magnitude of chemical instabilities within polymer microspheres. Herein, instabilities during manufacture, storage and release will be discussed with an emphasis of physical instability, followed by a brief overview of two important chemical degradation reactions: deamidation and oxidation.

### **Physical Instabilities During Manufacture**

During W/O/W encapsulation, proteins are exposed to conditions that are known to cause denaturing and aggregation, namely high shear [62, 63], elevated temperature, exposure to the air/liquid interface, organic solvents and the O/W interface [59, 64, 65]. Furthermore, stabilizing excipients that have solubility in the oil phase may diffuse into the polymer solution or be lost to the continuous aqueous phase. Higher energy emulsification methods, which may be necessary to achieve smaller particle sizes, are more detrimental to proteins than lower energy methods (e.g. sonicator > homogenizer > vortexer). High viscosity polymer solutions require more energy during emulsification and dissipate more energy as heat, and should be avoided. The addition of an aqueous protein solution to an organic solvent can lead to denaturing of proteins [59, 66]. Proteins, which are surface active, can diffuse to the O/W interface and aggregate non-covalently or covalently upon exposure of the hydrophobic core and subsequent disulfide scrambling.

For proteins where aggregation at O/W interfaces is a major instability, such as ribonuclease A (RNase A) [59], alternative encapsulation procedures, such as the S/O/W method may be necessary. The S/O/W encapsulation method decreases the stresses from exposure to the O/W interface as well as shear and high temperature during primary emulsification. The conformation of lyophilized protein is locked when it is added to organic solvent, because

the lack of lubricating water [65]. Therefore, retaining the native state during lyophilization is crucial for successful encapsulation using the S/O/W method. Decreased mobility of proteins upon dehydration stabilizes them against shear and elevated temperature encountered during emulsification. However, upon forming the O/W emulsion, proteins dispersed in the oil phase are rehydrated, sometimes unintentionally forming a W/O/W emulsion [67].

### **Physical and Chemical Instabilities During Storage**

Proteins and microspheres are often lyophilized prior to long term storage. The removal (and uptake) of water can destabilize proteins if excipients are not present to replace the hydrogen bonds [68]. Although degradation reactions occur at a much faster rate in solution, proteins in the solid state are not necessarily stable [53, 69]. Temperature, residual moisture, and interactions between protein, polymer, or excipients all threaten stability during storage in dehydrated polymer microparticles. The storage temperature should be maintained well below the protein  $T_g$  to minimize molecular mobility and chemical degradation reactions [70]. Residual moisture also increases molecular mobility, acts as a reactant or mobile phase for reactants in several degradation reactions, and lowers  $T_g$  and can thus compromise chemical stability of peptides and proteins encapsulated within polymeric microparticles [52]. Furthermore, residual moisture can prematurely degrade the polymer, altering the release profile and lowering pH, which in turn may accelerate deleterious reactions [71]. The lowered pH may also hydrolyze non-reducing sugars used as excipients, resulting in reducing sugars that may covalently bind to lysine residues [72]. Residual moisture also affects aggregation of polypeptides via thiol-disulfide exchange [73, 74, 75] or formaldehyde-mediated cross-linking [76, 77].

## Physical Instabilities During Release

During release from polymer microparticles, polypeptides are exposed to many stresses that can compromise their physical and chemical stability. These include rehydration, exposure to soluble oligomers, low  $\mu\text{pH}$ , interactions with the polymer, loss of stabilizing excipients, and physiological temperature.

Upon incubation in an aqueous release medium, water will diffuse into microspheres, causing them to swell. The rate of water uptake is dependent on the hydrophilicity of the polymer, microsphere porosity, and loading of drug and excipients. The uptake of water can result in moisture-induced aggregation, as previously mentioned. Moisture-induced aggregation occurs within a window of water content: at low water contents, an insufficient amount of water is present to act as a lubricant (e.g. insufficient conformational flexibility), to participate in deleterious processes, or to facilitate the diffusion of reactants [73]. At higher water concentrations, protein particles are diluted and are sufficiently hydrated properly refold [73].

Polymer degradation and the formation and enlargement of pores commences immediately upon water uptake. PLGA degrades to lower molecular weight oligomers and eventually LA and GA via a combination of chain end and bulk ester bond hydrolysis [78, 79]. As degradation proceeds, the molecular weight distribution decreases and the amount of acidic chain-ends increases. Oligomers up to 7–10 monomer units, depending on polymer composition, pH, etc., are soluble in water and diffuse into the aqueous pores. This increases the osmotic pressure inside the microsphere pores, resulting in additional water uptake [80]. Water soluble oligomers may also participate in a stabilizing or destabilizing co-solvent interaction with encapsulated proteins [81].

Acids generated during degradation autocatalyze PLGA hydrolysis [82]. Because of an increased resistance to oligomer diffusion at the center of microspheres, acidic degradation products accumulate resulting in heterogeneous degradation and  $\mu\text{pH}$  [83]. Even a dilute

lactic acid solution has substantially low pH that is detrimental to protein physical stability. For example the pH of 5% (w/w) lactic acid is 2.0 [84]. The extent of accumulation of acidic degradation products depends on the rate of formation and release of soluble oligomers, water uptake, and the presence of buffering salts [85]. The accumulation of acidic degradation products can be substantial in many microsphere formulations and is affected by the radial distance of a pore from the center as well as microsphere properties such as size, porosity, and drug loading. Using confocal microscopy, Fu et al. have shown that the  $\mu\text{pH}$  of 40  $\mu\text{m}$  microspheres increases from 1.5 in the center to 3.5 at the surface [86].

Many proteins denature at low pH, providing a driving force for non-covalent aggregation via non-covalent interactions. For example, simulations of the PLGA microclimate have shown that bovine serum albumin (BSA) aggregates non-covalently and undergoes peptide bond hydrolysis at  $\text{pH} < 3$  [60]. BSA undergoes a conformational transition from the partially denatured, F to the fully denatured E isoform at  $\text{pH} 2.7$  [87]. Poorly water soluble bases, such as  $\text{Mg}(\text{OH})_2$  or  $\text{MgCO}_3$ , can be added to neutralize the  $\mu\text{pH}$  and prevent acid-induced denaturing, aggregation, and peptide bond hydrolysis [60].

Adsorption of polypeptides can also affect their stability. Adsorption often results in the exposure of the hydrophobic interior of proteins and can often lead to the formation of insoluble aggregates or irreversible conformational changes [88]. Even when adsorption is reversible, it may accelerate other deleterious reactions by exposing previously buried residues or increasing side chain mobility. The double emulsion solvent evaporation technique produces highly porous microspheres with a large surface area for adsorption. Furthermore, as microspheres degrade and erode, the specific surface area may increase substantially [89]. Therefore, adsorption may become a greater factor in drug release and stability at later incubation times. Adsorption can be minimized by the addition of other proteins, such as BSA, or surfactants, such as SDS, that competitively interact with the polymer [89]. Pegylation has also been reported to decrease the adsorption of octreotide

and lysozyme to blank PLGA particles and microspheres, respectively [90, 91]. It is unclear, however, whether the loss of soluble protein was due to adsorption or a decrease in pH upon microsphere degradation.

### **Chemical Instabilities During Release**

Among irreversible chemical changes to peptides and proteins, deamidation and oxidation reactions are among the most common [92], and have been reported for human growth hormone encapsulated in PLGA microspheres [93]. In the presence of PLGA, acylation has also been reported to occur [94].

Crystal structures of deamidated lysozyme [95] and ribonuclease A [96] show that deamidation induced isoaspartate formation introduces a 90° bend to the polypeptide chain. Such alterations can result in decreased bioactivity if the labile Asn is near an active site. While deamidation does not affect the bioactivity of all proteins, the bioactivity of many proteins is affected by deamidation [97, 98, 99, 100, 101, 102, 103]. For examples, the bioactivity of rhGH, insulin, and IL-1 $\alpha$  and -2 are not significantly affected by deamidation, while calmodulin, EGF, growth hormone releasing factor, parathyroid hormone, triosephosphate isomerase (TPI), and RNase A all show decreased bioactivity upon deamidation [98]. IsoAsp formation may serve as a trigger for proteolytic degradation of some proteins, such as serine hydroxymethyltransferase [104] and TPI [105], or significantly increase autoimmunogenicity of others, for example cytochrome C peptide fragments [106]. The presence of isoaspartyl peptides have also been observed as a major component of the amyloid-containing brain plaques of patients with Alzheimers disease [107].

Oxidation or acylation may affect bioactivity of peptides and proteins in a similar manner– if a labile residue is near an active site, loss of activity may occur. Toxicity may also occur as a result of oxidation or acylation. For these reasons, chemical instabilities of therapeutic biomolecules may raise concerns of regulatory agencies, regardless of whether

the proteins bioactivity is affected. In the next section, we will review literature reports of peptide acylation, the reaction that is the focus of this dissertation. At this time, there have been no reports of the acylation of large proteins.

### **Acylation with PLGA**

PLGA can interact with nucleophiles (other than water), such as an amine-containing drug (peptide), resulting in an acylation reaction between the drug and the polymer. This reaction involves the nucleophilic attack by the drug on the lactate- or glycolate-endgroup, followed by hydrolysis [94]. Acylation is believed to only occur with oligomers and not with monomeric lactic or glycolic acid [108, 109]. The rate of this reaction is a function of pH, the reactivity of the polymer (e.g.  $M_W$  and LA:GA ratio), the nucleophilicity of the drug, and the concentration of water, drug, and polymer [108].

Several authors have investigated the effect of pH and lactic acid concentration on peptide acylation in lactic acid solutions [109, 110, 111]. However, increasing the concentration of lactic acid in solution results in a decreased pH as well a shift in the equilibrium between free and esterified lactic acid to higher amounts of oligomers [109, 110]. For example, in a study by Lucke and Gopferich [109], as the concentration of lactic acid increased from 1 to 50%, the pH decreased from 2.3 to 1.0 and the oligomer content increased from 0.1 to 14%. Because of this, one is unable to discriminate between the effect of pH and the equilibrium of free and esterified lactic acid in solutions at different pH values on peptide acylation. Nevertheless, reactions between peptides in lactic acid solutions have shown that the rate of acylation increases with lactic acid concentration as well as decreased pH. As the pH of 42.5% lactic acid solutions containing octreotide increased from 2.2 to 4.2, the amount of octreotide degradation products decrease, with none detected at pH 6.1 [111].

Murty et al. studied the effect of polymer composition, polymer  $M_W$ , and release medium buffer on the acylation of octreotide encapsulated in PLGA microspheres [112]. In both acetate and PBS, acylation decreases with increasing lactide composition (PLGA

50:50 > PLGA 85:15 > PLA 100) as well as decreasing  $M_W$  (high  $M_W$  PLGA 50:50 > low  $M_W$  PLGA 50:50). The decreased reactivity of octreotide with lactic acid units relative to glycolic acid units is hypothesized to result from steric hindrance of the additional methyl group on the  $\alpha$ -carbon. The authors suggest the increased reactivity of octreotide in high  $M_W$  PLGA may be a result of the longer exposure time of the peptide inside the microsphere due to the substantial decrease in the initial burst relative to the low  $M_W$  PLGA (50% release in acetate at 1 day vs. 21 days, respectively). However, the former suggestion is refuted by the PBS release data, where the amount of acylation is similar after the 21 day lag time in high  $M_W$  microspheres and after the 1 day burst release in low  $M_W$  microspheres.

Acylation was also significantly enhanced when the microspheres were incubated in PBS, relative to acetate buffer, possibly due to the plasticization of the polymer by acetic acid, facilitating the transport of reactive oligomers out of the microspheres. Further studies are required to elucidate the effects of release media buffer type and pH on the transport of buffer salts, oligomers, and peptide and their effect on the polymer degradation and acylation rates.

Later, Murty et al. investigated the effect of water uptake on octreotide acylation in PLGA 85:15 and PLA microspheres [111]. Octreotide in microspheres that were incubated under anhydrous conditions did not undergo acylation. The authors surmised that because of water uptake, the hydrolytic cleavage of the polymeric backbone created an acidic microenvironment to facilitate the covalent coupling of peptide with polymer. However, they could not discriminate between the effects of water as a plasticizer, solvent medium, or a direct participant in the acylation reaction.

Structural effects, such as differences in  $pK_a$ 's, net charge, and hydrophobicity, also play a role in the rate and extent of peptide acylation. Octreotide contains two reactive amino groups, one on the n-terminus and another on the Lys side chain. Mass spectrometry analysis on octreotide degradation products showed that the n-terminus is more likely to be



acylated than the lysine side-chain [112]. This is because the  $pK_a$  of the lysine is higher than the n-terminus, so at physiological pH a larger proportion of the n-terminal amine groups should be in the more nucleophilic deprotonated form. Lucke et al. performed a release study to compare acylation between atrial natriuretic peptide (ANP) and sCT in PLA and PLGA microspheres [94]. After 28 weeks, 50% of the ANP was released vs. 4% of the sCT. They found that the rate of acylation is substantially higher for ANP than sCT (60% vs 7% in PLA, respectively), demonstrating the unknown role structural effects play in peptide reactivity.

Na et al. studied the effect of PEGylation on octreotide sorption to free acid-endgroup and end-capped PLGA 50:50 subsequent acylation in phosphate buffer (0.1 M, pH = 7.4) [90]. Removing the reactive n-terminal amine by PEGylation was shown to completely eliminate the acylation of octreotide, suggesting that acid end-groups of PLGA are involved in interactions with amino groups of octreotide. PEGylation at lysine also substantially reduced acylation, possibly by reducing the ionic interaction between the peptide and the polymer or shielding the n-terminus from reacting.

### **Strategies to Stabilize Peptides and Proteins in PLGA Controlled Release Systems**

Peptides and proteins encapsulated within PLGA controlled release systems are exposed to many destabilizing stresses during manufacture, storage, and release that may result in incomplete release or release with reduced biological activity. A rational stabilization approach is necessary when formulating a therapeutic polypeptide delivery system in order to achieve complete release of active drug. Volkin and Klibanov have suggested a paradigm for rational stabilization of proteins [113], which has been the paradigm utilized in this research: 1) determine the major sources of inactivation, either directly or through simulation; 2) elucidate the molecular mechanisms of inactivation; and 3) devise methods to prevent, bypass, or minimize the specific mechanisms.

Several general approaches have been utilized to stabilize proteins by increasing their intrinsic stability [51]. These include the use of stabilizing excipients, chemical modification, and reduced mobility [113]. Excipients such as salts, sugars, and polyols stabilize proteins by preferentially hydrating the native state [81]. Additionally, excipients can react with species involved in deleterious reactions, for example ROS scavengers, such as thiourea or an oxidizing peptide, to minimize oxidation or non-oxidizing metals that bind to metal-binding sites, reducing MCO. Chemical modifications such as pegylation can physically stabilize peptides and proteins [91, 114]. Site-directed mutagenesis can be used to chemically stabilize polypeptides, by removing a labile residue, such as Asn or Asp [115]. Peptides and proteins in the solid state are more stable than in solution because of the decreased mobility of side chains and extended loops. The mobility of drugs can be reduced by loading them above their solubility, cross-linking with glutaraldehyde, or intentionally precipitating them (e.g. protein precipitation with zinc).

Several methods to minimize peptide acylation within PLGA microparticles have been proposed, based on the studies mentioned above, including: (a) increasing the microclimate pH from 2 to 6 [94, 109, 111], (b) reducing polymer hydrolysis rate by encapsulating with PLGAs of high lactic:glycolic ratio [94, 112], (c) facilitating the release of water soluble oligomers (for example by using PEG as a porosigen) [94], and (d) shielding the reactive amino-group on the peptide by PEGylation [90].

# Chapter 3

## Methodology

To study the acylation of peptides in PLGA, we selected a model system comprised of PLGA particles or films exposed to solutions of the model peptides, representing the aqueous pore/polymer phase interface and microenvironment within microspheres or other implant devices after injection and subsequent hydration.

### 3.1 Selection of polymers for investigation

The Boehringer-Ingelheim Resomer<sup>®</sup> family of PLGA 50:50 polymers were primarily used for this research. The Resomer<sup>®</sup> PLGAs were chosen to conveniently compare the effect of molecular-weight and capping of the carboxylic acid end-groups within a group of polymers with similar manufacturing methods and in order to validate our results against previously published work, which also primarily use Resomer<sup>®</sup> PLGAs. Table 3.1 summarizes several characteristics supplied from the manufacturer of the PLGAs typically studied that are particularly relevant to peptide acylation, namely the composition of the PLGA end-group, PLGA molecular-weight, number of acid end-groups, and dry glass transition temperature reported by the manufacturer. Upon incubation in water, PLGA 50:50 rapidly absorbs water, plasticizing the polymer and depressing  $T_g$  by up to 18°C [39, 40]. The  $T_g$  of RG503H was previously shown to be depressed from 45.5 → 31.7°C within 1h after incubation in water at 37°C [40] (see also Section 2.4.1).

**Table 3.1** Characteristics of Boehringer-Ingelheim Resomer<sup>®</sup> PLGAs. Molecular weight polydispersity (Mw/Mn) is  $\sim 1.7$ .

Polymer	Free acid end-group?	Molecular Weight, $M_n$ (kg/mol)	Acid Number (mg KOH/g PLGA)	Carboxylates ( $\mu\text{mol/g}$ PLGA)	Dry $T_g$ ( $^{\circ}\text{C}$ )
RG 502H	Yes	6.7	10.4	185	42-46
RG 503H	Yes	20.9	5.3	95	44-48
RG 504H	Yes	31.3	3.0	53	46-50
RG 502	No	6.9	<1.0	<17	42-46
RG 503	No	25.3	<1.0	<17	44-48

The PLGA RG502H was chosen as the 'base-case' polymer due to its high acid-content and low molecular weight, which were hypothesized to increase sorption and acylation as well as provide sustained release of peptides. All references to 'PLGA' in Chapters 6-7 refer to RG502H unless otherwise specified. It should be noted that due to its high number of acid end-groups, high fraction of soluble oligomers [116], and very low molecular-weight, this polymer could be considered an 'oligomer' with properties intermediate between higher molecular-weight 'polymers' and water soluble oligomers.

### 3.1.1 Characterization of PLGA particles

RG502H particles, as received from the manufacturer, had a very rough surface morphology with many pits and crevices (Figure 3.1(a)). The general surface morphology was not significantly affected by 24 hour incubation at typical experimental conditions (0.1M HEPES buffer, pH 7.4, 37°C, Figure 3.1(b)), indicating that peptide entrapment resulting from polymer rearrangements is unlikely. Multipoint Brunauer-Emmett-Teller (BET) analysis of N<sub>2</sub> sorption to RG502H particles shows a surface area of 4.6 m<sup>2</sup>/g (Figure 3.2).

**Table 3.2** Characteristics and manufacturing conditions of PLGA films.

Label	Thickness ( $\mu\text{m}$ )	PLGA concentration (wt%)	Solution Density (g/mL)	Spin Speed (rpm)	Spin Time (sec)	Volume ( $\mu\text{L}$ ) <sup>a</sup>	Volume ( $\mu\text{L}$ ) <sup>b</sup>
A	2 <sup>c</sup>	2	0.81	2000	15	150	60
B	7 <sup>c</sup>	7	0.82	1800	15	150	60
C	13 <sup>d</sup>	12	0.87	1600	15	150	60
D	24 <sup>c</sup>	17	0.87	1300	20	200	80
E	40 <sup>d</sup>	22	0.89	1000	20	250	100

<sup>a</sup> Volume used for 4cm diameter films.

<sup>b</sup> Volume used for 2.5cm diameter films.

<sup>c</sup> Estimated using PLGA density and mass of PLGA added.

<sup>d</sup> Measured by SEM.

### 3.1.2 PLGA film preparation and characterization

PLGA films of varying thicknesses were prepared for various studies of peptide sorption to PLGA. These films have been labelled A-E, as indicated in Table 3.2. To prepare the films, solutions of 2, 7, 12, 17, and 22 wt% PLGA 50/50 in acetone were added to a 4 or 2.5cm diameter glass microscope cover slide placed within a spin-coater (SCS G3-8, Indianapolis, IN). Spin-coating of the PLGA solutions were done at the conditions shown in Table 3.2. Following spin-coating, nascent PLGA films were placed in a Petri-dish with tight-fit lid (Beckton-Dickinson, Franklin Lakes, NJ) and dried for 48 hr at room temperature and pressure followed by 24 hr in a vacuum oven at 25°C.

The thickness and morphology of PLGA films were analyzed with a scanning electron microscope (Amray 1910). PLGA films appear to have a very smooth surface with even thickness throughout. The thickness of PLGA film E was determined to be  $\sim 40\mu\text{m}$ , as shown in Figure 3.3. The density of PLGA films was  $1\text{ g/cm}^3$ , based on the calculated mass of PLGA added, determined using the density of PLGA solutions (Table 3.2). The thickness of hydrated PLGA film C was also analyzed by SEM. Although the presence of otreotide induces some roughness on the surface (see Figure 7.3), the thickness of this film was  $\sim 13\mu\text{m}$ , corresponding to exactly the same PLGA density of  $1\text{ g/cm}^3$ . The thicknesses

of other films were estimated assuming constant PLGA density.

The zeta potential of PLGA Film B slides (9 x 18 mm) were evaluated using the SurPASS Electrokinetic Analyzer (Anton Paar USA, Ashland, VA). The samples were measured using the adjustable gap cell, containing two sample slides coated with PLGA, with a 1 mM potassium chloride electrolyte solution, pH 7.5. The measurements were able to differentiate between the surface properties of the three slide samples. Each sample was first rinsed at a maximum pressure of 300.0 mbar for 180 seconds before the streaming current was measured at a target pressure of 300.0 mbar for 20 seconds.

The zeta potential,  $\zeta$ , was calculated to be -70 mV, according to the following equation for streaming current measurements:

$$\zeta = \frac{dI}{dP} \times \frac{\eta}{\varepsilon \times \varepsilon_0} \times \frac{L}{A} \quad (3.1)$$

where  $\frac{dI}{dP}$  is the slope of the streaming current vs. the differential current,  $\eta$  is the electrolyte viscosity,  $\varepsilon$  is the dielectric constant of the electrolyte,  $\varepsilon_0$  is the permittivity of free space,  $L$  is the length of the streaming channel, and  $A$  is the cross-section of the streaming channel.

## 3.2 Model peptides

The model peptides used in this research included octreotide as the primary acylating model peptide, and leuprolide as a secondary non-acylating peptide for comparison of sorption. Both of these peptides have successful PLGA controlled release products on the market (See Section 2.4). Octreotide is a somatostatin analogue, used pharmacologically to treat acromegaly, that is a cyclic octapeptide with a molecular weight of 1019.3 g/mol, containing an intramolecular disulfide and two amino-groups— one at the n-terminus ( $\text{pK}_a \sim 7.8$ ) and one on the lysine side chain ( $\text{pK}_a \sim 10.1$ ) [117]— that are potential acylation sites.

Leuprolide is a gonadotropin-releasing hormone agonist, used pharmacologically to treat prostate cancer, that is a linear nonapeptide with a molecular weight of 1210. It does not contain any acylating amino-groups, but has an ionizable histidine imidazole ( $pK_a \sim 6.0$ ) [117].

Greater than 99% of native octreotide was recovered after 24 hr incubation at 37°C in all buffers typically used in these studies (e.g. HEPES, acetate, and phosphate), except at 100 mM phosphate concentration and PBST, where >85% of native octreotide was recovered.

### **3.3 General Methodology**

In this thesis, the sorption of model peptides and other divalent cations to PLGA is investigated. To assess the sorption, aqueous solutions of peptides were incubated in the presence of polymer particles or films. Peptide sorption to PLGA was determined primarily using the difference method for sorption to PLGA particles and by recovery from the polymer via two phase extraction for sorption to PLGA films. The concentration of peptide in solutions was measured by UV spectrophotometry after reverse phase-HPLC.

Validation studies were performed to ensure that the loss of peptide from solution did not result from sorption to the sample container or other degradation reactions, and that the presence of other excipients (e.g. divalent cations) did not affect the RP-HPLC/UV detection. (See Sections 4.2.8 and 4.2.2, respectively, for more details.) A mass balance on octreotide was also performed, showing that all of the octreotide is recoverable via two-phase extraction after 1 hr sorption (see Section 4.2.8).

Other auxiliary studies were also performed to analyze the peptide/cation/PLGA system, such as analysis of peptide-PLGA solubility, surface characterization by XPS, zeta-potential measurements.

### **3.4 Uncertainty and Error Analysis**

Uncertainties in reported values are presented as standard errors of the mean (s.e.m.) for an experimental sample size of 3, unless otherwise noted. The uncertainty of several measurements were propagated into the values of the s.e.m. These include uncertainties of: balance, pipette, HPLC injector, and standard curves for sorption studies using the difference method. In several cases, the s.e.m. values were smaller than the dimensions of the data point symbol and were omitted for clarity. In tables, the values of the s.e.m. values are shown except in cases where they are less than the order of the last significant digit reported.



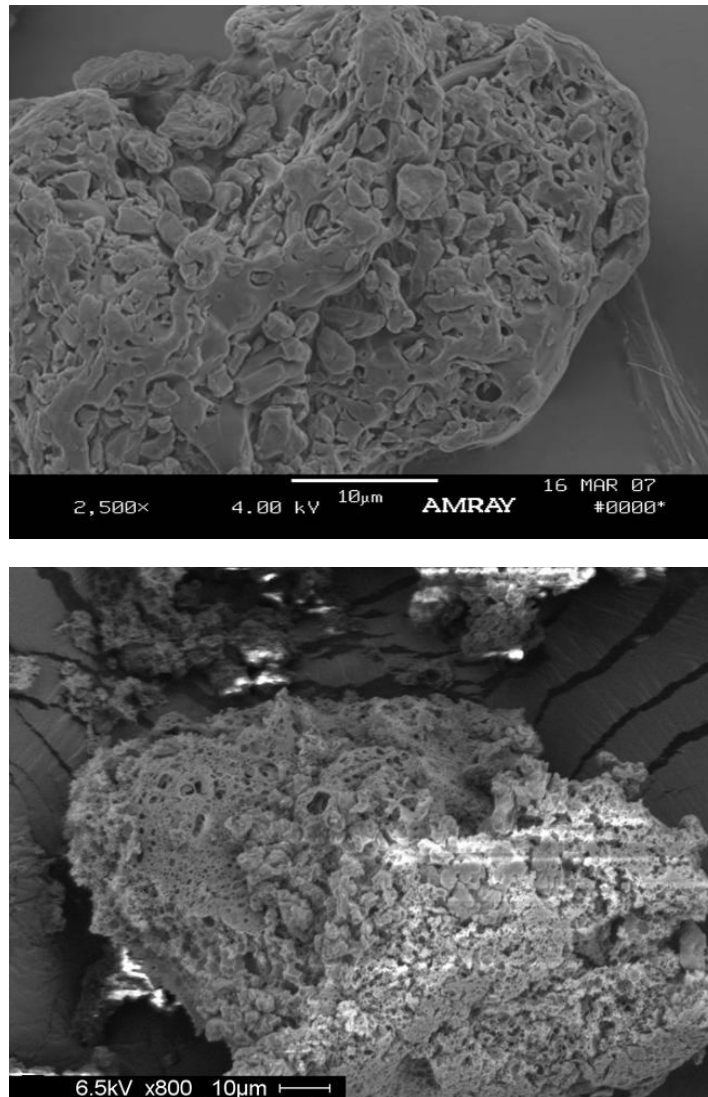


**Figure 3.1** Boehringer-Ingelheim Resomer<sup>®</sup> RG502H particles before (**top**) and after (**bottom**) 24 hour incubation at 37°C in 0.1M HEPES buffer, pH 7.4

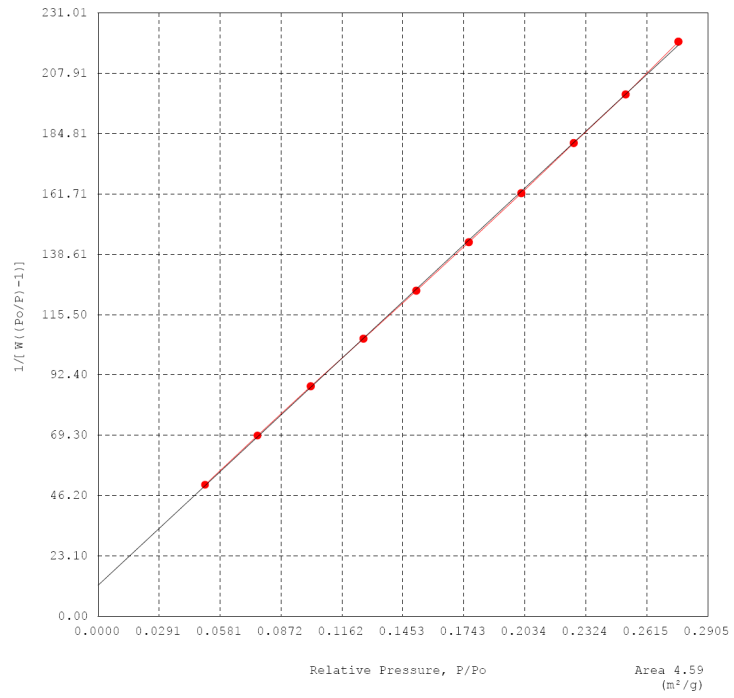


**Figure 3.2** Surface area determination via multi-point BET analysis of N<sub>2</sub> sorption to RG502H particles.

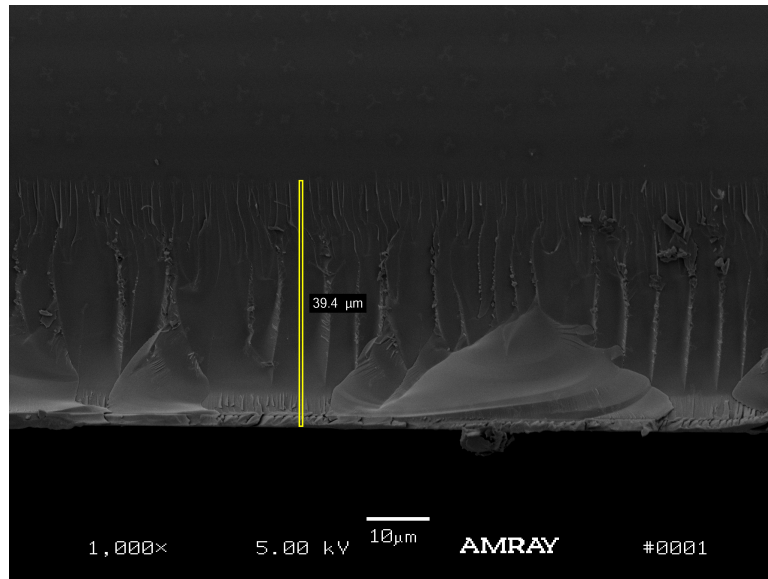


**Figure 3.3** Scanning electron micrograph of a cross section of a PLGA 50:50 film prepared according to E conditions (see Table 3.2) on a glass substrate.

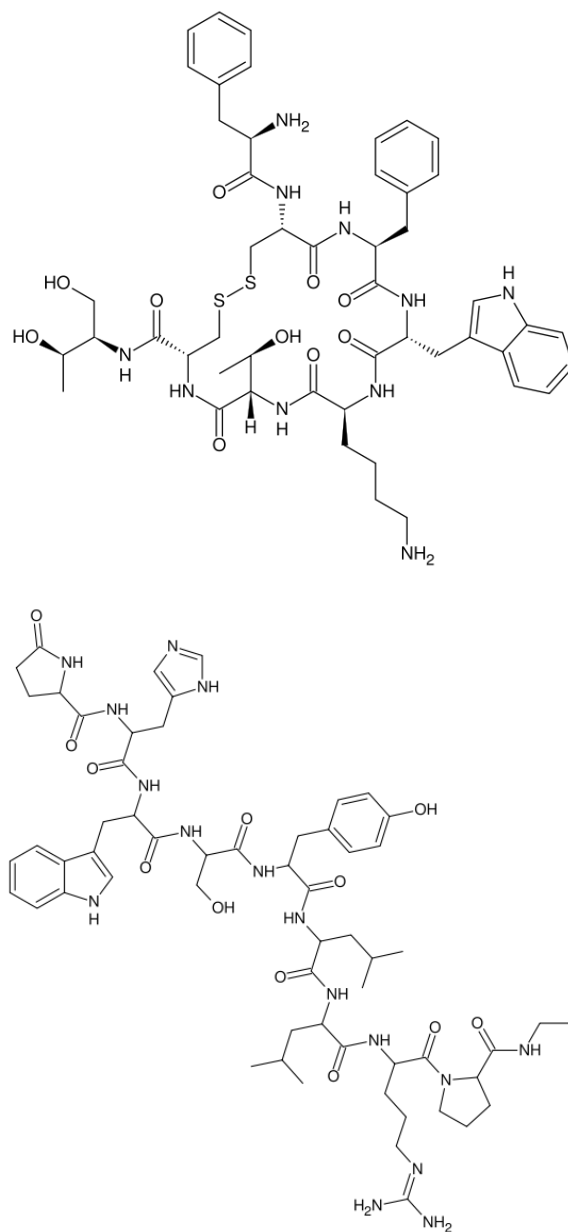


**Figure 3.4** Structure of octreotide, D-Phe-c(Cys-Phe-D-Trp-Lys-Thr-Cys)-Thr-ol (**left**). Structure of leuprolide, pGlu-His-Trp-Ser-Tyr-D-Leu-Leu-Arg-Pro-NHEt (**right**).

# Chapter 4

## A new class of inhibitors of peptide sorption and acylation in PLGA

### 4.1 Introduction

Injectable biodegradable microspheres and implants control the release of peptide or protein drugs over the course of weeks to months, providing a distinct advantage over daily injections in terms of patient acceptability and compliance. The PLGA family of copolymers of lactic and glycolic acids is one of the few biodegradable polymers used in US FDA approved pharmaceutical products or medical devices [118], and is widely used in commercially available controlled release peptide delivery systems, including the Lupron Depot<sup>®</sup> (leuprolide acetate), Sandostatin LAR<sup>®</sup> (octreotide acetate), and Zoladex<sup>®</sup> implant (goserelin acetate).

A very significant challenge in the development of controlled release PLGA systems is the instability of peptides and proteins. For larger protein molecules numerous physical and chemical pathways of instability have been extensively reviewed [51, 71, 119, 120]. Acylation was postulated [51] and later proven as a pathway of instability for peptides encapsulated in PLGA implants [94]. Nucleophilic primary amines, such as from the N-terminus and lysine side chain, can interact with solid PLGA and/or PLGA degradation products to form acylated peptide adducts [108]. Peptide acylation may potentially result in loss of activity [121], a change of receptor specificity, or immunogenicity (see [94] and citations therein). For the important, clinically used octreotide, acylation has been shown to occur

in both linear PLGA and glucose-star PLGA copolymers [111, 112], and a mechanism has been proposed to involve an ionic interaction between a protonated amine and the carboxylate PLGA end-group, followed by a nucleophilic attack of another nucleophilic amine on the lactic or glycolic carbonyl carbon and subsequent polymer hydrolysis [90].

Several methods to minimize acylation within PLGA microparticles have been proposed, including: (a) increasing the microclimate pH from 2 to 6 [94, 109, 111], (b) reducing polymer hydrolysis rate by encapsulating with PLGAs of high lactic:glycolic ratio [94, 112], (c) facilitating the release of water soluble oligomers (for example by using PEG as a porosigen) [94], and (d) shielding the reactive amino-group on the peptide by PEGylation [90]. Unfortunately, these methods either: do not strongly inhibit acylation, limit formulation options, or involve chemically modifying the drug molecule. Additional approaches, particularly the use of additives, are needed to optimize PLGA delivery of peptides susceptible to this reaction.

Na and Deluca [90] have shown that the interaction of octreotide with PLGA was attenuated when the polymer was end-capped and when octreotide was PEGylated, resulting in an inhibition of acylation. This important finding strongly suggests a critical precursor role of the ionic interaction between dicationic octreotide and the carboxylic acid end-groups of PLGA in acylation. This peptide-polymer interaction is the basis for our first effort to identify new acylation inhibitors.

PEGylating polypeptide therapeutics is an attractive option for molecules that would benefit from improved physical stability, resistance to proteases, reduced immunogenicity, or increased half-life. In some cases, PEGylation may be a useful strategy for extending an existing products patent-life by applying for regulatory approval of the new chemical entity. Unfortunately, there are many documented cases where PEGylation has resulted in a substantial decrease in receptor affinity [122] or may not be a feasible strategy because of financial concerns with gaining approval of a new drug entity.

The interaction of cations in the diffuse side of electric double layers of negatively charged surfaces is well documented [123]. Similarly, the binding mechanism of divalent cations to surfaces such as emulsion droplets [124] and phospholipid membranes [125, 126, 127, 128] has been the topic of extensive research. The specific interaction of divalent cations with biological membranes is essential for several cellular processes, including endo- and exo-cytosis, signal transduction, transport of molecules, and binding of proteins. This body of work motivated us to investigate the effect of water-soluble inorganic divalent cationic salts on the interaction between octreotide and PLGA. Indeed, we found for certain cations, such as  $\text{Ca}^{2+}$  and  $\text{Mn}^{2+}$ , which are significantly present in living systems, a very strong inhibition of both peptide sorption to PLGA and peptide acylation using octreotide as a model peptide.

## 4.2 Materials and Methods

### 4.2.1 Materials

Octreotide acetate was obtained from Novartis (Basel, Switzerland). PLGA 50:50 (Resomer<sup>®</sup> RG502H) was purchased from Boehringer-Ingelheim GmbH (Ingelheim, Germany). Poly(lactide) (i.v. 0.1-0.2 dL/g) and poly(ethyleneimine) ( $M_w \sim 25,000$  Da) were purchased from Polysciences, Inc. (Warrington, PA). Poly(arginine) ( $M_w \sim 10,000$  Da), (Hydroxyethyl)-piperazine-(ethanesulfonic acid) (HEPES), calcium chloride ( $\text{CaCl}_2$ ), magnesium chloride ( $\text{MgCl}_2$ ), manganese chloride ( $\text{MnCl}_2$ ), and sodium chloride ( $\text{NaCl}$ ) were purchased from Sigma-Aldrich Chemical Co. (St. Louis, MO). Nickel chloride ( $\text{NiCl}_2$ ) and strontium chloride ( $\text{SrCl}_2$ ) were purchased from Fisher Scientific. Standard solutions for inductively coupled plasma-optical emission spectroscopy (ICP-OES) were purchased from GFS Chemicals (Columbus, OH). All other reagents used were of analytical grade or purer and purchased from commercial suppliers.

### 4.2.2 Analysis of octreotide by HPLC

The concentration of native and acylated octreotide was determined by RP-HPLC and the octreotide degradation products were identified as acylated octreotide by HPLC-MS, similarly as described by Murty et al. [112]. Injection volumes of 20  $\mu$ L were loaded onto a Nova Pak C-18 column (3.9 x 150 mm, Waters) for RP-HPLC (Waters Alliance<sup>®</sup>) analysis using UV detection (280 nm). Solvent A was 0.1% TFA in acetonitrile and Solvent B was 0.1% TFA in water. A linear gradient of 25 to 35% A in 10 min, with a flowrate of 1.0 mL/min was used.

Solutions of octreotide (0.9 mM) before and after the addition of CaCl<sub>2</sub> and MnCl<sub>2</sub> (50 mM) were analyzed by HPLC after 24 hr incubation to validate that the divalent cations do not interfere with the HPLC analysis or degrade octreotide. The addition of CaCl<sub>2</sub> or MnCl<sub>2</sub> did not affect the concentration of octreotide detected (data not shown).

### 4.2.3 Analysis of octreotide by HPLC-MS

The formation of acylated octreotide was verified by HPLC-MS, where a linear gradient of 15 to 45% A in 30 min was used, with a flowrate of 1.0 mL/min, followed by infusion into an electrospray ionization mass spectrometer with ion-trap detection in positive ion mode (ThermoFinnigan Surveyor HPLC and LCQ MS, San Jose, CA). Acylated peak identification was performed against a reference sample that was previously analyzed by HPLC-MS, shown in Figure 4.1(a). The reference sample was prepared from octreotide, which was acylated using a PLGA-based polymer. Note that the concentration of the reference sample was high causing detector saturation and the appearance of two parent octreotide peaks. Figure 4.1(b) shows a sample HPLC chromatogram of octreotide incubated with PLGA for 28 days (see Figure 4.6) with the corresponding peak assignments obtained from the reference acylated sample in Figure 4.1(a). Table 4.1 gives the  $M_w$  and identification of the

**Table 4.1** LC-MS identification octreotide acylation products.

HPLC Peak	Observed Mass (m/z)	Expected Structure
1	1019	Octreotide
2	1077	Octreotide-1GA
3	1077	Octreotide-1GA
4	1135	Octreotide-2GA
5	1063	Octreotide-1GA-1LA
6	1077	Octreotide-1GA
7	1077	Octreotide-1GA
8	1077	Octreotide-1GA
9	n.d.	unknown
10	1135	Octreotide-2GA
11	1091	Octreotide-1LA

acylated HPLC-MS peaks. Peak 3 was not fully resolved in the reference sample, likely due to its higher concentration. Peak 9 was not present in the reference sample. Peaks 3 and 9 each accounted for 1.5% of the total peak area. All other peak retention times matched their corresponding reference peaks within 0.1 min, except peak 10, which matched within 0.2 min. Greater than 97% of the total peak area was accounted for by matching to the reference sample; all peaks other than the native octreotide peak were assumed to be acylated.

#### 4.2.4 Analysis of divalent cations by ICP-OES

The concentration of divalent cations were analyzed by ICP-OES (Perkin-Elmer Optima 2000 DV with Winlab software). Solutions containing divalent cations were diluted with water prior to analysis.  $\text{Ca}^{2+}$  was detected at 396.85 nm in the radial plasma mode;  $\text{Mn}^{2+}$  was detected at 257.61 nm in the axial plasma mode. Each measurement was an average of three scans.



#### **4.2.5 Preparation and Characterization of PLGA Nanoparticles in the Presence of Divalent Cations**

PLGA nanoparticles were prepared using a one-step, oil-in-water solvent evaporation method. Briefly, a dichloromethane solution (2 mL) containing PLGA (50 mg) was poured into a 50 mL glass beaker containing a 0.2% (w/v) water solution of PLA (40 mL), used as an emulsifier, and the mixture was sonicated for 1 min using a probe sonicator (Sonics VibraCell) at 50% power. The solvent was then evaporated for 3 hr under magnetic stirring to harden the particles. The resulting PLGA nanoparticles were then transferred to a 50 mL centrifuge tube and centrifuged at 919.7g for 20 min. The supernatant was discarded and the nanoparticles were resuspended in deionized water and centrifuged 3 times to remove excess PLA. After the final rinse, 20 mM HEPES buffer, pH 7.4 was added to a nanoparticle concentration of  $\sim 5$  mg/mL.

The size and zeta-potential ( $\zeta$ ) of PLGA nanoparticles were measured at 37°C using a Zetasizer Nano ZS (Malvern Instruments, UK). Each measurement was the average of 15 runs. To test the effect of divalent cations on the zeta potential of nanoparticles, concentrated aliquots of octreotide, CaCl<sub>2</sub> and MnCl<sub>2</sub> were added to the nanoparticles prior to the measurements. In order to prevent flocculation upon the addition of divalent cations, 0.1% (w/v) PVA was added to the HEPES buffer solution.

#### **4.2.6 Electron paramagnetic resonance (EPR) spectroscopy of Mn in the presence of octreotide acetate and PLGA**

EPR measurements were performed on the supernatant of a solution of 15 mM MnCl<sub>2</sub> and 2 mM octreotide in 0.1M HEPES (pH 7.4) that had been incubated in the presence and absence of PLGA as described in section 2.4. An unincubated control solution without PLGA was also analyzed. Prior to the EPR measurements, samples were diluted 3-fold with a solution containing 0.1 M HEPES and 0.1M NaCl, to avoid EPR saturation, and placed in

0.75 mm i.d. quartz capillary tubes. EPR measurements were obtained at 77K in the X-band region with a Bruker EMX (Billerica, MA) at a microwave frequency of 9.165 GHz and power of 1.013 mW. The 100 kHz field modulation width was 1.0 gauss. Each measurement was the average of 3 scans.

#### **4.2.7 Recovery of octreotide and divalent cation from PLGA via two-phase extraction**

Millicylinders or PLGA particles, which were loaded or sorbed with octreotide and/or salt (see below), were dissolved in 1 mL methylene chloride and the octreotide and salt were extracted with 2 mL acetate buffer (0.1 M, pH 4.0) three times. Octreotide concentration was determined by HPLC. The encapsulation efficiency of octreotide or divalent cation was determined by dividing the actual loading of octreotide, determined by HPLC, or divalent cation, determined by ICP-OES, by their theoretical loading.

#### **4.2.8 Octreotide sorption studies**

Solutions of octreotide (0.2–3.0 mM, 1 mL) in HEPES buffer (0.1 M, pH 7.4) were added to PLGA particles (10 mg, as received) and incubated (37°C) on a rotary shaker (320 rpm) (IKA KS 130 basic). For sorption inhibition studies, chloride salts of divalent cations (1-50 mM) or NaCl (50 mM) were added to octreotide solutions prior to incubation. HEPES buffer was necessary to solubilize the divalent cations, which can precipitate with conventionally used phosphate buffer ions. The amount of octreotide sorbed was determined by the loss of octreotide from solution. Samples were removed from the incubator, centrifuged (2 min at 9.0 rcf) (Eppendorf 5415 D), and the supernatant was analyzed by HPLC. To validate this method of sorption quantification, an octreotide mass balance was performed at 1 and 24 hr during the sorption experiment by recovering the sorbed octreotide from the polymer

**Table 4.2** Octreotide recovery via two-phase extraction with time after incubation in pH 7.4 buffers at 37°C (unless otherwise noted). Initial octreotide concentration ~0.42 mM.

Time (hr)	Buffer				
	A <sup>ab</sup>	B <sup>b</sup>	C <sup>c</sup>	D <sup>d</sup>	E <sup>e</sup>
1	1.01	0.99	0.98	1.06	0.99
3	0.98	0.98	0.94	0.96	0.98
6	0.99	0.97	0.95	0.95	0.97
12	0.98	0.96	0.93	0.90	0.95
18	0.99	0.91	0.92	0.85	0.92
24	0.99	0.92	0.85	0.86	0.90

<sup>a</sup> 25°C

<sup>b</sup> 100 mM HEPES

<sup>c</sup> 10 mM HEPES

<sup>d</sup> 10 mM phosphate

<sup>e</sup> 100 mM phosphate

via two-phase extraction (Table 4.2). The total amount of octreotide recoverable at 1 and 24 hr was 99±1% and 92±1%, respectively. Therefore, during sorption studies, virtually all sorbed octreotide was non-covalently bound to PLGA, with the likelihood that a small fraction had become covalently bound to the polymer or otherwise decomposed.

#### 4.2.9 Preparation of PLGA millicylinders

Sieved octreotide acetate powder, or octreotide acetate and salt powder (sodium chloride, calcium chloride or manganese chloride, <90µm), both at 5% theoretical loading (see Table 4.3), were suspended in 62.5% (w/w) PLGA/acetone or PLGA/methylene chloride solution. In some instances, PLGA was purified as described below prior to preparation of millicylinders (Sections 4.2.10 and 4.2.11). The suspension was then loaded into a 3 ml syringe and extruded into a silicone rubber tubing (0.8 mm) by a syringe pump (Harvard Apparatus, Holliston, MA) at approximately 0.01 mL/min. The silicone tubing loaded with suspension was dried at room temperature for 24 h followed by further drying in a vacuum oven at 40°C for another 48 h.

**Table 4.3** Summary of encapsulation of octreotide and salt in PLGA millicylinder formulations.

<b>Formulation</b>	<b>Theoretical Salt Loading (wt%)</b>	<b>Actual Salt Loading (wt%)</b>	<b>Salt Encapsulation Efficiency (%)</b>	<b>Theoretical Octreotide Loading (wt%)</b>	<b>Actual Octreotide Loading (wt%)</b>	<b>Octreotide Encapsulation Efficiency (%)</b>
No Salt	—	—	—	5.07	3.1±0.2	61±3
NaCl	5.2	3.1±0.1	59.7±0.1	5.2	3.6±0.2	69±4
CaCl <sub>2</sub>	5.1	3.4±1.0	67.5±1.9	5.08	4.1±0.2	81±4
MnCl <sub>2</sub>	5.1	3.8±0.1	74.7±0.9	4.94	4.0±0.1	81±2

#### 4.2.10 Purification of PLGA by precipitation method

100 mg of PLGA 50:50 (Absorbable Polymers International, i.v.= 0.6 dl/g) solution dissolved in methylene chloride (2 mL) was poured gently into excess anhydrous ether with stirring. The precipitated PLGA was dissolved in methylene chloride and precipitated into ether again; this process was repeated 5–6 times. Finally, the purified PLGA was dried under vacuum.

#### 4.2.11 Purification of PLGA by two-phase extraction method

100 mg of PLGA 50:50 (Absorbable Polymers International, i.v.= 0.6 dl/g) was dissolved in methylene chloride (4 mL). Deionized water was added (8 mL) at 20°C, and the mixture was vortexed (20 s). Water phase was removed and fresh deionized water was added, the process was repeated 5–6 times, finally the PLGA methylene chloride solution was poured into excess anhydrous ether. The precipitated PLGA was then dried under vacuum.

#### **4.2.12 Octreotide release from PLGA millicylinders**

PLGA millicylinders (3-4 mg) loaded with octreotide acetate and no salt, NaCl, CaCl<sub>2</sub>, or MnCl<sub>2</sub> (Table 4.3) were incubated in 1 mL PBS + 0.02% Tween 80, pH 7.4 (PBST) at 37°C for various preset times. To determine the rate of acylation and release of encapsulated octreotide, the acylated fraction of peptide was measured in both the extract and in the release media. For assessment in the release media, at each time point, the release media was removed and replaced with fresh buffer, and the native and acylated octreotide content was measured by HPLC. For assessment by extraction, release media was similarly replaced, and peptide extraction was determined similarly as for peptide loading in Section 4.2.7.

### **4.3 Results and Discussion**

#### **4.3.1 Effect of divalent cations on nanoparticle zeta-potential**

PLGA nanoparticles were prepared to conveniently verify that divalent cations interact with the electric double layer of PLGA particles. The zeta-potential of the prepared particles was -75 mV, indicating a highly negative surface potential. The presence of some surfactant was necessary during the assessment of the effect of divalent cations on  $\zeta$  to prevent flocculation of particles, reducing the cation-free value of the zeta-potential to -11 mV as a result of the interaction of the surfactant at the particle surface. Nevertheless, the addition of low concentrations of MnCl<sub>2</sub>, CaCl<sub>2</sub>, and octreotide clearly shift  $\zeta$  to less negative values (Table 4.4) in a concentration dependent manner, indicating that the cations do interact with the electric double layer of PLGA nanoparticles.

**Table 4.4** Zeta-potential of PLGA 50:50 nanoparticles (diameter = 250 nm) in the absence and presence of divalent cations at 37°C in 20 mM HEPES buffer with 0.1% poly(vinyl alcohol), pH 7.4.

<b>Solution Additives</b>	<b><math>\zeta</math> (mV)</b>
none <sup>a</sup>	-74.5
none	-11.4
5 mM MnCl <sub>2</sub>	-0.537
5 mM CaCl <sub>2</sub>	-0.832
0.35 mM Octreotide	-4.87
0.88 mM Octreotide	-0.543
0.35 mM Octreotide + 5 mM MnCl <sub>2</sub>	-0.231

<sup>a</sup> no PVA, diameter = 212 nm

### 4.3.2 Kinetics of octreotide sorption to PLGA

Before further evaluating cation inhibition of octreotide acylation, the baseline kinetics of octreotide sorption was determined for an initial octreotide concentration of 0.8 mM (see Chapter 5 for more detailed kinetic studies). As shown in Figure 4.2, the sorption of octreotide to PLGA was rapid up to 6 h. Subsequently, the increase in sorption with time was attenuated occurring at a very low and roughly constant rate. Although sorption never entirely reached equilibrium, possibly due to the generation of carboxylates by polymer hydrolysis, the rapid initial sorption was complete by 24 h. For reference, the sorption kinetics of one of the potential inhibitory divalent cations, Ca<sup>2+</sup>, was found to follow a similar trend as that with octreotide (Figure 4.2), indicating the usefulness of the 24-hour time point to characterize the binding behavior of the potential peptide acylation inhibitors. Therefore, this time point was designated as time to pseudo-equilibrium.

### 4.3.3 Effect of divalent cations on octreotide sorption

To determine the effect of the physical properties of divalent cations on their ability to inhibit octreotide sorption, 24-hour sorption isotherms were obtained using various concen-

trations of different cations in HEPES buffer (0.1 M, pH 7.4). Octreotide sorption isotherms containing 0, 1, 15, and 50 mM MgCl<sub>2</sub> or CaCl<sub>2</sub> are shown in Figure 4.3. Langmuir-like behavior was observed in the absence of salt and only for 1 mM divalent salt concentration; for higher concentrations of divalent salt, the amount of sorbed peptide appeared to increase sigmoidally with equilibrium octreotide concentration. Ca<sup>2+</sup> was more effective at inhibiting sorption than Mg<sup>2+</sup> at all concentrations tested.

Next, the effect of chloride salts of other divalent (Sr<sup>2+</sup>, Ni<sup>2+</sup>, Mn<sup>2+</sup>) and monovalent (Na<sup>+</sup>) cations were investigated to determine if such cations could inhibit sorption more effectively than Ca<sup>2+</sup> (Figure 4.4). The octreotide adsorption was very strongly inhibited in the presence of Mn<sup>2+</sup>, and in the presence of 15 mM divalent cations, inhibition decreased in the order: Mn<sup>2+</sup> > Ni<sup>2+</sup> > Sr<sup>2+</sup>, Ca<sup>2+</sup> > Mg<sup>2+</sup>. When 50 mM NaCl was added to the HEPES buffer, the amount of octreotide sorbed decreased slightly compared to the salt-free octreotide isotherm (see Figure 4.3), but was greater than in the presence of 15 mM divalent chlorides. For example, the amount of sorption from an initial concentration of 2 mM octreotide was reduced from 70 μmol/gPLGA for 50 mM Na<sup>+</sup> to 66, 32, and 2 for 15 mM Mg<sup>2+</sup>, Ca<sup>2+</sup>, and Mn<sup>2+</sup>, respectively.

The reduction in the amount of octreotide sorbed upon the addition of salt suggests that ionic strength may play a role in the interaction of octreotide with PLGA at pH 7.4. The ionic strength of octreotide solutions in HEPES buffer without salts is 50 mM, while the addition of 15 mM divalent cation chloride salt or 50 mM NaCl increased the ionic strength to approximately 100 mM. However, the increased ionic strength cannot account for the decreased sorption of octreotide to PLGA in the presence of divalent cations relative to Na<sup>+</sup>.

The overall binding strength of an ion with its ligand results from the balance of the intrinsic binding affinity of complexation (exothermic) and differences in hydration resulting from the liberation of water upon binding (endothermic) [129, 130]. The intrinsic binding affinity of divalent cations may change in solution for cations susceptible to oxidation, such

as  $\text{Mn}^{2+}$ , which may react to form ions with increased positive charge [131]. Furthermore, hydrolysis of hydrated aquo-cations,  $\text{X}[\text{H}_2\text{O}]_n^{2+}$ , where X is a cation in solution, may result in the reduction of their positive charge, (e.g.  $\text{X}[\text{H}_2\text{O}]_{n-1}[\text{OH}]^+$ ) [132]. The order of effectiveness for the group II cations suggests that with increasing size, the higher hydration energy of  $\text{Ca}^{2+}$  may compensate for the loss of intrinsic binding affinity present at lower charge densities (e.g., as for  $\text{Mg}^{2+}$ ). Thus, the relatively poor inhibition of  $\text{Mg}^{2+}$  may be due to a higher ratio of bound cation to PLGA carboxylates at quasi-equilibrium for  $\text{Ca}^{2+}$  than for  $\text{Mg}^{2+}$ .

For transition metal cations, complexation with a ligand causes field splitting of the d orbitals, resulting in crystal field stabilization. In the high-spin (weak field) electron configuration,  $\text{Mn}^{2+}$  is not stabilized by crystal field splitting, whereas  $\text{Ni}^{2+}$  is stabilized [131]. Thus, one would expect  $\text{Ni}^{2+}$  to be a more effective inhibitor of octreotide adsorption if the crystal field stabilization energy were the most significant component affecting cation binding. One possibility for the increased effectiveness of  $\text{Mn}^{2+}$  is the difference in rate constant for the exchange of water, which is three orders of magnitude higher for  $\text{Mn}(\text{H}_2\text{O})^{2+}$  than  $\text{Ni}(\text{H}_2\text{O})^{2+}$  [132]. There also exists a potential for  $\text{Mn}^{2+}$  oxidation to  $\text{Mn}^{3+}$  or other oxidized manganese species. In support of this notion, the Pourbaix diagram for manganese shows that the stability of  $\text{Mn}^{2+}$  decreases with increasing pH and is unstable above pH 7.6 [131].

To test the stability of  $\text{Mn}^{2+}$  in the chloride salt solution containing octreotide acetate in the presence and absence of PLGA, the hyperfine splitting of  $\text{Mn}^{2+}$  was evaluated using EPR spectroscopy. The typical hyperfine splitting of  $\text{Mn}^{2+}$  was observed for all spectra. No significant difference in the peak shape or intensity of the EPR spectra was observed for the incubated samples in the absence or presence of PLGA, relative to the non-incubated control (Figure 4.5). Therefore, the inherent inhibitory potential of  $\text{Mn}^{2+}$  in the presence of octreotide in the 24-h sorption isotherms was unlikely caused by other oxidized Mn-species,



such as  $\text{Mn}^{3+}$ , which is EPR silent [133].

#### **4.3.4 Long-term interaction of octreotide with PLGA**

Long-term sorption studies were performed to determine the effect of 15 mM  $\text{CaCl}_2$  and  $\text{MnCl}_2$  on the sorption and acylation of octreotide (Figure 4.6). In the absence of salt, the onset of octreotide sorption occurred rapidly (1 day), followed by a continuous increase in the total amount of octreotide in solution after 3 days. Octreotide acylation products appeared at 3 days and continuously increased to 32% of total octreotide in solution by 21 days. In the presence of modest concentrations of  $\text{CaCl}_2$  or  $\text{MnCl}_2$ , the peak amount of sorption occurred later (14 days). Exhibiting a similar delay, octreotide acylation products did not appear until 7 days and increased to 14% of total octreotide in solution by 21 days in the presence of  $\text{CaCl}_2$ . While the onset of acylation was not delayed in the presence of  $\text{MnCl}_2$ , the amount of acylation at 21 days was 13%, similar to that found with  $\text{CaCl}_2$  and less than half that of the salt-free value. The similar effectiveness of  $\text{Ca}^{2+}$  and  $\text{Mn}^{2+}$  is consistent with our suggestion that several mechanisms may contribute to the inhibition of sorption by divalent cations. The oxidation of  $\text{Mn}^{2+}$  to form  $\text{MnO(s)}$  may contribute to the reduced effectiveness of  $\text{MnCl}_2$  in long-term studies. Solutions of  $\text{MnCl}_2$  in HEPES buffer displayed visible signs of a solid brown precipitate, typical of  $\text{MnO}$ , after 2–3 weeks at room temperature. Another possibility is that differences between the microclimate environment within the pores and the HEPES buffer solution altered the water-exchange rates or the pKa of hydrolysis of the aquo-cations. Nevertheless, these results strongly support the previously formed hypothesis that some type of sorption to PLGA is involved in the acylation mechanism [90], and that inhibiting adsorption is a useful strategy to minimize octreotide acylation.

**Table 4.5** Effect of PLGA composition and excipients on octreotide acylation during millicylinder production. Theoretical octreotide and excipient loading were both 5 wt%.

Excipient	Native Octreotide (%)
—	35±3
— <sup>a</sup>	66 (1)
— <sup>b</sup>	65 (1)
NaCl	43±3
CaCl <sub>2</sub>	86±1
MnCl <sub>2</sub>	77±1
CaCl <sub>2</sub> <sup>a</sup>	91 (1)
MnCl <sub>2</sub> <sup>a</sup>	77 (1)

<sup>a</sup> PLGA purified as described in Section 4.2.10.

<sup>b</sup> PLGA purified as described in Section 4.2.11.

### 4.3.5 Effect of salts on peptide acylation when encapsulated in PLGA

The microclimate pH within PLGA controlled-release depots has been reported to be acidic [86], protonating the carboxylate groups responsible for the peptide interaction and making them unavailable for sorption. However, the polymer carboxylates can form a salt with the peptide during drying. During release, the microclimate pH is often acidic but variable [134]. Furthermore, the monomer and oligomers of lactic and glycolic acid have pKa's that are very low (e.g., 3.1–3.6), so a significant fraction of carboxylates will be ionized within the common microclimate pH range (e.g., 2.5–5) [135].

To determine if the divalent cations could inhibit acylation of encapsulated peptide, PLGA millicylinders containing octreotide acetate and either no salt, NaCl, CaCl<sub>2</sub>, or MnCl<sub>2</sub> (Table 4.3) were prepared by a solvent extrusion method [44], except that methylene chloride was used in place of acetone as a carrier solvent. In control studies, where extrusion was performed with an end-capped polymer (PLGA 50:50, i.v.=0.6 dl/g) and acetone, we observed strong acylation of 5% loaded octreotide (65±3% acylation) following solvent extrusion. This acylation was strongly inhibited by 5% loaded divalent salts (e.g., CaCl<sub>2</sub>: 14±1% and MnCl<sub>2</sub>: 23±1% acylation) relative to 5% loaded NaCl control (57±3% acylation) (Table 4.5).

The cause of this acylation is unknown, but low molecular-weight impurities may play a role. To test this hypothesis, PLGA was purified either by precipitation into ether or two-phase extraction prior to octreotide encapsulation. The amount of native octreotide recovered from the millicylinders made using purified PLGA was double the amount recovered from unpurified PLGA (Table 4.5), strongly suggesting that water-soluble oligomers are involved in octreotide acylation within PLGA millicylinders. Both purification methods appeared to remove PLGA impurities with equal efficiency, but did not significantly increase the amount of native octreotide recovered from millicylinders loaded with  $\text{CaCl}_2$  or  $\text{MnCl}_2$ .

Following encapsulation with methylene chloride, no peptide acylation was observed although encapsulation efficiency of both peptide and encapsulated salts was slightly lower, i.e., ~60–80% (Table 4.3), than traditionally with acetone [44]. The resulting millicylinders with initially native octreotide were then incubated in PBST at  $37^\circ\text{C}$  for 28 days. As encapsulated salts may modulate porosity, osmotic pressure, water uptake, transport of soluble oligomers, and pH, and therefore peptide acylation rate in the PLGA-peptide system [118], the addition of NaCl was used as an additional control. For the peptide release study, we recorded the fraction of extractable peptide remaining in the polymer, as octreotide is known to be unstable at physiological pH [136]. To assess acylation kinetics, we resolved the acylated peptide fraction from the acylated fraction appearing in the polymer extract (Table 4.6), as well as the total peptide in the release media (assuming similar decomposition rates between acylated and native peptide species, Table 4.7). The total extractable octreotide remaining within the millicylinders decreased steadily to approximately 25% over the course of 4 weeks for all formulations. Relative to the no-salt and NaCl controls, the addition of the divalent chlorides of  $\text{Ca}^{2+}$  or  $\text{Mn}^{2+}$  reduced the fraction of acylated octreotide extractable from the millicylinders at 7 days by approximately 75% from 8% to under 2%. The amount of acylation within the millicylinders formulated with divalent chlorides remained lower than the no-salt and NaCl control at all time-points, although the benefit from the addition of divalent chlorides decreased with time, likely due to the release of the salts during incubation.

Future studies will focus on maximizing salt content, distribution, and retention to maintain the highest competitive advantage for the anionic binding sites on the polymer.

## 4.4 Conclusions

A new class of inhibitors of the sorption and acylation of a model peptide, octreotide acetate, has been described. At neutral pH, all cations studied inhibited octreotide sorption to PLGA. The inhibiting effect of the cations increased in the order:  $\text{Na}^+ < \text{Mg}^{2+} < \text{Ca}^{2+}$ ,  $\text{Sr}^{2+} < \text{Ni}^{2+} < \text{Mn}^{2+}$ . Long-term sorption studies in the presence of  $\text{CaCl}_2$  and  $\text{MnCl}_2$  indicated that disrupting peptide sorption to PLGA with the inorganic divalent cation inhibitors translates to inhibition of peptide acylation. Acylation of octreotide encapsulated in PLGA millicylinders containing equivalent weight ratio  $\text{CaCl}_2$  or  $\text{MnCl}_2$  relative to peptide was also inhibited relative to no salt or  $\text{NaCl}$  controls during encapsulation or release incubation. In a future report we will demonstrate the strong inhibition of octreotide acylation afforded by divalent cations both during release of octreotide from PLGA microspheres.

**Table 4.6** Long-term stability of octreotide extracted from PLGA millicylinders.

Formulation	Time (day)	Native (%)	Acylated (%)	Total (%)
No Salt	7	88.7±6	7.8±1	96.5±6
	14	76.6±1	10.2±1	86.8±2
	21	36.3±4	5.8±2	42.1±5
	28	18.5±4	2.5±1	21.0±5
NaCl	7	88.2±5	7.0±1	95.1±5
	14	53.5±11	7.9±2	61.4±13
	21	31.5±5	5.2±1	36.7±6
	28	20.8±2	5.3±1	26.1±3
CaCl <sub>2</sub>	7	76.4±6	1.5±1	77.9±6
	14	61.3±3	3.0±1	64.3±3
	21	31.3±2	2.1±1	33.3±2
	28	18.9±2	3.5±1	22.4±3
MnCl <sub>2</sub>	7	82.6±3	1.7±1	84.3±3
	14	55.4±2	2.8±1	58.2±3
	21	31.5±2	3.2±1	34.7±2
	28	16.3±4	3.8±1	20.1±4

**Table 4.7** Long-term release of native and acylated octreotide from PLGA millicylinders.

Formulation	Time (day)	Native (%)	Acylated (%)	Total (%)
No Salt	7	0.8±0	0	0.8±0
	14	4.6±0	0.8±0	5.6±0
	21	32.0±3	7.6±1	39.6±4
	28	42.7±6	14.7±3	57.4±9
NaCl	7	1.7±1	0	1.7±1
	14	16.8±8	3.1±1	19.9±7
	21	37.0±12	12.6±3	49.6±14
	28	43.8±9	19.2±2	63.0±10
CaCl <sub>2</sub>	7	8.8±1	0	8.8±1
	14	17.7±1	0.9±0	18.6±1
	21	38.8±1	4.2±0	43.0±1
	28	43.7±2	7.2±1	50.9±3
MnCl <sub>2</sub>	7	11.7±2	0	11.7±2
	14	23.8±2	1.7±0	25.5±2
	21	32.2±2	4.8±2	37.0±0
	28	39.6±2	11.2±2	50.8±1

## 4.5 Appendix

Initial investigations for inhibitors of peptide sorption included water-soluble divalent cation salts, organic acids, and other excipients. This Appendix briefly reviews these preliminary studies and presents data for polycations as an additional class of sorption inhibitors..

### 4.5.1 Preliminary investigation into the effect of excipients on octreotide sorption to PLGA

The effect of various excipients and pretreatments on octreotide adsorption to PLGA was quantified by comparing the amount adsorbed at a given equilibrium concentration to the amount adsorbed at that concentration predicted by the Langmuir model for sorption from 0.1M phosphate buffer, pH 7.4 (data not shown). Acids with  $pK_a$ s below PLGA oligomers, such as maleic ( $pK_a=1.9$ ), oxalic (1.3), or trifluoroacetic acid (-0.2), were chosen to study whether they could displace octreotide by disrupting ionic interactions between octreotide and PLGA oligomers. The addition these acids at various molar excesses resulted in an inhibition of the amount adsorbed by 1–21% compared to value predicted by the Langmuir model (Table 4.8). These values of inhibition are not significant relative to the error of the

**Table 4.8** Effect of sodium salts of weak acids, trifluoroacetic acid, and Polysorbate 80 on octreotide adsorption to PLGA 50:50 in 0.1M phosphate buffer, pH 7.4. Standard error of the means in parentheses (n=3).

Excipient	Molar Excess	Final Concentration ( $\mu\text{g/mL}$ )	Octreotide Sorbed ( $\mu\text{g}$ )	Predicted Octreotide Sorbed ( $\mu\text{g}$ )	Inhibition (%)
Maleic acid	3x	103.8 (2.7)	81.1	90.8	11
Oxalic acid	3x	102.3 (5.0)	79.3	89.6	11
TFA	1x	119.3 (1.5)	90.0	103.3	13
TFA	3x	117.2 (2.0)	81.8	101.6	19
TFA	10x	128.7 (1.3)	77.1	97.1	21
TFA	30x	105.5 (2.0)	91.6	92.2	1

Langmuir model (i.e., the error in predicting the same standards used to fit the isotherm).

#### **4.5.2 Polycations as inhibitors of octreotide sorption to PLGA**

Polycations are another class of octreotide sorption inhibitors to PLGA. As shown in Figure 4.7, octreotide sorption was reduced in the presence of 0.24 mg/mL poly(arginine) or >0.2 mg/mL poly(ethyleneimine) (PEI). At PEI concentrations greater than 1.0 mg/mL, octreotide sorption to PLGA is minimal. This concentration of PEI contains ~24 mM positively charged monomeric units, comparing well to the concentration of divalent cations necessary for similar sorption inhibition. Unfortunately, most polycations are not generally regarded as safe for use in humans [137, 138, 139, 140].

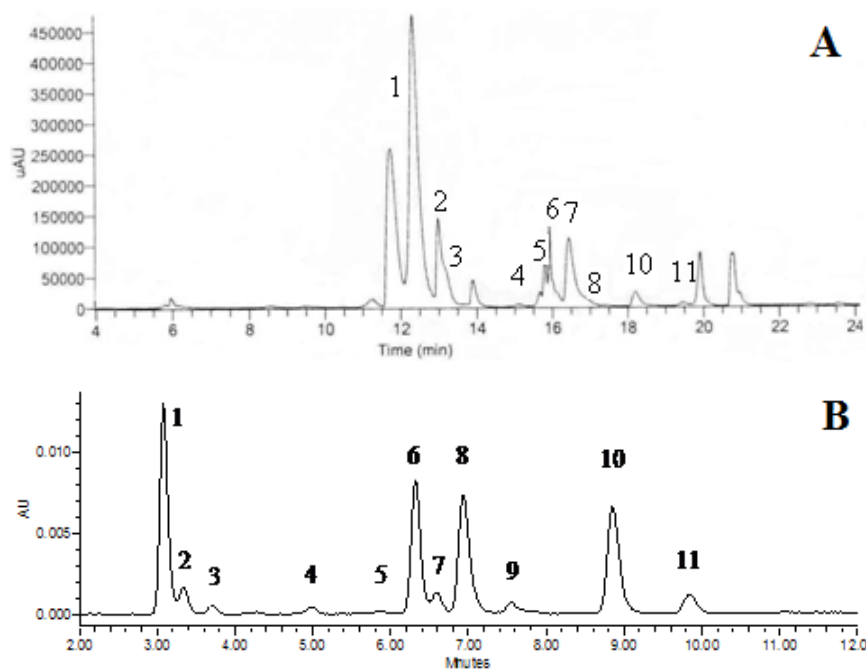


**Figure 4.1** (A) Sample chromatogram of reference sample of acylated octreotide products. (b) Sample chromatogram of acylated octreotide products in solution after 21 days incubation in the presence of PLGA 50:50 at 37°C.



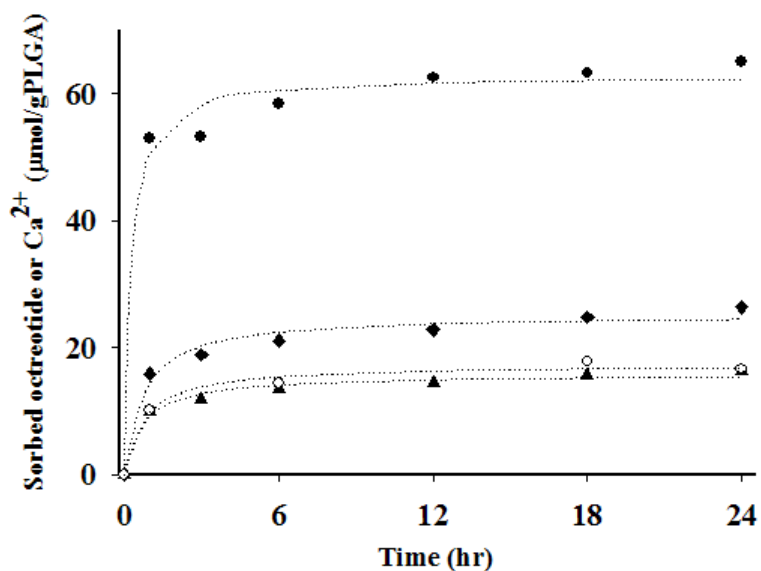


**Figure 4.2** Kinetics of octreotide acetate sorption to PLGA 50:50 in the presence of 15 mM CaCl<sub>2</sub> (◆), MnCl<sub>2</sub> (▲), no salt (●), and kinetics of Ca<sup>2+</sup> (○) sorption to PLGA during 24 h incubation in peptide-free 0.1M HEPES buffer solution, pH 7.4 at 37°C. PLGA was 10 mg in 1 mL of buffer solution. Initial octreotide and calcium chloride concentrations were 0.8 and 15 mM, respectively. Dotted trendlines shown for clarity.

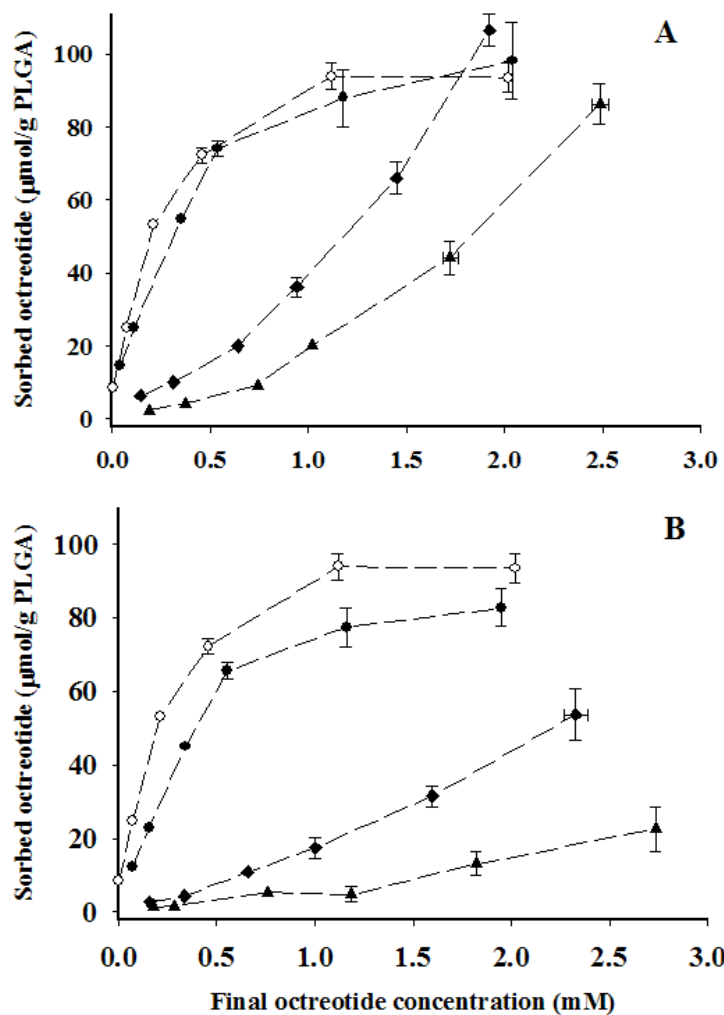


**Figure 4.3** Effect of (A) MgCl<sub>2</sub> and (B) CaCl<sub>2</sub> on octreotide acetate sorption to PLGA 50:50 at 0 (○), 1 (●), 15 (▲), and 50 (◆) mM salt concentrations after 24 hr incubation in 0.1M HEPES buffer solution, pH 7.4 at 37°C. PLGA was 10 mg in 1 mL of buffer solution.

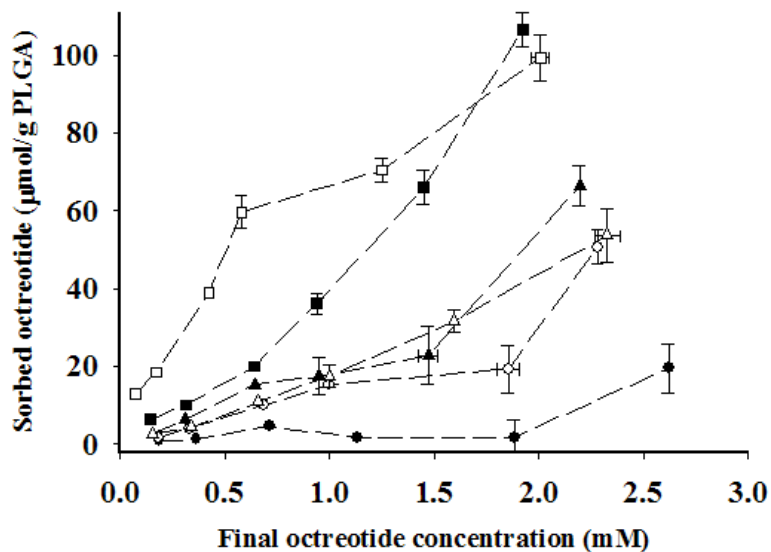


**Figure 4.4** Effect of 15 mM Mg<sup>2+</sup> (■), Ca<sup>2+</sup> (△), Sr<sup>2+</sup> (▲), Ni<sup>2+</sup> (○), and Mn<sup>2+</sup> (●) chloride and 50 mM NaCl (□) on octreotide sorption to PLGA 50:50 after 24 hr incubation in 0.1M HEPES buffer solution, pH 7.4 at 37°C. PLGA was 10 mg in 1 mL of buffer solution.

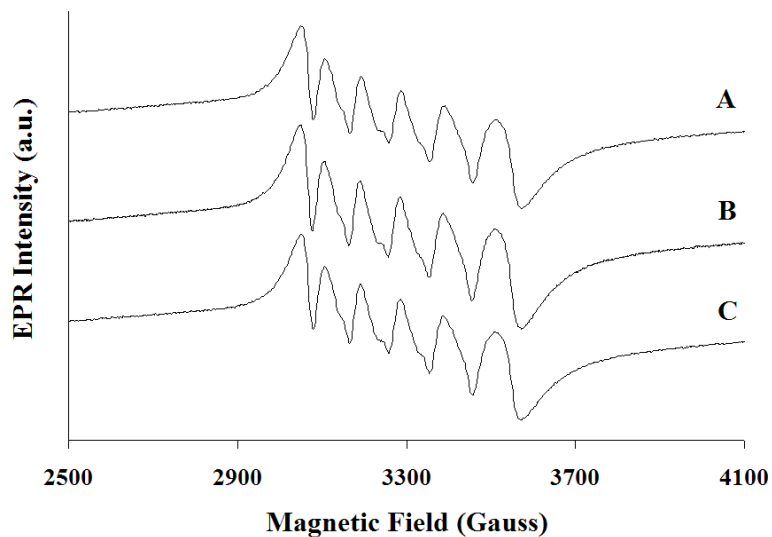


**Figure 4.5** EPR spectra of (A) unincubated MnCl<sub>2</sub>, (B) MnCl<sub>2</sub> and octreotide incubated without PLGA, and (C) MnCl<sub>2</sub> and octreotide incubated with PLGA.

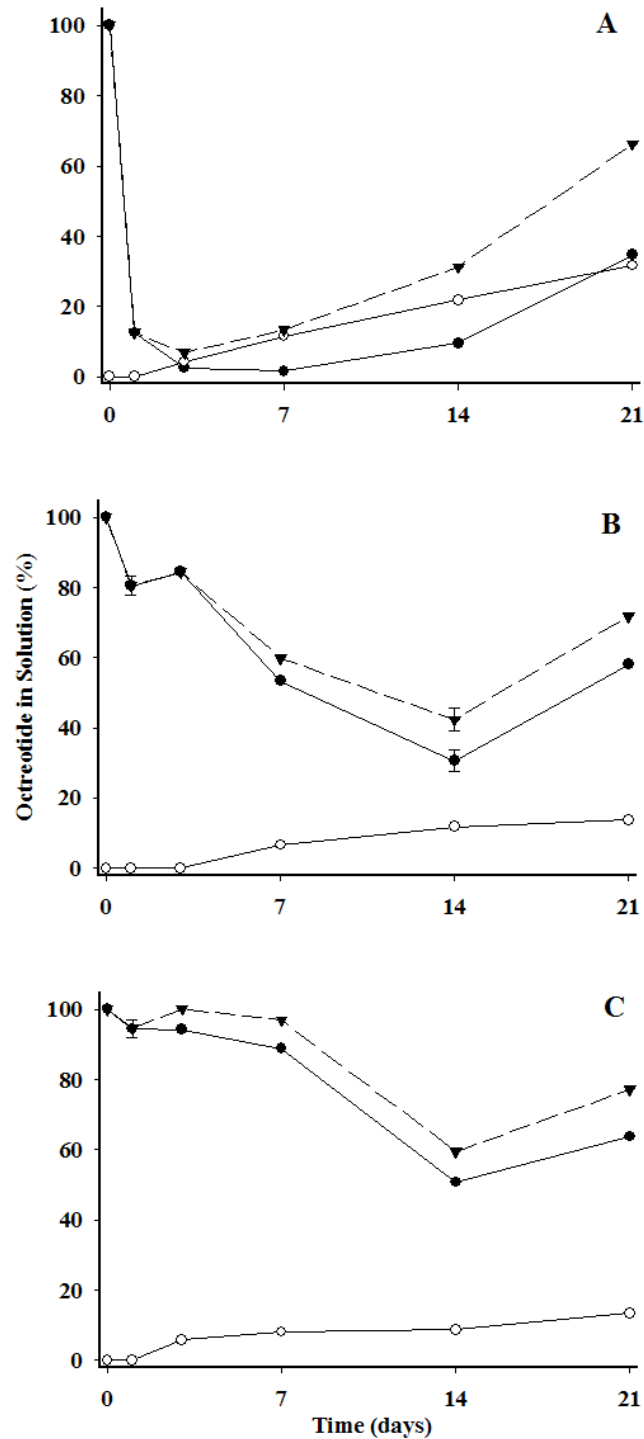


**Figure 4.6** Octreotide sorption and formation of acylated products, native (●), acylated (○), and total (▼) octreotide, during incubation of PLGA at 37°C in 0.1M HEPES buffer solution, pH 7.4 containing (A) no additional salt, (B) 15 mM CaCl<sub>2</sub>, and (C) 15 mM MnCl<sub>2</sub>. Initial octreotide concentration was 0.2 mM and PLGA was 10 mg in 1 mL of buffer solution.

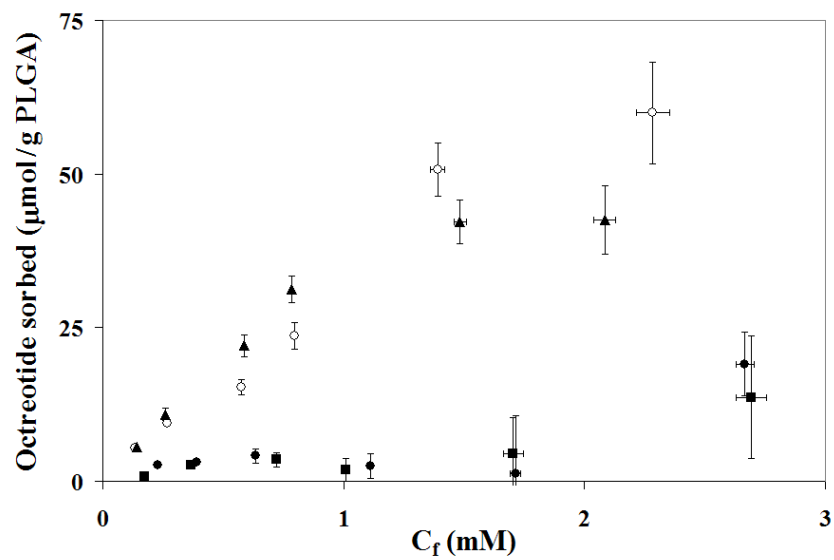


**Figure 4.7** Effect of 0.24 mg/mL poly(arginine) (▲) 0.2 (○), 1.0 (●), and 2.0 (■) mg/mL poly(ethyleneimine) on octreotide acetate sorption to PLGA 50:50 after 24 hr incubation in 0.1M HEPES buffer solution, pH 7.4 at 37°C. PLGA was 10 mg in 1 mL of buffer solution.

# Chapter 5

## Kinetics of Peptide Sorption to PLGA

### 5.1 Introduction

Due to the important role of peptide sorption to PLGA as the initial step on the acylation pathway, a detailed understanding of peptide sorption behavior is critical for the development of a rational formulation approach to minimize peptide acylation. The kinetics of peptide sorption is important to understand the mechanism of sorption and acylation with PLGA. Understanding peptide-polymer interactions is also useful because they can affect encapsulation into delivery systems and influence release behavior [89].

In this Chapter, we study the effect of initial concentration and ionic strength on the kinetics of peptide sorption to PLGA, compare the sorption kinetics of two model peptides, octreotide and leuprolide, which have different structures and conformational flexibility, and present a biexponential kinetic model that describes the sorption process well.

Understanding the mechanism and rate-limiting step of peptide sorption to PLGA is important to help identify potential strategies to inhibit sorption and acylation in PLGA. The sorption process is typically subdivided into the following steps:

1. diffusion of sorbate to the surface
2. interaction of sorbate with sorbing substance
3. structural rearrangements, if applicable
4. desorption from sorbing substance, if applicable
5. intraparticle diffusion, if applicable

The rate-limiting step of peptide sorption may be affected by solution properties, peptide concentration, the extent of surface coverage, or surface charge density, possibly resulting in a transition towards mass-transfer limited behavior.

Biexponential sorption kinetics have previously been observed for peptide sorption [141, 142], substrate binding [143], hydrogen-deuterium exchange in proteins [144, 145], and many other processes [146, 147, 148, 149]. The sorption of octreotide to PLGA was also found to follow biexponential kinetic behavior (see Figure 4.2):

$$P_{sorb}(t) = N_{fast}(1 - e^{-k_f t}) + N_{slow}(1 - e^{-k_s t}) \quad (5.1)$$

where  $P_{sorb}(t)$  is the amount of peptide sorbed,  $N_{fast}$  and  $N_{slow}$  are the population of peptide molecules sorbing under 'fast' and 'slow' kinetics ( $N_{fast} + N_{slow} = 185 \mu\text{mol/g}$  PLGA, the total number of PLGA acid end-groups for RG502H), and  $k_f$  and  $k_s$  are the apparent pseudo-first-order rate constants.

There is no common agreement in the literature concerning the meaning of the of the two rate constants for macromolecular binding/sorption interactions [150]. Three explanations for biexponential sorption kinetics have been discussed in the literature: surface site heterogeneity [150], conformational rearrangements [141, 142, 144, 151], and mass transport limitations [152, 153].

Surface heterogeneity may result from peptide binding to regions of the PLGA surface with different surface charge density or polymer functional groups at the interface (e.g. methyl side chains from lactic acid units). Furthermore, peptide binding to the PLGA surface may occur at different peptide orientations, or an equilibrium may exist between multiple peptide conformations, each with individual binding affinities. Evans et al. [154] noted that due to diverse interfacial features potentially available on a sorbing substance, binding peptides may reconform to recognize different surface features.

Conformational rearrangements upon adsorbing to surfaces, which are often observed for proteins [155, 156, 157, 158], have also been observed for peptides [141, 142, 159]. Furthermore, PLGA itself has been shown to rearrange upon changes in the hydrophobicity of the interface [160].

A detailed physical interpretation of the derived kinetic parameters is complicated and beyond the scope of this present work. The use of the biexponential model is not intended to imply that there are necessarily only two types of interactions (e.g. heterogeneous binding sites, multiple binding conformations, post-binding conformational reorientations, or a change in the rate-limiting step), but that the inclusion of a second exponential term acts to partially deconvolute the complex sorption behavior [161].

## **5.2 Materials and Methods**

### **5.2.1 Materials**

Octreotide acetate was obtained from Novartis (Basel, Switzerland). Leuprolide acetate (Lot No. 071002) was purchased from Shanghai Shinjn Modern Pharmaceutical Technology Co. (Shanghai, China). PLGA 50:50 (Resomer<sup>®</sup> RG502H) was purchased from Boehringer-Ingelheim GmbH (Ingelheim, Germany). (Hydroxyethyl)-piperazine-(ethanesulfonic acid) (HEPES) was purchased from Sigma-Aldrich Chemical Co. (St. Louis, MO). All other reagents used were of analytical grade or purer and purchased from commercial suppliers.

### **5.2.2 Investigation of octreotide sorption kinetics**

Solutions of octreotide (0.26–1.8 mM, 1 mL) or leuprolide (0.42 mM) in HEPES buffer (0.1 M, pH 7.4) were added to PLGA particles (10 mg, as received) and incubated (37°C) on a



rotary shaker (320 rpm) (IKA KS 130 basic). Samples were removed from the incubator at selected time-points, centrifuged (2 min at 9.0 rcf) (Eppendorf 5415 D), and the supernatant was analyzed by HPLC. The amount of octreotide sorbed was determined by the loss of octreotide from solution. Quantification of peptide sorption by the difference method was previously validated by mass balance after recovery of sorbed octreotide via two-phase extraction (Section 4.2.8).

### **5.2.3 Analysis of octreotide by HPLC**

The concentration of octreotide was determined by RP-HPLC, similarly as described by Murty, et al. [112]. Injection volumes of 20  $\mu\text{L}$  were loaded onto a Nova Pak C-18 column (3.9 x 150 mm, Waters) for RP-HPLC (Waters Alliance<sup>®</sup>) analysis using UV detection (280 nm). Solvent A was 0.1% TFA in acetonitrile and Solvent B was 0.1% TFA in water. A linear gradient of 25 to 35% A in 10 min, with a flowrate of 1.0 mL/min was used.

### **5.2.4 Model of peptide sorption to PLGA and estimation of kinetic parameters**

The parameters of the biexponential kinetic model (Equation 5.1) for peptide sorption to PLGA were obtained by non-linear regression to minimize the sum of the squared error between the amount of peptide sorbed determined experimentally and predicted by the model. The values of  $k_f$  and  $k_s$  were assumed to be independent of concentration and ionic strength. Although it is reasonable to presume that  $k_f$  and  $k_s$  could have a non-trivial dependence on ionic strength, it was assumed that the change in  $k_f$  and  $k_s$  with ionic strength was small relative to other contributions to the observed kinetics.

**Table 5.1** Parameters of biexponential kinetic model for data shown in 5.1(a), at various initial concentrations of octreotide.  $k_f = 1.38 \text{ hr}^{-1}$ ;  $k_s = 3.10 \times 10^{-3} \text{ hr}^{-1}$ .

Octreotide Initial Concentration (mM)	$N_{fast}$ ( $\mu\text{mol/gPLGA}$ )	$N_{slow}$ ( $\mu\text{mol/gPLGA}$ )	$N_{fast}$ (%)
0.26	8	177	4
0.39	13	172	7
0.54	22	163	12
0.87	42	143	23
1.80	93	92	50

## 5.3 Results and Discussion

### 5.3.1 Effect of Octreotide Concentration on Octreotide Sorption Kinetics

The kinetics of octreotide sorption to PLGA as a function of concentration is shown in Figure 5.1. As the initial concentration of octreotide increases, the initial rate of sorption increases, while the slope of the constant phase decreases (see Fig. 5.1(b)), suggesting a shift in the kinetic mechanism or rate-limiting step at higher concentrations.

Octreotide sorption to PLGA was well described by a biexponential model (Equation 5.1). Table 5.1 summarizes the fitted parameters for various initial concentrations of octreotide in the linear region of the octreotide sorption isotherm. A relationship between concentration and the model parameters is obvious, although we have not collected sufficient kinetic data (e.g. at high concentrations) to discern this relationship. The potential shift in the mechanism or rate-limiting step of octreotide sorption at various initial concentrations is shown quantitatively as the 'fast' component of the observed kinetics shifting towards the predominant pathway at higher initial concentrations of octreotide.

**Table 5.2** Parameters of biexponential kinetic model fit for data shown in Figure 5.2, with ionic strength modulated by buffer concentration and type. Initial octreotide concentration was 0.4 mM.  $k_f = 1.15 \text{ hr}^{-1}$ ;  $k_s = 2.56 \times 10^{-3} \text{ hr}^{-1}$ .

Buffer, Concentration (mM)	Ionic Strength (mM)	$N_{fast}$ ( $\mu\text{mol/gPLGA}$ )	$N_{slow}$ ( $\mu\text{mol/gPLGA}$ )	$N_{fast}$ (%)
HEPES, 10	5	31	154	17
Phosphate, 10	24	29	156	16
HEPES, 100	50	10	175	5
Phosphate, 100	237	7	178	4

### 5.3.2 Effect of Ionic Strength on Octreotide Sorption Kinetics

Having found that the amount of octreotide sorbed from solutions of constant ionic strength is independent of the concentration of HEPES buffer, and low concentrations of phosphate (see Section 3.2), the ionic strength of octreotide solutions was adjusted by varying the buffer type and concentrations. This allowed for the investigation of ionic strength without the addition of varying amounts of sodium cations to adjust ionic strength, which could act as weak inhibitors of octreotide sorption to PLGA (see Figure 4.4), although a later study found that the amount of octreotide sorbed from solutions of constant ionic strength is independent of the concentration of sodium, HEPES buffer, and low concentrations of phosphate (Figure 5.3)— at high phosphate concentrations, octreotide is unstable (see Section 3.2).

As the ionic strength was reduced from 237  $\rightarrow$  24 mM, the amount of octreotide sorbed increased substantially (Figure 5.2, model parameters in Table 5.2), in support of the concept of electrostatic interaction between octreotide and the PLGA carboxylates play a crucial role in the initial sorption mechanism. No significant difference in the amount of octreotide sorbed was observed at an ionic strength  $<24$  mM, possibly resulting from the convergence of the activity coefficient towards the value of 1.

**Table 5.3** Parameters of biexponential kinetic model fit for peptides sorbed to PLGA from solutions of 0.4 mM (A) octreotide in 0.1 M HEPES, pH 7.4 at 25°C (data shown in Fig. 5.5), (B) leuprolide in 0.1 M HEPES, pH 7.4 at 37°C (data shown in Fig. 5.4), and (C) octreotide in 0.1 M HEPES, pH 7.4 at 37°C (fit singularly for comparison).

Series	$N_{fast}$ ( $\mu\text{mol/gPLGA}$ )	$N_{slow}$ ( $\mu\text{mol/gPLGA}$ )	$N_{fast}$ (%)	$k_f$ ( $\text{hr}^{-1}$ )	$k_s$ ( $\text{hr}^{-1}$ )
A	3	182	1	0.74	$8.70 \times 10^{-4}$
B	21	164	12	2.65	$1.48 \times 10^{-3}$
C	14	171	8	1.15	$2.95 \times 10^{-3}$

### 5.3.3 Comparison of Leuprolide and Octreotide Sorption Kinetics

Peptide structural effects on acylation are not currently well understood [94], but may be due in part to their effect on sorption to PLGA. We compared the sorption kinetics of two model peptides, octreotide and leuprolide, which have different structures, net charge, and conformational flexibility. As shown in Figure 5.4 (also see Table 5.3), the initial rate of leuprolide sorption was substantially faster than for octreotide, increasing with a reduced slope at longer times, behaving in a less biexponential manner than octreotide. This suggests that one or more of the limiting steps in the octreotide sorption mechanism that are deconvoluted by the biexponential model occur at a faster rate for leuprolide.

Kang and Schwendeman [162] measured the diffusion coefficient of bodipy dye in an end-capped low molecular-weight PLGA 50:50. They found the diffusion coefficient to be  $\sim 1 \times 10^{-11}$   $\text{cm}^2/\text{s}$  at 37°C. The water uptake of free-acid RG502H should substantially increased relative to the more hydrophobic end-capped PLGA used in the Kang and Schwendeman study, possibly increasing diffusivity of octreotide, relative to bodipy, by a factor 10-100, a value high enough to potentially allow for kinetic control of the sorption process.

Assuming that the sorption of either peptide is not mass-transfer limited in the well-mixed conditions of the sorption experiment or in the polymer phase, if partitioning occurs, differences in the observed kinetics would likely be due to structural effects.

While we cannot ascertain how structural effects or flexibility play a role in the different sorption kinetics of octreotide and leuprolide, Peelle et al. [163] has shown that increased flexibility improved peptide affinity to II-VI semiconductors by mitigating the effects of down-regulating amino acids that decreased adsorption affinity upon restructuring conformationally post-binding. Conversely, affinity may be improved in conformationally restricted peptides that retain up-regulating amino acids at spatially proximal distances.

Furthermore, based on peptide adsorption kinetics obtained using SPR, Seker et al. [141] provide evidence that molecular features, such as a loop constraint, can exert significant influence on peptide adsorption onto surfaces. The fact that linear-PTSTGQA peptide exhibited biexponential adsorption behavior, while cyclic-CPTSTGQAC adsorption was described by a single exponential, suggests that the adsorption process for the linear form may involve an additional event or step that does not occur in the cyclic-CPTSTGQAC adsorption process. They suggested this additional step may involve peptide conformational rearrangement or repositioning of the linear peptide on the surface that occurs after the initial peptide binding event. However, the exact nature of the proposed mechanism is unclear and inconsistent— in a subsequent review by the same authors [154], they presented the same graph with the peptide assignments flip-flopped and stated that the cyclic peptide, rather than the linear one, displayed the biexponential kinetics because it required an additional folding step that was inaccessible to the linear one.

### **5.3.4 Temperature Dependence of Octreotide Sorption**

Octreotide sorption to PLGA was significantly temperature dependent (Figure 5.5). Reducing the temperature below the hydrated  $T_g$  ( $\sim 30^\circ\text{C}$ ), from  $37 \rightarrow 25^\circ\text{C}$ , dramatically attenuated the rate and extent of sorption (Table 5.3), while no octreotide sorption was observed at  $4^\circ\text{C}$ . Several factors could contribute to the temperature effect on octreotide sorption, including its effect on hydrophobic interactions [164], hydration of the polymer

[40], polymer mobility, and diffusivity of species within the polymer phase. For example, Kang and Schwendeman [162] found that the diffusion coefficient of bodipy dye in an end-capped PLGA 50:50 of similar molecular weight as RG502H varied over 3 orders of magnitude from 22 → 45°C, a temperature range spanning the hydrated glass-transition temperature [40], and was too slow to measure at 4°C.

## 5.4 Conclusions

The kinetic profiles of peptide sorption to PLGA were investigated at various solution conditions. The rate and extent of sorption is reduced at low octreotide concentrations, high solution ionic strength and low temperature, becoming completely attenuated at 4°C, suggesting polymer mobility plays a critical role in the sorption interaction. Leuprolide sorbs to PLGA at a greater rate and extent than octreotide, possibly due to structural differences, although mass-transfer limitations may also contribute. A biexponential model described the sorption profiles extremely well, and a relationship between concentration and the model parameters is obvious, although kinetic data at high concentrations will be required in order to discern this relationship.

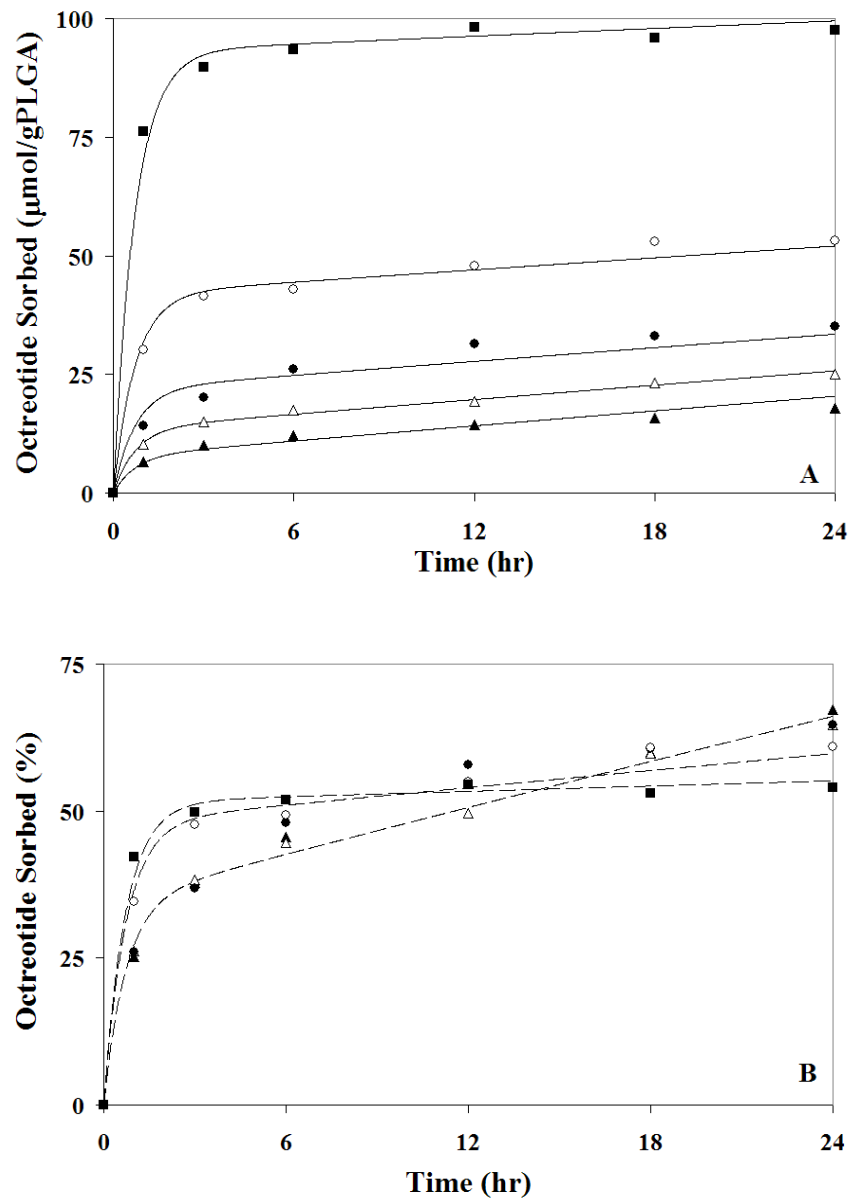


**Figure 5.1** (A) Kinetics of octreotide sorption to PLGA 50:50 from solutions of 0.26 (▲), 0.39 (△), 0.54 (●), 0.87 (○), 1.80 (■) mM octreotide in 0.1 M HEPES, pH 7.4 at 37°C and fits to biexponential model (solid lines). (B) Normalized kinetic data (same symbols). Model fits for 0.26 and 0.54 mM omitted for clarity.

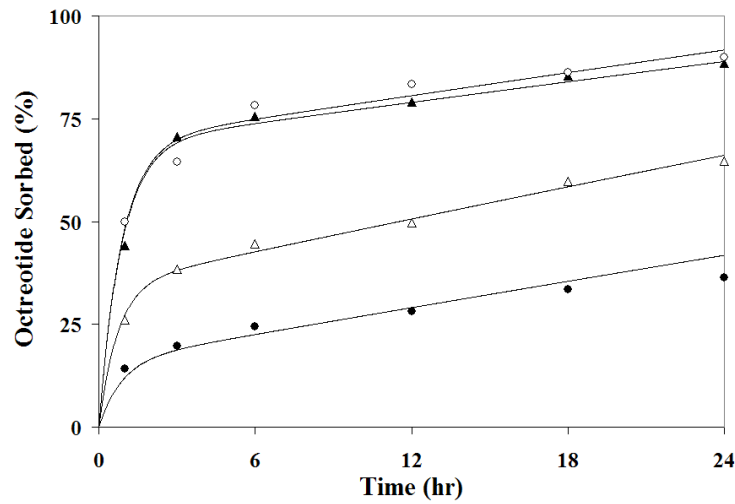


**Figure 5.2** Effect of ionic strength on octreotide sorption kinetics to PLGA 50:50 (Boehringer-Ingelheim RG502H) at 37°C in solutions of pH 7.4. The ionic strength was adjusted using buffer type and concentration: 10mM HEPES buffer (I = 4 mM, ▲), 10 mM phosphate buffer (23 mM, ○), 0.1M HEPES buffer (49 mM, △), 0.1 M phosphate buffer (236 mM, ●). Initial octreotide concentration was 0.4 mM.

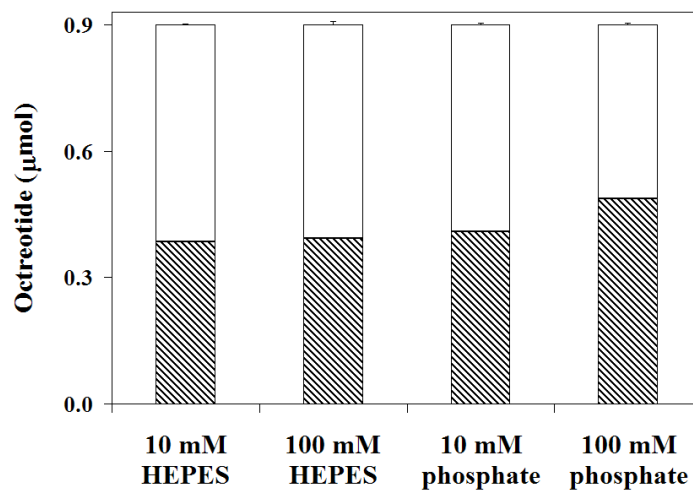


**Figure 5.3** Effect of buffer type and concentration (pH 7.4) on octreotide sorption to 10 mg PLGA 50:50 (Boehringer-Ingelheim RG502H) from 300 mM ionic strength solutions (adjusted by NaCl) at 37°C. Amount sorbed: shaded area; amount remaining in solution: white area.



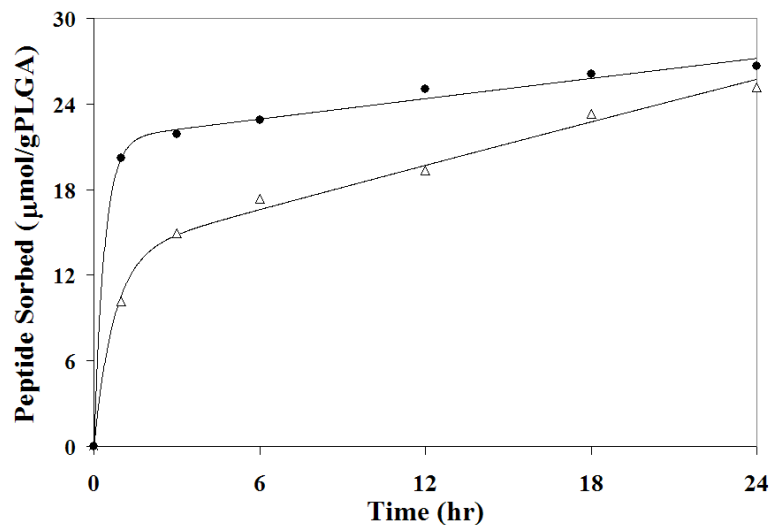


**Figure 5.4** Comparison of leuprolide (●) and octreotide (△) sorption to PLGA 50:50 (Boehringer-Ingelheim RG502H) at 37°C in solutions of 0.1 M HEPES buffer, pH 7.4. Initial peptide concentration was 0.4 mM.

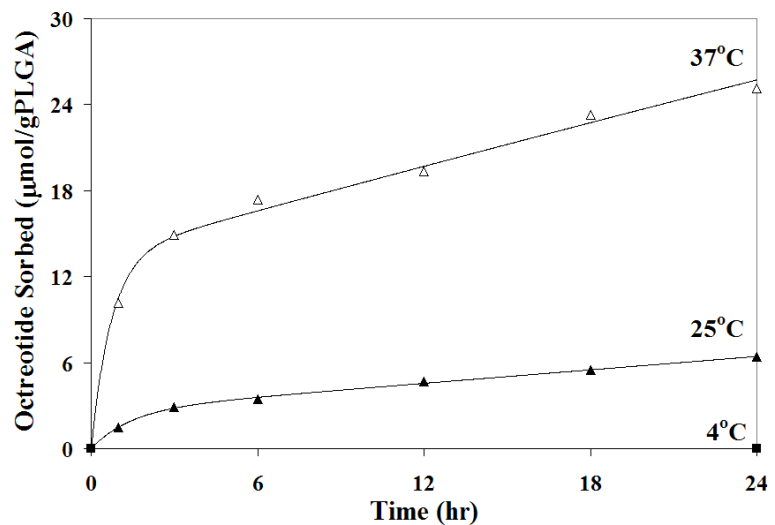


**Figure 5.5** Effect of temperature on octreotide sorption to PLGA 50:50 (Boehringer-Ingelheim RG502H) in solutions of 0.1 M HEPES buffer, pH 7.4. Initial octreotide concentration was 0.4 mM.

# Chapter 6

## Sorption Behavior of Peptides to PLGA

### 6.1 Introduction

Due to the important role of peptide sorption to PLGA as the initial step on the acylation pathway, a detailed understanding of peptide sorption behavior is important for the development of a rational formulation approach to minimize peptide acylation. Understanding peptide-polymer interactions is also useful because they can affect encapsulation into delivery systems and influence release behavior [89].

Although there are multiple reports of peptide adsorption to surfaces [141, 142, 165, 166], detailed studies of the sorption of peptides to PLGA have been limited. For example, Tsai et al. [167, 168] investigated in detail the effect of physical factors and solution properties on the adsorption kinetics and isotherms of salmon calcitonin, the 8-22 amino acid portion of salmon calcitonin (CT15), triptorelin, and vapreotide to end-capped RG503 (see Table 3.1 for characteristics of RG503). Calcitonin is a 32-amino acid hormone that may sorb similarly to proteins due to its larger molecular weight and secondary structure. Triptorelin is a gonadotropin-releasing hormone agonist and vapreotide is somatostatin analogue, similar in structure to leuprolide and octreotide, respectively—peptides used in this study. The authors selected two peptides, CT15 and vapreotide, that did not sorb to RG503. They also reported limited solubilities for both vapreotide and triptorelin. As a result, only data for calcitonin and triptorelin at low concentrations was reported. The authors presumed

the sorption was multilayer based on geometric calculations, and presented hypothetical schemes of peptide aggregating prior to sorption or peptide aggregation induced by sorption. The absence of CT15 sorption suggests that physical instabilities may play a role in the adsorption of calcitonin, although it is also possible that the deleted sequences specifically interact with PLGA. The selection of poorly soluble small peptides, which are unstable in solution, limit the applicability of their conclusions to more soluble peptides such as leuprolide or octreotide.

In this study, the first detailed investigation into the sorption of water-soluble low molecular weight peptides to free-acid PLGA, we obtain sorption isotherms across a broad range of peptide concentration at various pH and assess the reversibility of sorption at various solution conditions, with the goal of gaining insight into the factors and forces influencing the type and extent of sorption.

## **6.2 Materials and Methods**

### **6.2.1 Materials**

Octreotide acetate was obtained from Novartis (Basel, Switzerland). Leuprolide acetate (Lot No. 071002) was purchased from Shanghai Shnjin Modern Pharmaceutical Technology Co. (Shanghai, China). PLGA 50:50 (Resomer<sup>®</sup> RG502H, RG503H, and RG504H) was purchased from Boehringer-Ingelheim GmbH (Ingelheim, Germany). (Hydroxyethyl)-piperazine-(ethanesulfonic acid) (HEPES), calcium chloride (CaCl<sub>2</sub>), and trifluoroacetic acid (TFA) were purchased from Sigma-Aldrich Chemical Co. (St. Louis, MO). Diethylpiperazine (DEPP) was purchased from Acros Organics (Geel, Belgium). All other reagents used were of analytical grade or purer and purchased from commercial suppliers.

## 6.2.2 Analysis of octreotide by HPLC

The concentration of octreotide, was determined by RP-HPLC, similarly as described by Murty, et al. [112]. Injection volumes of 20  $\mu$ L were loaded onto a Nova Pak C-18 column (3.9 x 150 mm, Waters) for RP-HPLC (Waters Alliance<sup>®</sup>) analysis using UV detection (280 nm). Solvent A was 0.1% TFA in acetonitrile and Solvent B was 0.1% TFA in water. A linear gradient of 25 to 35% A in 10 min, with a flowrate of 1.0 mL/min was used.

## 6.2.3 Octreotide sorption studies

For desorption studies, solutions of 1 mM octreotide (1 mL for particles, 4 mL for film) in 0.1 M HEPES buffer, pH 7.4 were added to PLGA particles (10 mg, as received) or a PLGA film prepared according to D conditions (see Table 3.2 for more information) and incubated (37°C) on a rotary shaker (320 rpm) (IKA KS 130 basic). HEPES buffer was necessary to solubilize the calcium used in the desorption study and the divalent cations used for inhibition studies (see Section 6.2.4, and Chapter 4, respectively), which can precipitate with conventionally used phosphate buffer ions. For 24-hr sorption isotherms, peptide solutions with initial concentration of 0.2–4.0 mM in 0.1 M HEPES buffer, pH 7.4, 0.1 M MES buffer, pH 5.5, or 0.05 M DEPP buffer, pH 4.0 were used. Samples were removed from the incubator, centrifuged (2 min at 9.0 rcf) (Eppendorf 5415 D), and the supernatant was analyzed by HPLC. The amount of peptide sorbed was determined by the loss of peptide from solution for particles, and by two-phase extraction of sorbed peptide for films.

## 6.2.4 Desorption of octreotide from PLGA 50:50

Samples prepared as described above were gently centrifuged and the supernatant was removed; the amount initially sorbed was  $\sim$ 650 nmol for RG 502H particles,  $\sim$ 360 nmol

for RG503H particles, and ~300 nmol for RG 502H films. After removal of the supernatant and rinsing with deionized water twice, desorption solutions containing 50 vol% methanol (MeOH) in water, 0.1 M diethylpiperazine (DEPP, pH 4.0), 2 M CaCl<sub>2</sub> in 0.1 M HEPES (pH 7.4), 1 mg/mL PEI in 0.1 M acetate buffer, pH 4.0, 0.1% TFA in 0.1 M HEPES, pH 7.0, 5% SDS, or only 0.1 M HEPES, pH 7.4 were separately added to the residual PLGA and incubated for 24 hr at 37°C. Additionally, samples containing 0.1 M HEPES, pH 7.4 desorption buffer were incubated for 24 hr at 4°C. All samples except the 5% SDS were then removed from the incubator, centrifuged, and the supernatant analyzed by HPLC. Because SDS interferes with the RP-HPLC analysis, desorption was assessed by recovering sorbed octreotide by two-phase extraction after rinsing with deionized water three times to remove excess SDS. Octreotide was found to be stable after 24 hr incubation at 37°C in all solutions.

### **6.2.5 Two-phase extraction of octreotide sorbed to PLGA 50:50**

PLGA particles, sorbed with octreotide, were dissolved in 1 mL methylene chloride and the octreotide was extracted with 2 mL acetate buffer (0.1 M, pH 4.0) three times. Octreotide concentration was determined by HPLC.

## **6.3 Results and Discussion**

### **6.3.1 Investigation of peptide sorption mechanism to PLGA from 24-hr isotherms.**

To determine the characteristics of peptide sorption to PLGA, such as the stoichiometry, binding affinity, and maximal amount of peptide sorbed, 24-hour sorption isotherms were obtained for two model peptides, octreotide and leuprolide (Figure 6.1). No true equilibrium is typically reached for peptide sorption to PLGA, as several complicating dynamic phenomena

occur upon incubation in aqueous solution, such as polymer hydration/swelling/plasticization, rearrangement, hydrolysis, peptide acylation, and the release of soluble monomers and oligomers. See below for possible exceptions. The net effect of these phenomena is to alter the microenvironment of the polymer phase (e.g. water activity, free-volume between polymer chains, dielectric constant, and diffusivity) and the total number of acid end-groups with time, possibly affecting the surface potential and surface-to-bulk exchange of acid end-groups. For these reasons, we chose a time (24 hours) where a pseudo-equilibrium has been achieved (see Section 4.3.2).

The sorption of both peptides to PLGA were similar and behaved in a Langmuir-like manner, increasing in a linear manner at low concentrations and transitioning to a saturation point where the amount sorbed does not increase with additional increases in peptide concentration. Octreotide sorption appears to have a slightly higher affinity to PLGA than leuprolide, while leuprolide sorbs to a marginally greater extent at high concentrations.

It has previously been suggested that the presence of free carboxylates are a prerequisite for octreotide sorption to PLGA [90]. This suggestion was validated by obtaining octreotide sorption isotherms at neutral and acidic pH near the  $pK_a$  of the PLGA carboxylic acids ( $\sim 3.5$ ), shown in Figure 6.2. Lowering the pH from 7.4  $\rightarrow$  4.0 substantially inhibits octreotide sorption, suggesting that the presence of ionized carboxylates is a necessary prerequisite to octreotide sorption. However, it is also possible that pH may affect sorption through its effect on the charge or solubility of the peptide or peptide-oligomer complexes. Note that octreotide becomes completely dicationic (i.e. 1000:1 mole ratio of dication:monocation) by pH 4.8.

The effect of the number of acid end-groups on octreotide sorption to PLGA was also studied using a series of PLGA with varying molecular weights (see Table 3.1 for polymer properties, including  $M_n$ ), as shown in Figure 6.3. Sorption to RG 503H also followed Langmuir-like behavior, while sorption to the higher molecular-weight RG 504H polymer

was minimal. As shown in Table 3.1, the total number of acid end-groups is reduced by 50% from RG 502H → RG 503H, and another 50% from RG 503H → RG 504H. Interestingly, the maximum amount of octreotide sorbed from the isotherms also appears to be reduced by 50% from RG 502H → RG 503H, although this is not the case for RG504H. It is possible that above a certain molecular-weight, the PLGA microenvironment is substantially less amenable to octreotide sorption, perhaps due insufficient polymer mobility, the reduction in the diffusivity of oligomers, or differences in other factors mentioned above. For example, reduced uptake and subsequent plasticization by water would lead to a higher hydrated  $T_g$  relative to lower molecular-weight PLGA (recall that the dry  $T_g$  increases by 2–4°C from RG503H to RG504H, see Table 3.1). The trend of the sorption isotherms for RG502H and RG503H in Figure 6.3 suggests that maximum sorption to PLGA may be governed by the total number of acid end-groups in the polymer, while the unexpectedly low sorption for RG504H appears consistent with microenvironmental factors such as polymer mobility also playing an important role under certain circumstances.

### 6.3.2 Quantification of the maximal amount of peptide sorbed using a modified Langmuir model

To further investigate the stoichiometry of peptide sorption to PLGA, the maximal amount of peptide sorbed,  $\Gamma_{max}$ , was estimated from the 24-hour sorption isotherms for octreotide and leuprolide (Figure 5) by fitting the sorption data to the modified Langmuir equation by non-linear regression (see Table 6.1):

$$\Gamma = \Gamma_0 + \frac{\Gamma_1 K C_f}{(1 + K C_f)} \quad (6.1)$$

where  $C_f$  is the final concentration of peptide in solution,  $\Gamma$  is the amount of peptide sorbed,  $\Gamma_0$  and  $\Gamma_1$  are model parameters related to the amount of peptide sorbed,  $\Gamma_{max} = \Gamma_0 + \Gamma_1$ , and  $K$  is the 'binding affinity' in the classical sense described by Langmuir. The Langmuir

**Table 6.1** Langmuir model fitted parameters and estimated fraction of acids occupied at maximal sorption, calculated using Equation 6.1.

Peptide	Polymer	K (mM <sup>-1</sup> )	$\Gamma_0$ ( $\mu\text{mol/g}$ PLGA)	$\Gamma_{max}^a$ ( $\mu\text{mol/g}$ PLGA)	Total Acids ( $\mu\text{mol/g}$ PLGA)	Fraction of Acids Occupied <sup>b</sup>
Leuprolide	RG 502H	0.77	1.5	229	185	1.24
Octreotide	RG 502H	1.6	8.5	163	185	0.88
Octreotide	RG 503H	1.2	2.9	81	94	0.86
Octreotide	RG 504H	n.d.	n.d.	$\sim 6^c$	53	n.d.

<sup>a</sup>  $\Gamma_{max} = \Gamma_0 + \Gamma_1$

<sup>b</sup> Fraction of Acids Occupied =  $\Gamma_{max} / \text{Total Acids}$

<sup>c</sup>  $\Gamma_{max}$  estimated visually from isotherm

model requires that the adsorption process be reversible. Although Figures 6.1 and 6.3 show typical reversible adsorption isotherms, most of octreotide sorption is irreversible at the conditions tested (see Section 6.3.3, below). Such a tendency is often observed in the sorption of peptides and proteins onto surfaces [165, 169], although the mechanism for this remains unclear [170]. Therefore, the parameter  $K$  in Equation 6.1 does not imply the adsorption affinity as defined in the original Langmuir equation. Nevertheless, it is common to use Langmuir-type experiments to compare the binding of peptides and proteins to surfaces and to estimate maximal surface coverage, regardless of the reversibility of the process [165, 169].

As quantified in Table 6.1, the  $\Gamma_{max}$  values for leuprolide and octreotide sorption to RG502H, and octreotide sorption to RG503H appear to be approximately equal to the total acid-content of the polymers (185  $\mu\text{mol/g}$  for RG502H and 94  $\mu\text{mol/g}$  for RG503H), suggesting that in these polymers the peptides sorb until a 1:1 stoichiometry is attained.

The amount of acid end-groups was increased by pre-hydrolyzing the PLGA and decreased by incubating the PLGA in PBST buffer to release soluble monomers and oligomers. The net change in the number of accessible PLGA end-groups is related to the amount generated by polymer hydrolysis and lost by release of monomer and small oligomer impu-



rities. Pre-incubating PLGA particles in PBST for 24 hr at 37°C prior to octreotide sorption resulted in an inhibition of the amount adsorbed by 49% relative to the amount predicted by the Langmuir model, strongly suggesting that the number of accessible ionized end-groups is decreased by pre-incubation with, and removal of, the PBST pre-incubation buffer. It is likely that the acid content and possibly the zeta-potential of the particles was reduced after pre-incubation via the release of monomers and soluble oligomers or PLGA.

The number of acidic end-groups in the PLGA was increased by pre-degrading the PLGA in water for 24 hr at 60°C. When the degraded PLGA was incubated with octreotide solution, the amount adsorbed increased by 64% relative to the amount predicted by the Langmuir model, suggesting that the amount adsorbed correlates with the number of acidic end-groups. These results are consistent with the hypothesis that the extent of adsorption is primarily due to the total number of acid end-groups in the polymer.

While we have not measured the zeta-potential of the polymer particles due to their large size ( $>1 \mu\text{m}$ ), the surface potential of PLGA particles is likely on the order of -70–80 mV, based on zeta-potential measurements of PLGA nanoparticles and films. For the former,  $\zeta = -75 \text{ mV}$  in 20 mM HEPES, pH 7.4 (Table 4.4) and for the latter,  $\zeta = -70 \text{ mV}$  in 1 mM KCl, pH 7.5 (see Section 3.1.2). Assuming the particles have a zeta-potential near the values for nanoparticles and films, the density of charges on the surface calculated using Equation 7.1 (see Section 7.3.2 below) is  $65 \text{ nmol/m}^2$ , corresponding to  $0.3 \mu\text{mol/g}$ , or 0.16% of the total acids at the surface, based on a total surface area of  $4.6 \text{ m}^2/\text{g}$  obtained from BET isotherms (Section 3.1.1).

Furthermore, the surface area available for sorption of one molecule of octreotide at maximal sorption was calculated to be  $4.7 \text{ \AA}^2$ . Based on a study of proteins at interfaces [171], it has been estimated that an average amino acid occupies  $\sim 15 \text{ \AA}^2$  area on the surface [167]. Given that it is highly unlikely that all of the acid end-groups are at the surface or that peptide can adsorb at such high density, this result indicates that octreotide either

forms a multilayer, precipitates with soluble oligomers, or partitions into the polymer phase. Assuming no partitioning into the polymer, and that octreotide occupies a space equivalent to the area of 4 average amino acids ( $\sim 60 \text{ \AA}^2$ ), monolayer coverage of octreotide would require  $12.7 \mu\text{mol/g}$  PLGA and a multilayer of  $\sim 13$  layers would form at maximal octreotide sorption to RG502H ( $163 \mu\text{mol/g}$  PLGA).

At this point, some indirect evidence suggests that following the initial adsorption, octreotide may partition into the polymer phase: the 1:1 sorption stoichiometry of both octreotide and leuprolide to RG502H and RG503H, and the curiously low sorption to high molecular-weight RG504H. As previously mentioned, it is likely that RG504H, having a  $M_n \sim 5x$  greater than RG502H, is less mobile than RG502H or RG503H, possibly due its increased dry  $T_g$  and reduced plasticization [40] resulting from decreased water uptake or other factors affecting partitioning of octreotide into the polymer phase. While it is also possible that octreotide forms multilayers on PLGA, if this were the case, the Langmuir-like saturation of octreotide and leuprolide at values similar to the total number of acid end-groups, would be a rather fortuitous result. Yet another possibility is that sorption requires PLGA release of acid oligomers which would combine with the peptide to adsorb, precipitate, and/or partition into the polymer phase. The physical state and localization of sorbed octreotide is investigated further in subsequent chapters.

### **6.3.3 Effect of solution conditions on desorption of octreotide from PLGA**

Desorption studies were initially performed to investigate the appropriateness of an analysis of peptide sorption using the Langmuir assumptions and later to investigate the nature of the irreversibility. Various desorption solutions were chosen to selectively disrupt a variety of molecular interactions. The high ionic strength and  $[\text{Ca}^{2+}]$  in the 2M  $\text{CaCl}_2$  + HEPES solution was intended to disrupt ionic interactions existing between octreotide and PLGA on

the surface and compete for PLGA carboxylates, respectively. Similarly, trifluoroacetic acid (TFA) was selected to potentially compete with PLGA carboxylates for octreotide amino groups because it is more acidic than PLGA carboxylic acids, having a  $pK_a = 0.2$  versus  $\sim 3.5$  for PLGA. The acidic pH obtained using the Goods buffer diethylpiperazine (DEPP) or acetate buffer (0.1 M, pH 4.0) should protonate some surface carboxylates, releasing surface-bound ion-pairs, assuming that disrupting the ionic interaction is sufficient to desorb octreotide. Desorption was also attempted at 4°C because sorption was inhibited at this temperature. None of these conditions tested led to substantial octreotide desorption, both in absolute value (5% desorption) or relative to HEPES buffer control (Figure 6.4).

Poly(ethyleneimine) in 0.1 M acetate buffer, pH 4.0 resulted in the greatest extent of desorption (15%) of the aqueous solutions tested, a 3-fold increase over the HEPES buffer control (5%). Desorption of octreotide from PLGA in the presence of this solution may have been enhanced simultaneously by a combination of several factors: protonation of PLGA carboxylates, diffusion of acetic acid into the polymer phase, with concomitant plasticization of the PLGA, increased ionic strength, competition for PLGA carboxylates by PEI, and hydrophobic contacts between PEI and PLGA. The incomplete desorption of octreotide from PLGA, despite of the large number of potentially disruptive interactions, suggest these factors do not dominate the irreversibility of sorption. However, the addition of 5% SDS or organic solvent (50 vol% methanol in water) led to the desorption of  $65 \pm 3\%$  and  $55 \pm 5\%$  of the originally sorbed octreotide, respectively, strongly suggesting the predominate interaction leading to irreversibility of sorption are hydrophobic contacts between octreotide and PLGA. It is unclear whether methanol or SDS only act to desorb surface associated octreotide, or whether they interact with octreotide that could potentially be dissolved in the bulk polymer phase. Methanol can permeate into PLGA, plasticize and swell the polymer, and potentially increase the solubility of the ion-pair in solution or the diffusivity of the ion-pair within the bulk. It is also possible that the bulk polymer phase has sufficient dielectric and permeability to support partitioning of the SDS into the PLGA.

Octreotide sorption to the higher molecular weight RG503H polymer (see Table 3.1) was also mostly irreversible. The amount of octreotide sorbed to RG503H is  $\sim 1/2$  of the amount sorbed to RG502H (Figure 6.3 and Table 6.1), while the absolute amount of desorption from both (33 nmol) was the same.

## 6.4 Conclusions

Octreotide desorption from PLGA was found to be no greater than 15% for various aqueous solution conditions tested. Only the addition of 50 wt% methanol resulted in a substantial desorption from PLGA, indicating the irreversibility was due to hydrophobic interactions or hydrogen-bonding between the peptide and PLGA or low mass-transfer rates of absorbed peptide-PLGA ion-pairs between bulk and the surface of the polymer. Although kinetically irreversible, octreotide (and leuprolide) sorption follow Langmuir-like behavior. Sorption of octreotide decreased as the pH of the solutions tested was decreased towards the  $pK_a$  of PLGA carboxylates. Reducing the number of total acid end-groups by increasing the PLGA molecular weight also decreased octreotide sorption. These results indicate the critical role of ionized PLGA acid end-groups during the peptide sorption pathway. Quantification of the maximal amount of peptide sorbed at high solution concentration from a modified Langmuir equation show that this number is similar to the total number of PLGA acid end-groups for RG502H and RG503H, suggesting the possibility of peptide partitioning into the polymer phase. The low amount of sorption to the higher molecular-weight RG504H is also consistent with peptide partitioning into the polymer, as the decreased polymer mobility with increasing molecular weight eventually prevents peptide partitioning. Future studies will investigate this possibility in greater detail.

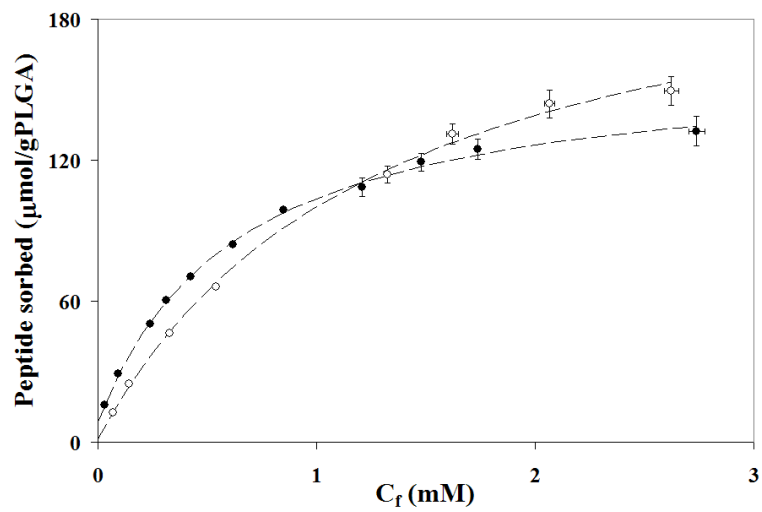


**Figure 6.1** 24-hour sorption isotherms of leuprolide (○) and octreotide (●) on PLGA 50:50 (Boehringer-Ingelheim RG 502H) in 0.1 M HEPES buffer, pH 7.4 at 37°C.

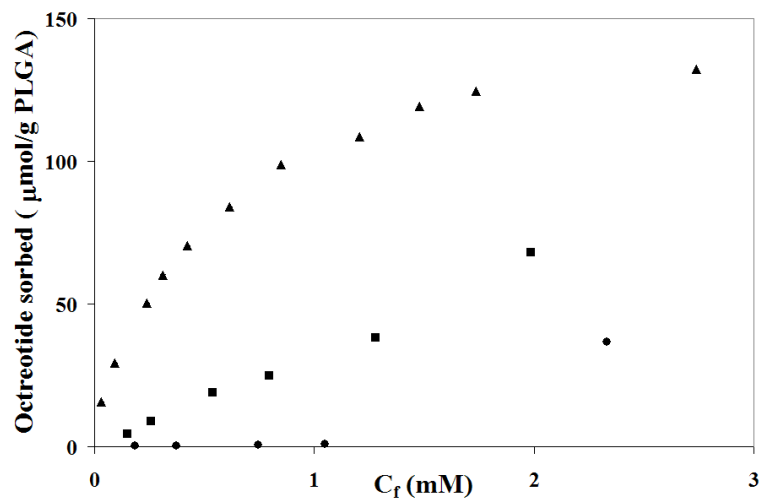


**Figure 6.2** Effect of pH on octreotide sorption to PLGA 50:50 (Boehringer-Ingelheim RG502H) in solutions of 0.1 M HEPES buffer, pH 7.4 (▲), 0.1 M MES buffer, pH 5.5 (■), and 0.05 M DEPP buffer, pH 4.0 (●) after 24 hours incubation at 37°C.

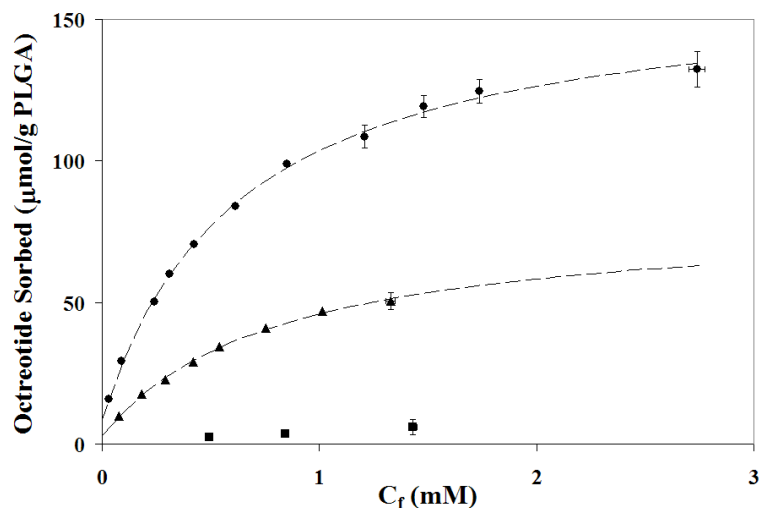


**Figure 6.3** Effect of PLGA 50:50 molecular weight on 24-hr octreotide sorption isotherms at 37°C from solutions of 0.1 M HEPES buffer, pH 7.4. Boehringer-Ingelheim Resomer<sup>®</sup> (●) RG 502H, (▲) RG 503H, and (■) RG 504H.

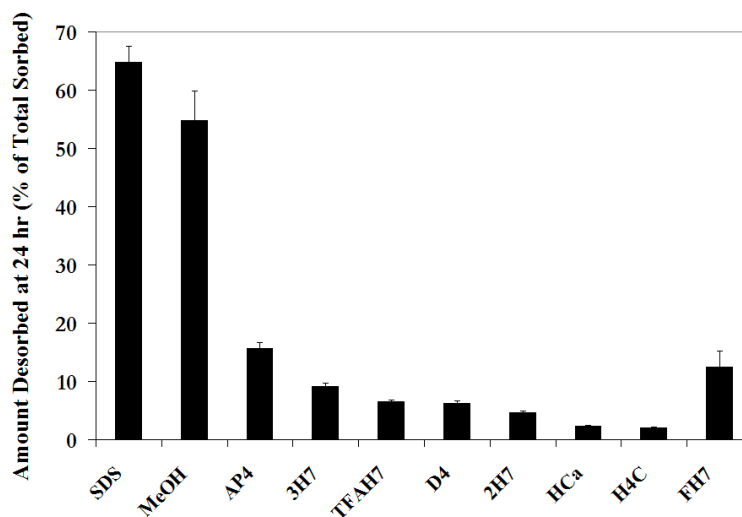


**Figure 6.4** Desorption of octreotide from PLGA 50:50 particles and films (FH7) after 24 hr incubation at 37°C with 1 mM octreotide acetate in 0.1 M HEPES buffer, pH 7.4 (~650 nmol octreotide sorbed to RG502H particles (10 mg), ~360 nmol to RG503H particles (10 mg), and ~300 nmol to RG502H Film D (30 mg)). Desorption solutions: 5 wt% SDS in water (**SDS**); 50 vol% methanol in water (**MeOH**); 1 mg/mL PEI in 0.1 M acetate buffer, pH 4.0 (**AP4**); 0.1 M HEPES, pH 7.4 (**3H7**); 0.1% TFA in 0.1 M HEPES, pH 7.0 (**TFAH7**); 0.1 M DEPP, pH 4.0 (**D4**); 0.1 M HEPES, pH 7.4 (**2H7**: particles and **FH7**: films); 2 M CaCl<sub>2</sub> in HEPES (**HCa**); 0.1 M HEPES, pH 7.4 (**H4C**). All desorptions were at 37°C, except H4C, which was at 4°C. PLGA RG502H was used in all cases, except 3H7, which used RG503H. SDS desorption was assessed by recovering sorbed octreotide via two-phase extraction.

# Chapter 7

## Octreotide Localization Upon Sorption to PLGA

### 7.1 Introduction

It has previously been suggested that the presence of free carboxylates are a prerequisite for octreotide sorption to PLGA [90]. Previous studies have shown that both octreotide and leuprolide sorption to RG502H follows Langmuir-like behavior and saturates at values near the number of total acid end-groups of the polymer (163  $\mu\text{mol/g}$  PLGA). This was also observed for octreotide sorption to RG503H, but not for RG504H. It is likely that RG504H, having a  $M_w$   $\sim 5$  times greater than RG502H, is less mobile than RG502H or RG503H, due its increased dry  $T_g$  and reduced plasticization [40] resulting from decreased water uptake. Furthermore, sorption to PLGA was shown to be significantly temperature dependent, with no sorption observed at 4°C (Section 5.3). These results are consistent with peptide absorption into the bulk of the polymer or the requirement of oligomer release.

Assuming no partitioning into the polymer, and that octreotide occupies a space equivalent to the area of 4 average amino acids ( $\sim 60\text{\AA}^2$ ) (Section 5.3), monolayer coverage of octreotide on PLGA particles would require 12.7  $\mu\text{mol/g}$  PLGA and a multilayer of  $\sim 13$  layers would form at maximal octreotide sorption. Thus, the location of octreotide sorbed to PLGA must either be exclusively within a multilayer, as a solid precipitate (for PLGA particles), or partially absorbed within the bulk of the polymer. The specific aim of this

Chapter is to build on previous data suggesting peptide partitioning into the polymer and to rigorously test this hypothesis.

In lieu of traditional methods used to study multilayer formation, such as in-situ ellipsometry, atomic force microscopy, or quartz crystal microgravimetry, which can be complicated by polymer water uptake, swelling, hydrolysis, and rearranging, and may not resolve whether peptides were present in the polymer phase, we chose to investigate the possibility of octreotide partitioning into PLGA by attempting to physically localize the peptide in the polymer phase. In this Chapter, this is done by investigating the solubility of sorbed octreotide in organic solvent, study the effect of film thickness on peptide sorption, recover peptide from sectioned films, and perform x-ray photoelectron spectroscopy (XPS) surface analysis on PLGA films.

## **7.2 Materials and methods**

### **7.2.1 Materials**

Octreotide acetate was obtained from Novartis (Basel, Switzerland). PLGA 50:50 (Resomer<sup>®</sup> RG502H) was purchased from Boehringer-Ingelheim GmbH (Ingelheim, Germany). *d*<sub>3</sub>-Acetonitrile and *d*<sub>6</sub>-dimethylsulfoxide were obtained from Cambridge Isotope Laboratories (Andover, MA). All other reagents used were of analytical grade or purer and purchased from commercial suppliers.

### **7.2.2 PLGA film preparation and characterization**

PLGA film preparation and characterization by SEM was described in detail in Section 3.1.2. Briefly, PLGA in acetone solutions were placed on glass (for film thickness study) or



gold coated glass substrate (for XPS analysis) and spread using a spin coater (SCS G3-8, Indianapolis, IN). See Table 3.2 for the conditions used to spin-coat PLGA solutions onto glass microscope cover-slides. Following spin-coating, nascent PLGA films were dried for 48 hr at room temperature and pressure followed by 24 hr in a vacuum oven at 40°C.

### **7.2.3 Analysis of octreotide solution concentration by HPLC**

The concentration of octreotide was determined by HPLC, by loading solutions (20  $\mu$ L) onto a Nova Pak C-18 column (3.9 x 150 mm, Waters) for RP-HPLC (Waters Alliance<sup>®</sup>) analysis using UV for detection (280 nm). Solvent A: 0.1% TFA in acetonitrile; Solvent B: 0.1% TFA in water; Linear gradient: 25 to 35% A in 10 min.

### **7.2.4 Sorption of octreotide to PLGA films**

Solutions of octreotide (1 mM, 4.5 mL) in HEPES buffer (0.1M, pH 7.4) were added to PLGA films of varying thicknesses (2, 7, 13, 24, and 40  $\mu$ m) with constant surface area (see Section 3.1.2 for detailed description of manufacturing method) placed in a Petri-dish with tight-fit lid (Beckton-Dickinson, Franklin Lakes, NJ) and incubated at 25 and 37°C for 24 hr. After incubation, the amount of octreotide sorbed was determined by recovering sorbed octreotide via two-phase extraction. PLGA films were first broken and placed within a 15 mL polypropylene centrifuge tube prior to extraction. The films were then dissolved by adding methylene chloride (1 mL) and using 50 mM acetate buffer, pH 4.0 (2 mL), followed by a second extraction with acetate buffer containing 1 M NaCl, which was useful to minimize saponification. The extracts were pooled and analyzed by HPLC as described in Section 7.2.3.

### **7.2.5 $^1\text{H}$ Nuclear magnetic resonance of sorbed octreotide**

Solutions of 1 mM octreotide (1 mL) in HEPES buffer were added to PLGA particles, as received (10 mg), and incubated at 37°C on a rotary shaker (320 rpm). After sorption, samples were removed from the incubator, centrifuged, the supernatant was removed, and the PLGA was rinsed with deionized water. PLGA-octreotide was freeze-dried, dissolved in  $\text{d}_3$ -acetonitrile (1 mL, Cambridge Isotope Laboratories, Andover, MA), and filtered (Millipore Millex<sup>®</sup>-FG PTFE syringe filter, 0.2  $\mu\text{m}$  pore diameter) prior to NMR analysis (Bruker Avance DRX500). As controls, PLGA and octreotide were dissolved individually in  $\text{d}_6$ -dimethylsulfoxide.

### **7.2.6 Sectioning and analysis of PLGA films sorbed with octreotide**

PLGA films were cast onto specially prepared plastic cylinders (8 x 13 mm) for microtoming. To achieve even sectioning of the PLGA films, a 2 x 2 mm circular groove was cut out from the 8mm diameter face to leave a 4 mm diameter face. The PLGA film was cast by placing 4  $\mu\text{L}$  of a 22% PLGA in acetone solution on the 4 mm diameter face of the plastic cylinder. The films were then dried at room temperature for 24 h, then for another 24-48 h in a vacuum oven at 40°C. Cylinders with PLGA films were then immersed into 2 mL of 0.5 mM octreotide acetate in 0.1 M HEPES, pH 7.4 and incubated for 24 h at 37°C. After incubation, the films were removed from the octreotide solution, rinsed, and dried for 24-48 h in a vacuum oven at 40°C. The dried films were then sectioned using a Reichert Ultracut-E ultramicrotome (Vienna, Austria). The films were viewed through the microscope on the Ultracut-E and appear to have a very rough morphology as well as some curvature. The thickness of the film was estimated to be  $\sim 80 \mu\text{m}$  by slicing through the entire film in 0.5  $\mu\text{m}$  increments. Two groups of 5-7 films were cut to a depth of  $\sim 20 \mu\text{m}$  and  $\sim 40 \mu\text{m}$ . Each group sectioned films, as well as a non-sectioned control, were then carefully dissolved

together in 1 mL methylene chloride and extracted similarly as described in Section 4.2.7 prior to HPLC analysis with detection at 215 nm.

### **7.2.7 Surface analysis by x-ray photoelectron spectroscopy**

XPS analysis of PLGA films on gold-coated glass cover-slides was performed using a Kratos AXIS spectrometer in constant analyser energy transmission mode. Gold-coating was performed as a safeguard against detection of elements in the glass substrate or to indicate the presence of film defects. The source employed was monochromated Al K $\alpha$  radiation (1486.6 eV) with a photoelectron take-off angle of 90° to the surface, operated at 10 mA emission current and 15 kV anode potential. A low-energy electron flood gun was employed for charge neutralisation. High resolution scans of the C 1s and O 1s core levels were obtained with a pass energy of 20 eV. Atomic compositions were calculated based on atomic sensitivity factors obtained from Reference [172]. Data analysis was performed using Casa XPS version 2.3.14.

## **7.3 Results and Discussion**

### **7.3.1 <sup>1</sup>H-NMR of octreotide-PLGA ion-pair dissolved in *d*<sub>3</sub>-acetonitrile**

The presence of sorbed octreotide in acetonitrile was assessed by <sup>1</sup>H-NMR in order to test the hypothesis that the octreotide-PLGA ion-pair would have enhanced solubility in low-dielectric solvents, a condition that would appear to be required for partitioning into the bulk of the polymer phase. The characteristic proton shifts at 6.7–7.5 ppm attributable to protons on the aromatic side chains of octreotide [173] present in the octreotide control sample also appear in the test sample containing PLGA incubated with octreotide in acetonitrile (Figure 7.1). As free octreotide acetate is not soluble in acetonitrile, the presence of the characteris-

tic octreotide proton shifts in the test sample indicate that octreotide is solubilized by the formation of a PLGA-octreotide ion-pair, confirming the hypothesis that upon ion-pairing with PLGA, the solubility of octreotide increases in low dielectric solvent.

### 7.3.2 Peptide sorption to PLGA films

The localization of sorbed octreotide, whether adsorbed as multilayer or absorbed within the bulk of the polymer, was investigated using PLGA films with constant surface area (12.6 cm<sup>2</sup>) of varying mass and thickness (2, 7, 13, 24, 40  $\mu\text{m}$ ). The amount of octreotide and leuprolide sorbed to PLGA films at 37°C increased linearly with the amount of PLGA added (e.g. film thickness) with an approximate slope of 9.7 nmol/mg PLGA (Figure 7.4). Negligible octreotide sorption was observed at 22°C, a temperature likely below the glass-transition temperature of the hydrated PLGA film, suggesting that the mobility of the polymer is likely necessary for octreotide sorption to PLGA. Interestingly, sorption at 30°C showed biphasic behavior, increasing linearly for thin films and plateauing for thicker films, suggesting this temperature is near the  $T_g$ , although thickness-dependent surface compositional effects could potentially play a role [160]. At temperatures near the glass-transition temperature, the reduced polymer mobility could limit peptide sorption by either prohibiting the release of oligomers or decreasing the diffusivity of both the polymer and peptide-polymer adduct in the polymer phase.

The effect of film thickness on octreotide sorption could potentially be a result of differences in release of acid oligomers, different chemical composition of the surface layer, film thickness total surface area (e.g. due to roughness), or differences in the surface-potential.

Using ATR-FTIR spectroscopy, Thanki et al. [160] found that in PLGA films, thicker films (46  $\mu\text{m}$ ) contained a larger number of methyl side chains from the lactic acid units at the polymer/air surface than thinner films (< 2  $\mu\text{m}$ ) and the population of methyl side groups

on the film surface decreased with decreasing the film thickness. The reduced number of methyl groups on the surface for thin films was attributed to the decreased availability of bulk polymer that can provide methyl groups to the surface.

Thanki et al. [160] also found, based on contact angle relaxation measurements, that 15  $\mu\text{m}$ -thick films with relatively higher number of hydrophobic groups on the surface, relative to 1  $\mu\text{m}$ -thick films, rapidly undergo restructuring as their surface comes into contact with water, with the methyl side chains orientating away from the interface. This was not observed for thin films, indicating that potential for conformational rearrangement in PLGA is thickness-dependent. Although it is possible that thickness effects could play a role in differences in the surface composition between the thinnest films studied and the thicker ones, this effect is unlikely to be significant at the 13, 24, and 40  $\mu\text{m}$  thicknesses. Furthermore, the extremely linear relationship at 37°C between the amount of octreotide sorbed and film thickness over the entire range of thicknesses studied strongly suggests that surface compositional effects were insignificant.

The morphology of hydrated PLGA films in the absence of octreotide was generally smooth (Figure 7.2(a)). The addition of octreotide resulted in the formation of circular areas of rough morphology (Figure 7.2(b)), increasing in diameter and density with increasing film thickness. It could be possible that the increased sorption with increasing film thickness could result from the increased total surface area of the hydrated PLGA. We estimate that  $\sim 35$  nmol octreotide would form monolayer coverage on the 4 cm diameter films ( $2.8$  nmol/cm<sup>2</sup>), based on an analysis similar to the one performed in Section 6.3.2. The estimated value of 35 nmol octreotide per monolayer corresponds to 12 monomer thicknesses for Film E, the thickest film studied, which sorbed 418 nmol octreotide. Assuming a multilayer 20 monomers thick and no partitioning into the polymer phase (e.g.  $55.4$  nmol/cm<sup>2</sup>), the surface area of the 7, 13, 24, and 40  $\mu\text{m}$  thick PLGA films would need to increase by 1.3, 2.9, 5.6, and 8.6 times the surface area of the 2  $\mu\text{m}$  film to account for the observed increase

**Table 7.1** Effect of zeta-potential on solution concentration at the surface in [mM], calculated using Equation 7.2, for a bulk concentration of 1 mM.

$\zeta$ (mV)	Net Charge (+1)	Net Charge (+2)
-70	13.7	188.8
-71	14.3	203.5
-72	14.8	219.3
-73	15.4	236.4
-74	16.0	254.7
-75	16.6	274.5
-80	20.0	399.2

in peptide sorption at 37°C.

It is also possible that increasing the thickness of PLGA films could affect the zeta-potential, as thicker films have a larger content of acid end-groups, which may be preferentially presented at the surface. The following relationship between  $\psi_0$ , the electrostatic potential in the aqueous phase at the surface, and  $\sigma$ , the charge density, derived from the Poisson-Boltzmann equation was applied to calculate the change in surface charge density with surface potential:

$$A\sigma/\sqrt{C} = \sinh(ze\psi_0/2kT) \quad (7.1)$$

where  $k$  is the Boltzmann constant,  $T$  is the temperature  $e$  is the electronic charge,  $z$  is the valence of the electrolyte,  $C$  is the bulk electrolyte concentration, and  $A = 1/(8N_a\epsilon\epsilon_0kT)^{1/2}$ , where  $N_a$  is Avogadro's number,  $\epsilon$  is the dielectric constant, and  $\epsilon_0$  is the permittivity of free space. A 5 mV change in zeta-potential only changes the total number of charges on the surface by 10 pmol, far to little to account for the >50 nmol increment in peptide sorbed (Figure 7.4).

The surface concentration  $C_s$  can be related to the bulk concentration  $C_b$  using the

Boltzmann factor as shown in the following expression:

$$C_s = C_b \exp(z_i e \psi_0 / kT) \quad (7.2)$$

where  $z_i$  is the valency of the ion in solution. A 1mV difference in zeta-potential has a significant impact on the solution concentration of the peptide at the surface, especially when  $z_i = 2$ . For the divalent octreotide, a 1 mV increment in zeta-potential can increase the surface concentration by 15–20-fold relative to the bulk concentration and by 8% relative to the surface concentration (Table 7.1). This effect is less significant for the monovalent leuprolide. If the increased peptide sorption were explainable as resulting from the effect of zeta-potential on  $C_s$ , we would not expect to observe similar sorption behavior between divalent octreotide and monovalent leuprolide (e.g. in the slope of sorption plots with mass/thickness, see Figure 7.4). Thus, we conclude that the effect of PLGA film mass/thickness cannot be explained by differences in film zeta-potential.

### 7.3.3 Localization of sorbed octreotide within PLGA

An additional experiment was performed to confirm that the peptide was partitioning into the polymer phase. PLGA films were incubated in the presence of octreotide solution and sectioned prior to recovery by two-phase extraction. The results of two pools of 5-7 4 mm diameter films  $\sim 80 \mu\text{m}$  thick are shown in Table 7.2. Between 73-80% and 60-65% of the amount of octreotide sorbed to the control film was recovered after, removing roughly 25% and 50% of the top section of the PLGA film. Due to substantial surface roughness, the starting point for sectioning may have varied somewhat between samples. Also, the films displayed some curvature due to edge effects on the small substrate. Due to this, as well as exposure of the side of the film to the octreotide solution, it was likely that some of the recovered octreotide was present on the surface of the remaining film. Nevertheless,

**Table 7.2** Octreotide recovery from sectioned PLGA films incubated in the presence of 1 mM octreotide acetate solution.

Distance Sectioned ( $\mu\text{m}$ )	Octreotide Recovered (pmol/film)	
	Group 1	Group 2
0	376	435
$\sim 20$	275	346
$\sim 40$	224	281

it is unlikely that the large amount of remaining octreotide is only an artifact of these observations and not partially due to peptide solubility in the bulk polymer phase.

### 7.3.4 Surface analysis by X-ray Photoelectron Spectroscopy

The wide-scan survey spectrum covering the binding energy range of 0-1000 eV with a pass energy of 160 eV showed that only carbon and oxygen were present and that, prior to incubation, PLGA films were free from any unexpected elements within the top  $\sim 10$  nm of the polymer surface (Figure 7.5). The atomic composition of PLGA and octreotide powder were calculated from the XPS high resolution spectra and compared to their theoretical compositions (see Figure 7.6 for octreotide survey spectrum). As shown in Table 7.3, the calculated atomic compositions for both PLGA and octreotide closely matched the theoretical atomic compositions, validating that the atomic sensitivity factors [172] used were accurate.

The XPS spectrum of a PLGA film prepared according to D conditions after incubation in 1 mM octreotide acetate solution showed the presence of nitrogen, sulfur, and trace sodium, indicating that sorbed octreotide is present in the top layer of the film (Figure 7.7). The calculated atomic compositions for the spectrum was intermediate between pure PLGA and octreotide, consistent with the presence of  $\sim 40\%$  octreotide in the top-most  $\sim 10$  nm of the film, estimated by least-squares minimization of the atomic compositions  $X_i$  using the equation:  $X_i = X_{i,oct}F_{oct} + X_{i,plga}F_{plga}$ , where  $X_{i,oct}$  and  $X_{i,plga}$  are the atomic compositions of pure



**Table 7.3** Atomic compositions of PLGA films determined from XPS spectra shown in Figures 7.5 – 7.7. Trace amounts of sodium were not included.

Sample	Calculated Composition (%)				Theoretical Composition (%)			
	C	O	N	S	C	O	N	S
PLGA control	57	43	—	—	56	44	—	—
octreotide control	68	16	13	3	69	14	14	3
PLGA + 1mM octreotide <sup>a</sup>	65	29	4	2	—	—	—	—

<sup>a</sup> Standard Deviation (n=2): C(1.1), O(3.4), N(0.7), S(1.6)

octreotide or PLGA, and  $F_{oct}$  and  $F_{plga}$  are the mole fraction present in the layer analyzed by XPS.

## 7.4 Conclusions

In this study, we investigated the solubility properties of ion-paired octreotide-PLGA in two low-dielectric mediums, acetonitrile and PLGA. The presence of octreotide-PLGA in acetonitrile was confirmed by <sup>1</sup>H-NMR, and absorption of octreotide into PLGA is strongly suggested by the increased sorption with increasing polymer thickness, which is unlikely due to differences in surface roughness or zeta-potential. A second experiment where octreotide was recovered from sectioned PLGA films is also consistent with octreotide absorption within PLGA. However, XPS analysis suggests the composition of octreotide in the 10 nm-surface layer is 40 mol%. Hence, currently data supports both absorption and multilayer adsorption.

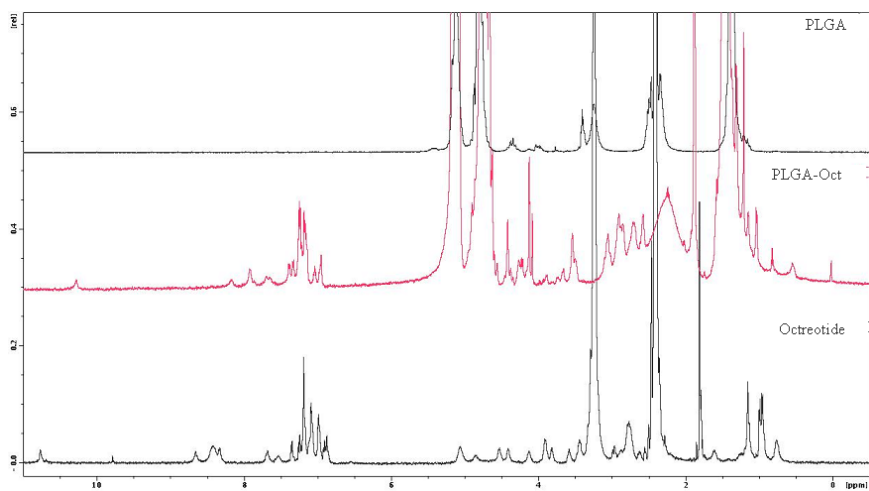


**Figure 7.1** <sup>1</sup>H-NMR of PLGA 50:50 in *d*<sub>6</sub>-dimethylsulfoxide (top), sorbed octreotide-PLGA 50:50 in *d*<sub>3</sub>-acetonitrile (middle), and octreotide acetate in *d*<sub>6</sub>-dimethylsulfoxide (bottom).

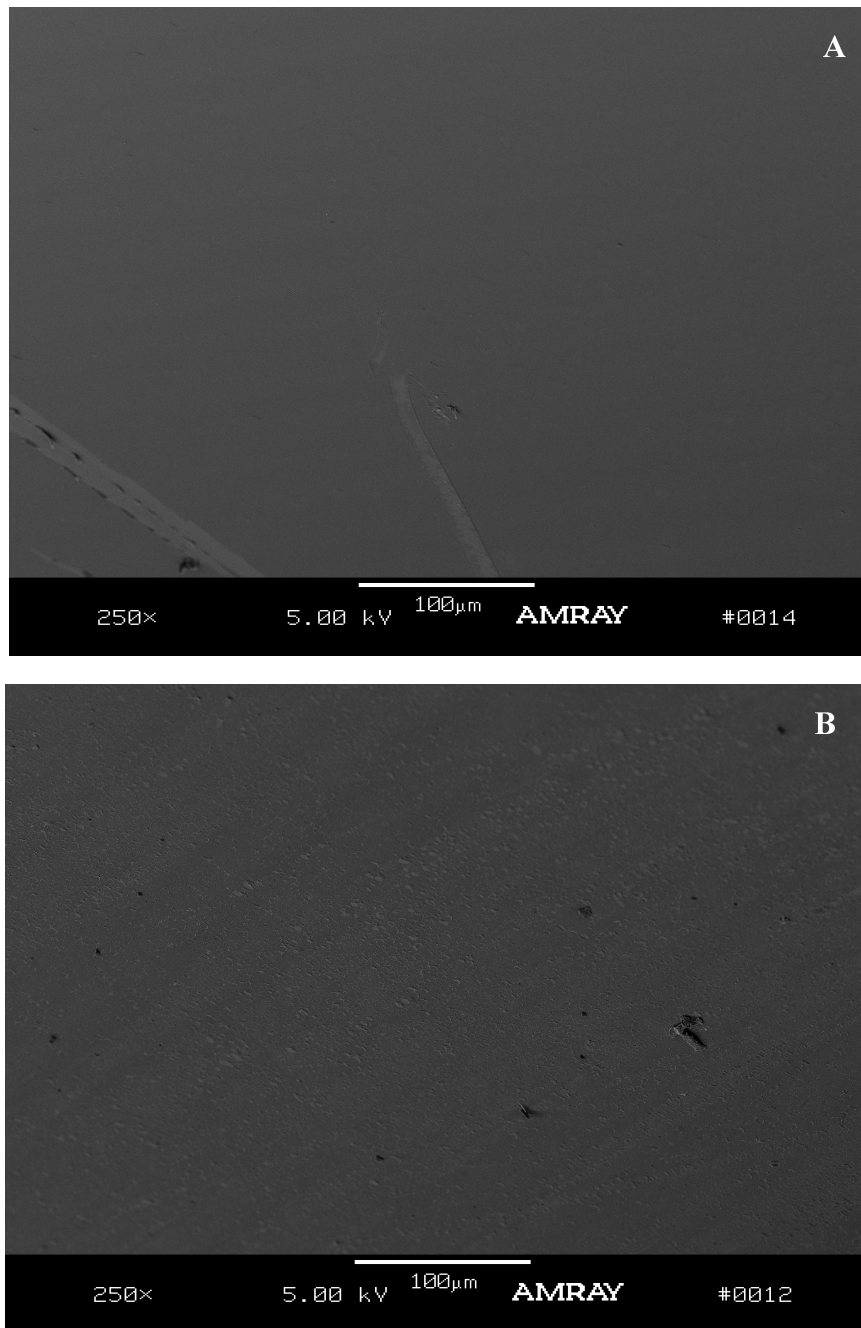


**Figure 7.2** Scanning electron micrograph of the surface of a PLGA 50:50 film prepared according to A conditions (see Table 3.2) after 24 h incubation in 0.1M HEPES buffer, pH 7.4 **A** without and **B** with 1 mM octreotide acetate at 37°C.

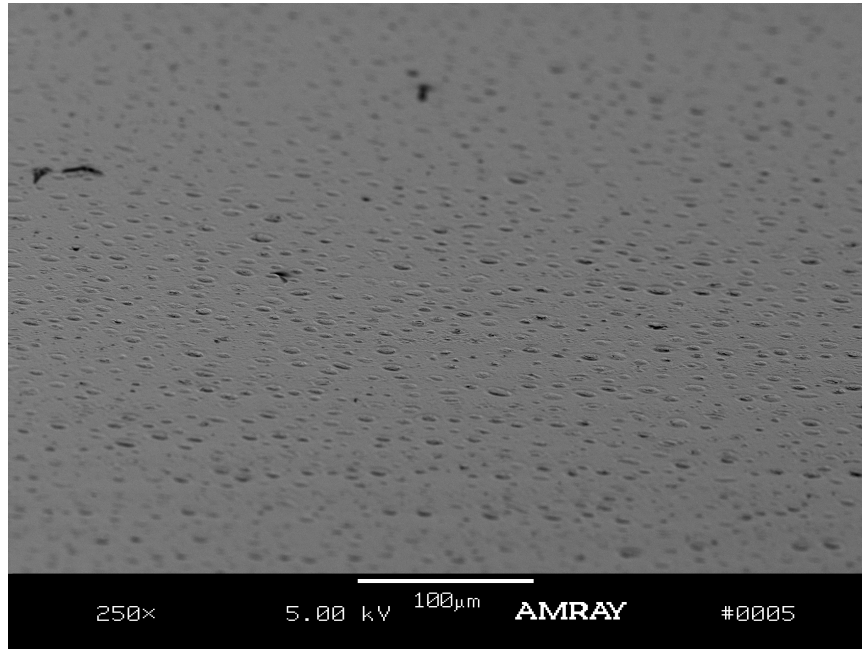


**Figure 7.3** Scanning electron micrograph of the surface of a PLGA 50:50 film prepared according to C conditions (see Table 3.2) after 24 h incubation with 1 mM octreotide acetate in 0.1 M HEPES buffer, pH 7.4 at 37°C.

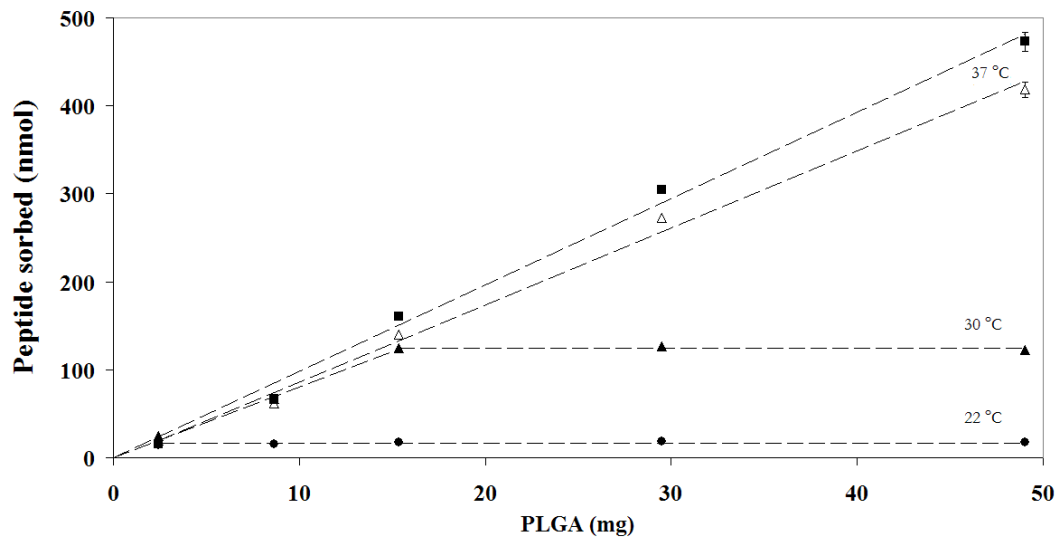


**Figure 7.4** Effect of mass/thickness on peptide sorption to PLGA 50:50 (Boehringer-Ingelheim RG502H) films in 0.1 M HEPES buffer, pH 7.4 at 22°C (octreotide: ●), 30°C (octreotide: ▲), and 37°C (octreotide: △, leuprolide: ■). Initial peptide concentration was 1.0 mM.

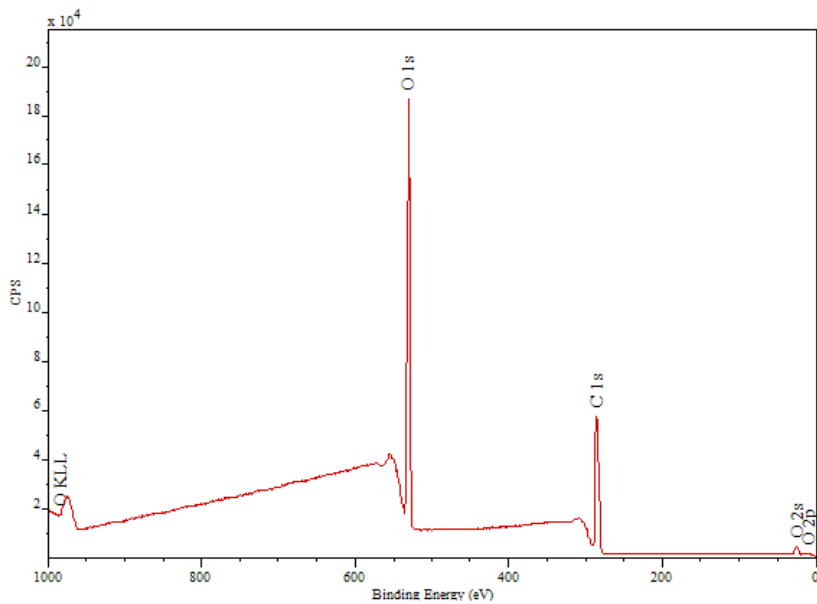


**Figure 7.5** The XPS survey spectra of a PLGA 50:50 film prepared according to D conditions (see Table 3.2).

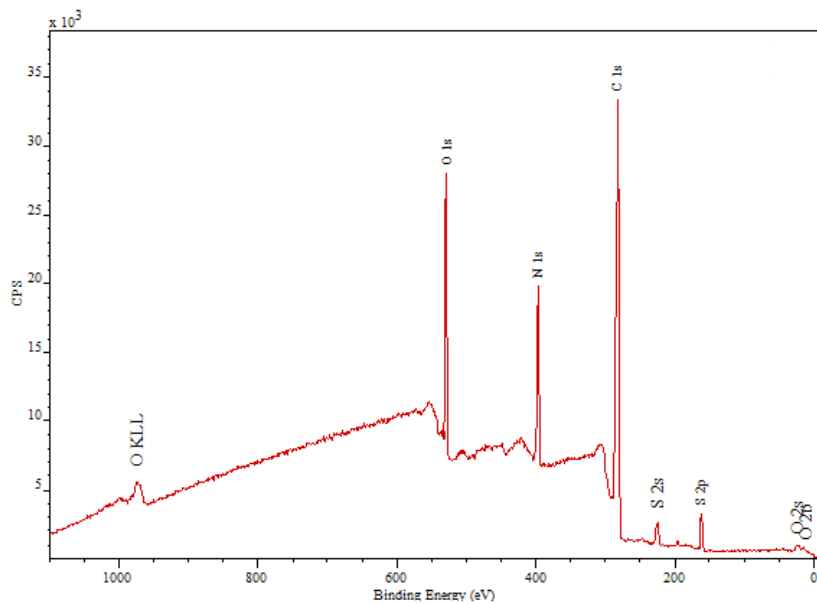


**Figure 7.6** The XPS survey spectra of octreotide acetate powder.

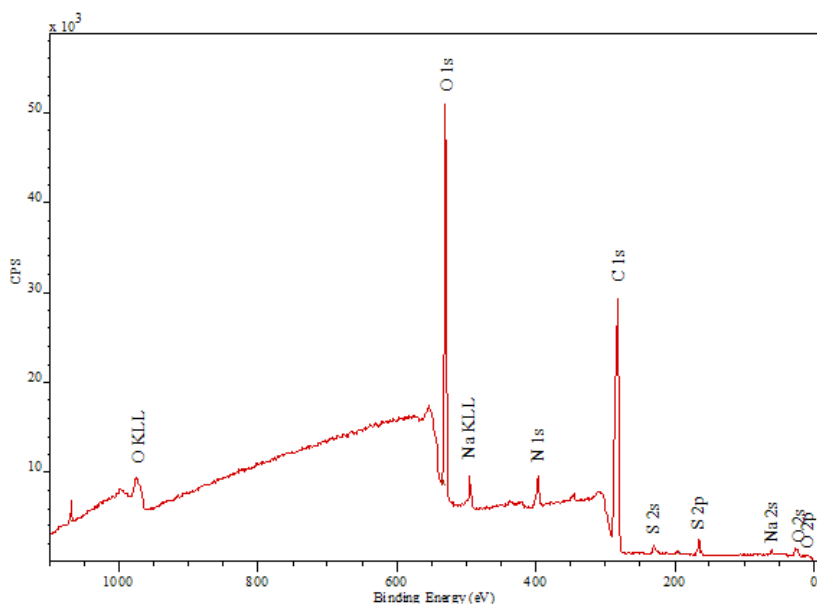


**Figure 7.7** The XPS survey spectra of a PLGA 50:50 film prepared according to D conditions (see Table 3.2) after 24 hr incubation at 37°C with 1mM octreotide acetate in 0.1 mM HEPES, pH 7.4.

# Chapter 8

## Contributions

This dissertation has focused on understanding peptide sorption to PLGA mechanistically, with the goal of utilizing this understanding for a rational formulation approach to stabilize octreotide and similar peptides against acylation within PLGA controlled release drug delivery systems. Surprisingly, these studies are the first detailed investigations of peptide sorption to low molecular-weight free-acid PLGA, perhaps due to the challenges these polymers present (e.g. water uptake and degradation) preventing straight-forward use of many traditional methods used to study sorption behavior.

A new class of inhibitors of the sorption and acylation of a model peptide, octreotide, has been described. Long-term sorption studies in the presence of  $\text{CaCl}_2$  and  $\text{MnCl}_2$  indicated that disrupting peptide sorption to PLGA with the inorganic divalent cation inhibitors translates to inhibition of peptide acylation. Acylation of octreotide encapsulated in PLGA millicylinders containing equivalent weight ratio  $\text{CaCl}_2$  or  $\text{MnCl}_2$  relative to peptide was also inhibited relative to no salt or  $\text{NaCl}$  controls both during encapsulation or release incubation.

We have shown that the octreotide-PLGA interactions are mostly kinetically irreversible in aqueous solutions and changes the solubility properties of octreotide in acetonitrile, confirmed by  $^1\text{H-NMR}$ . Only the addition of solvent or 5% SDS resulted in a substantial desorption from PLGA, strongly suggesting the irreversibility was due to hydrophobic interactions or hydrogen-bonding between the peptide and PLGA or low mass-transfer rates

of absorbed peptide-PLGA ion-pairs between bulk and the surface of the polymer.

The kinetic profiles of peptide sorption to PLGA were also investigated at various solution conditions. The rate and extent of sorption is reduced at low octreotide concentrations, high solution ionic strength and low temperature, becoming completely attenuated at 4°C, suggesting polymer mobility plays a critical role in the sorption interaction. A biexponential model described the sorption profiles extremely well, and a relationship between concentration and the model parameters is obvious, although further research will need to be conducted in order to discern this relationship.

Although kinetically irreversible, octreotide (and leuprolide) sorption follow Langmuir-like behavior. Sorption of octreotide decreased as the pH of the solutions tested was decreased towards the  $pK_a$  of PLGA carboxylates. Reducing the number of total acid end-groups by increasing the PLGA molecular weight also decreased octreotide sorption. These results indicate the critical role of ionized PLGA acid end-groups during the peptide sorption pathway. Quantification of the maximal amount of peptide sorbed at high solution concentration from a modified Langmuir equation show this value to be similar to the total number of PLGA acid end-groups for RG502H and RG503H, suggesting the possibility of peptide partitioning into the polymer phase or dependence on acid release from the polymer. The low amount of sorption to the higher molecular-weight RG504H is also consistent with peptide partitioning into the polymer, as the decreased polymer mobility with increasing molecular weight eventually prevents peptide partitioning.

The localization of sorbed octreotide, whether adsorbed as multilayer, precipitated, or absorbed within the bulk of the polymer, was directly investigated using PLGA films with constant surface area of varying thickness and by recovering sorbed octreotide from sectioned PLGA films. These studies strongly suggest that some peptide is indeed absorbed within the bulk of the polymer. While we cannot completely rule out the presence of some multilayer sorption or precipitation, the calculations presented in this dissertation suggest



that multilayer sorption alone cannot support the large body of evidence consistent with internalization of octreotide within PLGA.

There have been no prior reports of peptide internalization into the PLGA phase, making this central conclusion of this thesis—that octreotide can absorb in RG502H, the first of its kind.

# Bibliography

- [1] Anonymous, “Biotechnology industry statistics,” 2003.
- [2] T. J. Kamerzell and C. R. Middaugh, “The complex inter-relationships between protein flexibility and stability,” *Journal of Pharmaceutical Sciences*, vol. 97, no. 9, pp. 3494–3517, 2008.
- [3] W. Wang, S. Singh, D. L. Zeng, K. King, and S. Nema, “Antibody structure, instability, and formulation,” *Journal of Pharmaceutical Sciences*, vol. 96, no. 1, pp. 1–26, 2007.
- [4] S. Frokjaer and D. E. Otzen, “Protein drug stability: A formulation challenge,” *Nature Reviews Drug Discovery*, vol. 4, no. 4, pp. 298–306, 2005.
- [5] W. Wang, “Protein aggregation and its inhibition in biopharmaceutics,” *International Journal of Pharmaceutics*, vol. 289, no. 1-2, pp. 1–30, 2005.
- [6] W. Wang, “Instability, stabilization, and formulation of liquid protein pharmaceuticals,” *International Journal of Pharmaceutics*, vol. 185, no. 2, pp. 129–188, 1999.
- [7] V. H. L. Lee, S. Dodda-Kashi, G. M. Grass, and W. Rubas, “Oral route of peptide and protein drug delivery,” in *Peptide and protein drug delivery* (V. H. L. Lee, ed.), pp. 691–738, New York: Marcel Dekker, 1990.
- [8] J. A. Fix, “Oral controlled release technology for peptides: Status and future prospects,” *Pharmaceutical Research*, vol. 13, no. 12, pp. 1760–1764, 1996.
- [9] L. Chen, R. N. Apte, and S. Cohen, “Characterization of plga microspheres for the controlled delivery of il-1 alpha for tumor immunotherapy,” *Journal of Controlled Release*, vol. 43, no. 2-3, pp. 261–272, 1997.
- [10] G. J. Russell-Jones, “Use of vitamin b-12 conjugates to deliver protein drugs by the oral route,” *Critical Reviews in Therapeutic Drug Carrier Systems*, vol. 15, no. 6, pp. 557–586, 1998.
- [11] J. G. Still, “Development of oral insulin: progress and current status,” *Diabetes-Metabolism Research and Reviews*, vol. 18, pp. S29–S37, 2002. Suppl. 1.

- [12] S. J. Milstein, H. Leipold, D. Sarubbi, A. Leone-Bay, G. M. Mlynek, J. R. Robinson, M. Kasimova, and E. Freire, "Partially unfolded proteins efficiently penetrate cell membranes - implications for oral drug delivery," *Journal of Controlled Release*, vol. 53, no. 1-3, pp. 259–267, 1998.
- [13] J. L. Cleland, A. Daugherty, and R. Mrsny, "Emerging protein delivery methods," *Current Opinion in Biotechnology*, vol. 12, no. 2, pp. 212–219, 2001.
- [14] J. S. Patton, P. Trincherio, and R. M. Platz, "Bioavailability of pulmonary delivered peptides and proteins - alpha-interferon, calcitonins and parathyroid hormones," *Journal of Controlled Release*, vol. 28, no. 1-3, pp. 79–85, 1994.
- [15] L. Borgstrom, L. Asking, O. Beckman, E. Bondesson, A. Kallen, and B. Olsson, "Discrepancy between in vitro and in vivo dose variability for a pressurized metered dose inhaler and a dry powder inhaler," *Journal of Aerosol Medicine-Deposition Clearance and Effects in the Lung*, vol. 11, pp. S59–S64, 1998. Suppl. 1.
- [16] D. Cipolla, I. Gonda, and S. J. Shire, "Characterization of aerosols of human recombinant deoxyribonuclease-i (rhdnase) generated by jet nebulizers," *Pharmaceutical Research*, vol. 11, no. 4, pp. 491–498, 1994.
- [17] Y. W. Chien, "Transdermal route of peptide and protein drug delivery," in *Peptide and protein drug delivery* (V. H. L. Lee, ed.), pp. 667–689, New York: Marcel Dekker, 1991.
- [18] G. Cleary, "Transdermal delivery systems: a medical rationale," in *Topical drug bioavailability, bioequivalence, and penetration* (V. Shah and H. Maibach, eds.), pp. 17–68, New York: Plenum Press, 1993.
- [19] A. Naik, Y. N. Kalia, and R. H. Guy, "Transdermal drug delivery: overcoming the skin's barrier function," *Pharmaceutical Science and Technology Today*, vol. 3, no. 9, pp. 318–326, 2000.
- [20] S. Mitragotri, D. Blankschtein, and R. Langer, "Ultrasound-mediated transdermal protein delivery," *Science*, vol. 269, no. 5225, pp. 850–853, 1995.
- [21] P. Ledger, "Skin biological issues in electrically enhanced transdermal delivery," *Advanced Drug Delivery Reviews*, vol. 9, pp. 289–307, 1992.
- [22] J. L. Cleland, E. Duenas, A. Daugherty, M. Marian, J. Yang, M. Wilson, A. C. Celniker, A. Shahzamani, V. Quarmby, H. Chu, V. Mukku, A. Mac, M. Roussakis, N. Gillette, B. Boyd, D. Yeung, D. Brooks, Y. F. Maa, C. Hsu, and A. J. S. Jones, "Recombinant human growth hormone poly(lactic-co-glycolic acid) (plga) microspheres provide a long lasting effect," *Journal of Controlled Release*, vol. 49, no. 2-3, pp. 193–205, 1997.
- [23] M. J. Alonso, S. Cohen, T. G. Park, R. K. Gupta, G. R. Siber, and R. Langer, "Determinants of release rate of tetanus vaccine from polyester microspheres," *Pharmaceutical Research*, vol. 10, no. 7, pp. 945–953, 1993.

- [24] J. L. Cleland, "Single-administration vaccines: controlled-release technology to mimic repeated immunizations," *Trends in Biotechnology*, vol. 17, no. 1, pp. 25–29, 1999.
- [25] H. Okada, Y. Doken, Y. Ogawa, and H. Toguchi, "Preparation of 3-month depot injectable microspheres of leuporelin acetate using biodegradable polymers," *Pharmaceutical Research*, vol. 11, no. 8, pp. 1143–1147, 1994.
- [26] G. D. Yancopoulos, S. Davis, N. W. Gale, J. S. Rudge, S. J. Wiegand, and J. Holash, "Vascular-specific growth factors and blood vessel formation," *Nature*, vol. 407, no. 6801, pp. 242–248, 2000.
- [27] C. A. Kirker-Head, "Potential applications and delivery strategies for bone morphogenetic proteins," *Advanced Drug Delivery Reviews*, vol. 43, no. 1, pp. 65–92, 2000.
- [28] K. E. Uhrich, S. M. Cannizzaro, R. S. Langer, and K. M. Shakesheff, "Polymeric systems for controlled drug release," *Chemical Reviews*, vol. 99, no. 11, pp. 3181–3198, 1999.
- [29] P. Menei, J. P. Benoit, M. Boisdroncelle, D. Fournier, P. Mercier, and G. Guy, "Drug targeting into the central nervous system by stereotaxic implantation of biodegradable microspheres," *Neurosurgery*, vol. 34, no. 6, pp. 1058–1064, 1994.
- [30] F. F. Eide, D. H. Lowenstein, and L. F. Reichardt, "Neurotrophins and their receptors - current concepts and implications for neurologic disease," *Experimental Neurology*, vol. 121, no. 2, pp. 200–214, 1993.
- [31] A. O. Eniola and D. A. Hammer, "Artificial polymeric cells for targeted drug delivery," *Journal of Controlled Release*, vol. 87, no. 1-3, pp. 15–22, 2003.
- [32] R. S. Schwartz and E. R. Edelman, "Drug-eluting stents in preclinical studies - recommended evaluation from a consensus group," *Circulation*, vol. 106, no. 14, pp. 1867–1873, 2002.
- [33] R. R. Chen and D. J. Mooney, "Polymeric growth factor delivery strategies for tissue engineering," *Pharmaceutical Research*, vol. 20, no. 8, pp. 1103–1112, 2003.
- [34] A. Perets, Y. Baruch, F. Weisbuch, G. Shoshany, G. Neufeld, and S. Cohen, "Enhancing the vascularization of three-dimensional porous alginate scaffolds by incorporating controlled release basic fibroblast growth factor microspheres," *Journal of Biomedical Materials Research Part A*, vol. 65A, no. 4, pp. 489–497, 2003.
- [35] C. M. Agrawal, G. G. Niederauer, D. M. Micallef, and K. A. Athanasiou in *Encyclopedic Handbook of Biomaterials and Bioengineering, Part A: Materials* (D. L. Wise, D. J. Trantolo, D. E. Altobelli, M. J. Yaszemski, J. D. Gresser, and E. Schwartz, eds.), p. 1055, New York: Marcel Dekker, 1995.

- [36] J. B. Eilert, P. Binder, P. W. McKinney, J. M. Beal, and J. Conn, "Polyglycolic acid synthetic absorbable sutures," *American Journal of Surgery*, vol. 121, no. 5, pp. 561–565, 1971.
- [37] D. L. Wise, "Biopolymer system design for sustained release of biologically active agents," in *Biopolymeric controlled release systems* (D. L. Wise, ed.), vol. 1, pp. 3–10, Boca Raton, FL: CRC Press, 1984.
- [38] A. Kumar and R. K. Gupta, *Fundamentals of polymers*. New York: McGraw-Hill, 1998.
- [39] T. G. Park, "Degradation of poly(d,l-lactic acid) microspheres - effect of molecular-weight," *Journal of Controlled Release*, vol. 30, no. 2, pp. 161–173, 1994.
- [40] P. Blasi, S. D'Souza, F. Selmin, and P. DeLuca, "Plasticizing effect of water on poly(lactide-co-glycolide)," *Journal of Controlled Release*, vol. 108, pp. 1–9, NOV 2 2005.
- [41] M. A. Tracy, K. L. Ward, L. Firouzabadian, Y. Wang, N. Dong, R. Qian, and Y. Zhang, "Factors affecting the degradation rate of poly(lactide-co-glycolide) microspheres in vivo and in vitro," *Biomaterials*, vol. 20, no. 11, pp. 1057–1062, 1999.
- [42] D. Blanco and M. J. Alonso, "Protein encapsulation and release from poly(lactide-co-glycolide) microspheres: effect of the protein and polymer properties and of the co-encapsulation of surfactants," *European Journal of Pharmaceutics and Biopharmaceutics*, vol. 45, no. 3, pp. 285–294, 1998.
- [43] J. Herrmann and R. Bodmeier, "Biodegradable, somatostatin acetate containing microspheres prepared by various aqueous and non-aqueous solvent evaporation methods," *European Journal of Pharmaceutics and Biopharmaceutics*, vol. 45, no. 1, pp. 75–82, 1998.
- [44] X. C. Zhang, U. P. Wyss, D. Pichora, B. Amsden, and M. F. A. Goosen, "Controlled-release of albumin from biodegradable poly(dl-lactide) cylinders," *Journal of Controlled Release*, vol. 25, no. 1-2, pp. 61–69, 1993.
- [45] S. Takada, Y. Uda, H. Toguchi, and Y. Ogawa, "Application of a spray drying technique in the production of trh-containing injectable sustained-release microparticles of biodegradable polymers.," *PDA Journal of Pharmaceutical Science and Technology*, vol. 49, no. 4, pp. 180–184, 1995.
- [46] O. L. Johnson, W. Jaworowicz, J. L. Cleland, L. Bailey, M. Charnis, E. Duenas, C. C. Wu, D. Shepard, S. Magil, T. Last, A. J. S. Jones, and S. D. Putney, "The stabilization and encapsulation of human growth hormone into biodegradable microspheres," *Pharmaceutical Research*, vol. 14, no. 6, pp. 730–735, 1997.
- [47] P. Herbert, K. Murphy, O. Johnson, N. Dong, W. Jaworowicz, M. A. Tracy, J. L. Cleland, and S. D. Putney, "A large-scale process to produce microencapsulated proteins," *Pharmaceutical Research*, vol. 15, no. 2, pp. 357–361, 1998.

- [48] M. C. Manning, K. Patel, and R. T. Borchardt, "Stability of protein pharmaceuticals," *Pharmaceutical Research*, vol. 6, no. 11, pp. 903–918, 1989.
- [49] J. L. Cleland, M. F. Powell, and S. J. Shire, "The development of stable protein formulations - a close look at protein aggregation, deamidation, and oxidation," *Critical Reviews in Therapeutic Drug Carrier Systems*, vol. 10, no. 4, pp. 307–377, 1993.
- [50] T. Brennan and S. Clarke, "Deamidation and isoaspartate formation in model synthetic peptides: The effects of sequence and solution environment," in *Deamidation and isoaspartate formation in peptides and proteins* (D. Aswad, ed.), pp. 65–90, Boca Raton, FL: CRC Press, 1995.
- [51] S. P. Schwendeman, M. Cardamone, M. Brandon, A. Klibanov, and R. Langer, "Stability of proteins and their delivery from biodegradable polymer microspheres," in *Microparticulate systems for the delivery of proteins and vaccines* (S. Cohen and H. Bernstein, eds.), pp. 1–50, New York: Marcel Dekker, Inc., 1996.
- [52] S. P. Schwendeman, H. R. Costantino, R. K. Gupta, and R. Langer, "Peptide, protein, and vaccine delivery from implantable polymeric systems," in *Controlled drug delivery: challenges and strategies* (K. Park, ed.), pp. 229–267, Washington, D. C.: American Chemical Society, 1997.
- [53] M. C. Lai and E. M. Topp, "Solid-state chemical stability of proteins and peptides," *Journal of Pharmaceutical Sciences*, vol. 88, no. 5, pp. 489–500, 1999.
- [54] P. M. Bummer and S. Koppenol, "Chemical and physical consideration in protein and peptide stability," in *Protein Formulation and Delivery* (E. McNally, ed.), pp. 5–69, New York: Marcel Dekker, 2000.
- [55] J. Meyer, B. Ho, and M. C. Manning, "Effects of conformation on the chemical stability of pharmaceutically relevant peptides," in *Rational design of stable protein formulations* (J. Carpenter and M. C. Manning, eds.), pp. 85–107, New York: Kluwer Academic/Plenum Publishers, 2002.
- [56] G. Zhu, *Stabilization and controlled release of proteins encapsulated in poly(lactide-co-glycolide) delivery systems*. Ph.d. thesis, The Ohio State University, 1999.
- [57] I. J. Castellanos, G. Cruz, R. Crespo, and K. Griebenow, "Encapsulation-induced aggregation and loss in activity of gamma-chymotrypsin and their prevention," *Journal of Controlled Release*, vol. 81, no. 3, pp. 307–319, 2002.
- [58] K. Fu, K. Griebenow, L. Hsieh, A. M. Klibanov, and R. Langer, "Ftir characterization of the secondary structure of proteins encapsulated within plga microspheres," *Journal of Controlled Release*, vol. 58, no. 3, pp. 357–366, 1999.
- [59] H. Sah, "Protein behavior at the water/methylene chloride interface," *Journal of Pharmaceutical Sciences*, vol. 88, no. 12, pp. 1320–1325, 1999.

- [60] G. Z. Zhu, S. R. Mallery, and S. P. Schwendeman, "Stabilization of proteins encapsulated in injectable poly (lactide-co-glycolide)," *Nature Biotechnology*, vol. 18, no. 1, pp. 52–57, 2000.
- [61] J. C. Kang and S. P. Schwendeman, "Comparison of the effects of mg(oh)<sub>2</sub> and sucrose on the stability of bovine serum albumin encapsulated in injectable poly(d,l-lactide-co-glycolide) implants," *Biomaterials*, vol. 23, no. 1, pp. 239–245, 2002.
- [62] Y. F. Maa and C. C. Hsu, "Effect of high shear on proteins," *Biotechnology and Bioengineering*, vol. 51, no. 4, pp. 458–465, 1996.
- [63] V. Sluzky, J. A. Tamada, A. M. Klibanov, and R. Langer, "Kinetics of insulin aggregation in aqueous solutions upon agitation in the presence of hydrophobic surfaces," *Proceedings of the National Academy of Sciences of the United States of America*, vol. 88, no. 21, pp. 9377–9381, 1991.
- [64] U. R. Desai and A. M. Klibanov, "Assessing the structural integrity of a lyophilized protein in organic-solvents," *Journal of the American Chemical Society*, vol. 117, no. 14, pp. 3940–3945, 1995.
- [65] K. Griebenow and A. M. Klibanov, "On protein denaturation in aqueous-organic mixtures but not in pure organic solvents," *Journal of the American Chemical Society*, vol. 118, no. 47, pp. 11695–11700, 1996.
- [66] H. Sah, "Stabilization of proteins against methylene chloride water interface-induced denaturation and aggregation," *Journal of Controlled Release*, vol. 58, no. 2, pp. 143–151, 1999.
- [67] M. Iwata, T. Tanaka, Y. Nakamura, and J. W. McGinity, "Selection of the solvent system for the preparation of poly(d,l-lactic-co-glycolic acid) microspheres containing tumor necrosis factor-alpha (tnf-alpha)," *International Journal of Pharmaceutics*, vol. 160, no. 2, pp. 145–156, 1998.
- [68] L. Kreilgaard, S. Frokjaer, J. M. Flink, T. W. Randolph, and J. F. Carpenter, "Effects of additives on the stability of recombinant human factor xiii during freeze-drying and storage in the dried solid," *Archives of Biochemistry and Biophysics*, vol. 360, no. 1, pp. 121–134, 1998.
- [69] H. R. Costantino, R. Langer, and A. M. Klibanov, "Solid-phase aggregation of proteins under pharmaceutically relevant conditions," *Journal of Pharmaceutical Sciences*, vol. 83, no. 12, pp. 1662–1669, 1994.
- [70] E. D. Breen, J. G. Curley, D. E. Overcashier, C. C. Hsu, and S. J. Shire, "Effect of moisture on the stability of a lyophilized humanized monoclonal antibody formulation," *Pharmaceutical Research*, vol. 18, no. 9, pp. 1345–1353, 2001.
- [71] M. van de Weert, W. E. Hennink, and W. Jiskoot, "Protein instability in poly(lactic-co-glycolic acid) microparticles," *Pharmaceutical Research*, vol. 17, no. 10, pp. 1159–1167, 2000.

- [72] A. Sanchez, B. Villamayor, Y. Y. Guo, J. McIver, and M. J. Alonso, "Formulation strategies for the stabilization of tetanus toxoid in poly(lactide-co-glycolide) microspheres," *International Journal of Pharmaceutics*, vol. 185, no. 2, pp. 255–266, 1999.
- [73] W. R. Liu, R. Langer, and A. M. Klibanov, "Moisture-induced aggregation of lyophilized proteins in the solid-state," *Biotechnology and Bioengineering*, vol. 37, no. 2, pp. 177–184, 1991.
- [74] H. R. Costantino, R. Langer, and A. M. Klibanov, "Moisture-induced aggregation of lyophilized insulin," *Pharmaceutical Research*, vol. 11, no. 1, pp. 21–29, 1994.
- [75] G. Crotts and T. G. Park, "Protein delivery from poly(lactic-co-glycolic acid) biodegradable microspheres: release kinetics and stability issues," *Journal of Microencapsulation*, vol. 15, no. 6, pp. 699–713, 1998.
- [76] W. L. Jiang and S. P. Schwendeman, "Formaldehyde-mediated aggregation of protein antigens: comparison of untreated and formalinized model antigens," *Biotechnology and Bioengineering*, vol. 70, no. 5, pp. 507–517, 2000.
- [77] S. P. Schwendeman, H. R. Costantino, R. K. Gupta, G. R. Siber, A. M. Klibanov, and R. Langer, "Stabilization of tetanus and diphtheria toxoids against moisture-induced aggregation," *Proceedings of the National Academy of Sciences of the United States of America*, vol. 92, no. 24, pp. 11234–11238, 1995.
- [78] A. Gopferich, "Mechanisms of polymer degradation and erosion," *Biomaterials*, vol. 17, pp. 103–114, JAN 1996.
- [79] C. Shih, "Chain-end scission in acid-catalyzed hydrolysis of poly(d,l-lactide) in solution," *Journal of Controlled Release*, vol. 34, pp. 9–15, APR 1995.
- [80] A. Brunner, K. Mader, and A. Gopferich, "pH and osmotic pressure inside biodegradable microspheres during erosion," *Pharmaceutical Research*, vol. 16, no. 6, pp. 847–853, 1999.
- [81] T. Arakawa and S. N. Timasheff, "Stabilization of protein structure by sugars," *Biochemistry*, vol. 21, no. 25, pp. 6536–6544, 1982.
- [82] S. Li, H. Garreau, and M. Vert, "Structure property relationships in the case of the degradation of massive poly(alpha-hydroxy acids) in aqueous media .2. Degradation of lactide-glycolide copolymers - PLA37.5GA24 and PLA75GA25," *Journal of Materials Science- Materials in Medicine*, vol. 1, pp. 131–139, OCT 1990.
- [83] I. Grizzi, H. Garreau, S. LI, and M. Vert, "Hydrolytic degradation of devices based on poly(dl-lactic acid) size-dependence," *Biomaterials*, vol. 16, pp. 305–311, MAR 1995.
- [84] C. Holten, A. Muller, and D. Reh binder, *Lactic acid: properties and chemistry of lactic acid and derivatives*. Weinheim, Germany: Verlag Chemie, 1971.



- [85] S. P. Schwendeman, A. Shenderova, G. Zhu, and W. Jiang, "Stability of encapsulated substances in poly(lactide-co-glycolide) delivery systems," in *Handbook of pharmaceutical controlled release technology* (D. L. Wise, ed.), pp. 393–411, New York: Marcel Dekker, 2000.
- [86] K. Fu, D. W. Pack, A. M. Klibanov, and R. Langer, "Visual evidence of acidic environment within degrading poly(lactic-co-glycolic acid) (plga) microspheres," *Pharmaceutical Research*, vol. 17, no. 1, pp. 100–106, 2000.
- [87] T. J. Peters, *All about albumin: biochemistry, genetics, and medical applications*. San Diego: Academic Press, 1996.
- [88] P. R. Van Tassel, L. Guemouri, J. J. Ramsden, G. Tarjus, P. Viot, and J. Talbot, "A particle-level model of irreversible protein adsorption with a postadsorption transition," *Journal of Colloid and Interface Science*, vol. 207, no. 2, pp. 317–323, 1998.
- [89] G. Crotts, H. Sah, and T. G. Park, "Adsorption determines in-vitro protein release rate from biodegradable microspheres: Quantitative analysis of surface area during degradation," *Journal of Controlled Release*, vol. 47, no. 1, pp. 101–111, 1997.
- [90] D. H. Na and P. P. DeLuca, "Pegylation of octreotide: I. separation of positional isomers and stability against acylation by poly(d,l-lactide-co-glycolide)," *Pharmaceutical Research*, vol. 22, no. 5, pp. 736–742, 2005.
- [91] M. Diwan and T. G. Park, "Pegylation enhances protein stability during encapsulation in plga microspheres," *Journal of Controlled Release*, vol. 73, no. 2-3, pp. 233–244, 2001.
- [92] S. H. Li, C. Schoneich, and R. T. Borchardt, "Chemical-instability of protein pharmaceuticals - mechanisms of oxidation and strategies for stabilization," *Biotechnology and Bioengineering*, vol. 48, no. 5, pp. 490–500, 1995.
- [93] J. L. Cleland, A. Mac, B. Boyd, J. Yang, E. T. Duenas, D. Yeung, D. Brooks, C. Hsu, H. Chu, V. Mukku, and A. J. S. Jones, "The stability of recombinant human growth hormone in poly(lactic-co-glycolic acid) (plga) microspheres," *Pharmaceutical Research*, vol. 14, no. 4, pp. 420–425, 1997.
- [94] A. Lucke, J. Kiermaier, and A. Gopferich, "Peptide acylation by poly(alpha-hydroxy esters)," *Pharmaceutical Research*, vol. 19, no. 2, pp. 175–181, 2002.
- [95] S. Noguchi, K. Miyawaki, and Y. Satow, "Succinimide and isoaspartate residues in the crystal structures of hen egg-white lysozyme complexed with tri-n-acetylchitotriose," *Journal of Molecular Biology*, vol. 278, no. 1, pp. 231–238, 1998.
- [96] S. Capasso, A. DiDonato, L. Esposito, F. Sica, G. Sorrentino, L. Vitagliano, A. Zagari, and L. Mazzarella, "Deamidation in proteins: the crystal structure of bovine pancreatic ribonuclease with an isoaspartyl residue at position 67," *Journal of Molecular Biology*, vol. 257, no. 3, pp. 492–496, 1996.

- [97] P. K. Tsai, M. W. Bruner, J. I. Irwin, C. C. Y. Ip, C. N. Oliver, R. W. Nelson, D. B. Volkin, and C. R. Middaugh, "Origin of the isoelectric heterogeneity of monoclonal immunoglobulin h1b4," *Pharmaceutical Research*, vol. 10, no. 11, pp. 1580–1586, 1993.
- [98] G. Teshima, W. Hancock, and E. Canova-Davis, "Effects of deamidation and isoaspartate formation on the activity of proteins," in *Deamidation and isoaspartate formation in peptides and proteins* (D. Aswad, ed.), pp. 167–192, Boca Raton, FL: CRC Press, 1995.
- [99] J. Cacia, R. Keck, L. G. Presta, and J. Frenz, "Isomerization of an aspartic acid residue in the complementarity-determining regions of a recombinant antibody to human ige: Identification and effect on binding affinity," *Biochemistry*, vol. 35, no. 6, pp. 1897–1903, 1996.
- [100] Y. R. Hsu, W. C. Chang, E. A. Mendiaz, S. Hara, D. T. Chow, M. B. Mann, K. E. Langley, and H. S. Lu, "Selective deamidation of recombinant human stem cell factor during in vitro aging: Isolation and characterization of the aspartyl and isoaspartyl homodimers and heterodimers," *Biochemistry*, vol. 37, no. 8, pp. 2251–2262, 1998.
- [101] D. W. Aswad, M. V. Paranandi, and B. T. Schurter, "Isoaspartate in peptides and proteins: formation, significance, and analysis," *Journal of Pharmaceutical and Biomedical Analysis*, vol. 21, no. 6, pp. 1129–1136, 2000.
- [102] M. Perkins, R. Theiler, S. Lunte, and M. Jeschke, "Determination of the origin of charge heterogeneity in a murine monoclonal antibody," *Pharmaceutical Research*, vol. 17, no. 9, pp. 1110–1117, 2000.
- [103] R. J. Harris, B. Kabakoff, F. D. Macchi, F. J. Shen, M. Kwong, J. D. Andya, S. J. Shire, N. Bjork, K. Totpal, and A. B. Chen, "Identification of multiple sources of charge heterogeneity in a recombinant antibody," *Journal of Chromatography B*, vol. 752, no. 2, pp. 233–245, 2001.
- [104] V. Schirch, "Deamidation and isoaspartate formation in serine hydroxymethyltransferase," in *Deamidation and isoaspartate formation in peptides and proteins* (D. Aswad, ed.), pp. 115–132, Boca Raton, FL: CRC Press, 1995.
- [105] R. Gracy, K. Yuksel, and A. Gomez-Puyou, "Deamidation of triosephosphate isomerase in vitro and in vivo," in *Deamidation and isoaspartate formation in peptides and proteins* (D. Aswad, ed.), pp. 133–155, Boca Raton, FL: CRC Press, 1995.
- [106] M. J. Mamula, R. J. Gee, J. I. Elliott, A. Sette, S. Southwood, P. J. Jones, and P. R. Blier, "Isoaspartyl post-translational modification triggers autoimmune responses to self-proteins," *Journal of Biological Chemistry*, vol. 274, no. 32, pp. 22321–22327, 1999.
- [107] A. E. Roher, J. D. Lowenson, S. Clarke, C. Wolkow, R. Wang, R. J. Cotter, I. M. Reardon, H. A. Zurcherneely, R. L. Heinrikson, M. J. Ball, and B. D. Greenberg,

- “Structural alterations in the peptide backbone of beta-amyloid core protein may account for its deposition and stability in alzheimers-disease,” *Journal of Biological Chemistry*, vol. 268, no. 5, pp. 3072–3083, 1993.
- [108] A. J. Domb, L. Turovsky, and R. Nudelman, “Chemical interactions between drugs containing reactive amines with hydrolyzable insoluble biopolymers in aqueous solutions,” *Pharmaceutical Research*, vol. 11, no. 6, pp. 865–868, 1994.
- [109] A. Lucke and A. Gopferich, “Acylation of peptides by lactic acid solutions,” *European Journal of Pharmaceutics and Biopharmaceutics*, vol. 55, no. 1, pp. 27–33, 2003.
- [110] D. Na, S. Murty, K. Lee, B. C. Thanoo, and P. DeLuca, “Preparation and stability of poly(ethylene glycol) (peg)ylated octreotide for application to microsphere delivery,” *AAPS PharmSciTech*, vol. 4, no. 3, p. Article 72, 2003.
- [111] S. B. Murty, D. H. Na, B. C. Thanoo, and P. P. DeLuca, “Impurity formation studies with peptide-loaded polymeric microspheres. part ii. in vitro evaluation,” *International Journal of Pharmaceutics*, vol. 297, no. 1-2, pp. 62–72, 2005.
- [112] S. B. Murty, J. Goodman, B. C. Thanoo, and P. P. DeLuca, “Identification of chemically modified peptide from poly(d,l-lactide-co-glycolide) microspheres under in vitro release conditions,” *AAPS PharmSciTech*, vol. 4, no. 4, pp. 392–405, 2003. 50.
- [113] D. B. Volkin and A. M. Klibanov, “Minimizing protein inactivation,” in *Protein function: a practical approach* (T. E. Creighton, ed.), pp. 1–24, Oxford: Oxford University Press, 1985.
- [114] M. Diwan and T. G. Park, “Stabilization of recombinant interferon-alpha by pegylation for encapsulation in plga microspheres,” *International Journal of Pharmaceutics*, vol. 252, no. 1-2, pp. 111–122, 2003.
- [115] H. T. Wright, “Nonenzymatic deamidation of asparaginy and glutaminy residues in proteins,” *Critical Reviews in Biochemistry and Molecular Biology*, vol. 26, no. 1, pp. 1–52, 1991.
- [116] S. Fredenberg, M. Reslow, and A. Axelsson, “Effect of divalent cations on pore formation and degradation of poly(D,L-lactide-co-glycolide),” *Pharmaceutical Development and Technology*, vol. 12, no. 6, pp. 563–572, 2007.
- [117] S. Wong, *Chemistry of protein conjugation and cross-linking*. CRC Press, Boca Raton, FL, 1991.
- [118] S. P. Schwendeman, “Recent advances in the stabilization of proteins encapsulated in injectable plga delivery systems,” *Critical Reviews in Therapeutic Drug Carrier Systems*, vol. 19, no. 1, pp. 73–98, 2002.
- [119] S. D. Putney and P. A. Burke, “Improving protein therapeutics with sustained-release formulations,” *Nature Biotechnology*, vol. 16, no. 2, pp. 153–157, 1998.

- [120] V. R. Sinha and A. Trehan, "Biodegradable microspheres for protein delivery," *Journal of Controlled Release*, vol. 90, no. 3, pp. 261–280, 2003.
- [121] D. H. Na, J. E. Lee, S. W. Jang, and K. C. Lee, "Formation of acylated growth hormone-releasing peptide-6 by poly(lactide-co-glycolide) and its biological activity," *AAPS PharmSciTech*, vol. 8, no. 2, pp. E1–E5, 2007. 41.
- [122] T. Peleg-Shulman, H. Tsubery, M. Mironchik, M. Fridkin, G. Schreiber, and Y. Shechter, "Reversible pegylation: A novel technology to release native interferon alpha 2 over a prolonged time period," *Journal of Medicinal Chemistry*, vol. 47, no. 20, pp. 4897–4904, 2004.
- [123] P. Hiemenz and R. Rajagopalan, *Principles of Colloid and Surface Chemistry*. New York: Marcel Dekker, Inc., 2nd ed., 1997.
- [124] S. B. Hall, P. W. Gaskin, J. R. Duffield, and D. R. Williams, "An interfacial equilibria model for the electrokinetic properties of a fat emulsion," *International Journal of Pharmaceutics*, vol. 70, no. 3, pp. 251–260, 1991.
- [125] S. Ohki, N. Duzgunes, and K. Leonards, "Phospholipid vesicle aggregation- effect of monovalent and divalent ions," *Biochemistry*, vol. 21, no. 9, pp. 2127–2133, 1982.
- [126] C. Altenbach and J. Seelig, "Ca<sup>2+</sup> binding to phosphatidylcholine bilayers as studied by deuterium magnetic resonance- evidence for the formation of a ca<sup>2+</sup> complex with 2 phospholipid molecules," *Biochemistry*, vol. 23, no. 17, pp. 3913–3920, 1984.
- [127] J. Seelig, "Interaction of phospholipids with ca<sup>2+</sup> ions- on the role of the phospholipid head groups," *Cell Biology International Reports*, vol. 14, no. 4, pp. 353–360, 1990.
- [128] S. McLaughlin, N. Mulrine, T. Gresalfi, G. Vaio, and A. McLaughlin, "Adsorption of divalent cations to bilayer membranes containing phosphatidylserine," *Journal of General Physiology*, vol. 77, no. 4, pp. 445–473, 1981.
- [129] M. Satoh, M. Hayashi, J. Komiyama, and T. Iijima, "Competitive counterion binding and hydration change of na poly(acrylate)/mgcl<sub>2</sub>, cac<sub>l</sub>2 in aqueous solution," *Polymer*, vol. 31, no. 3, pp. 501–505, 1990.
- [130] M. Satoh, T. Kawashima, and J. Komiyama, "Competitive counterion binding and dehydration of polyelectrolytes in aqueous solutions," *Polymer*, vol. 32, no. 5, pp. 892–896, 1991.
- [131] D. Shriver, P. Atkins, and C. Langford, *Inorganic Chemistry*. New York: W.H. Freeman, 2nd ed., 1994.
- [132] F. Basolo and R. Pearson, *Mechanisms of Inorganic Reactions: A Study of Metal Complexes in Solution*. New York: John Wiley and Sons, Inc., 2nd ed., 1967.

- [133] S. K. Smoukov, J. Telser, B. A. Bernat, C. L. Rife, R. N. Armstrong, and B. M. Hoffman, "Epr study of substrate binding to the mn(ii) active site of the bacterial antibiotic resistance enzyme fosa: A better way to examine mn(ii)," *Journal of the American Chemical Society*, vol. 124, no. 10, pp. 2318–2326, 2002.
- [134] A. G. Ding and S. P. Schwendeman, "Acidic microclimate ph distribution in plga microspheres monitored by confocal scanning laser microscopy," *Journal of Controlled Release*, vol. 25, no. 9, pp. 2041–2052, 2008.
- [135] A. G. Ding, A. Shenderova, and S. P. Schwendeman, "Prediction of microclimate ph in poly(lactic-co-glycolic acid) films," *Journal of the American Chemical Society*, vol. 128, no. 16, pp. 5384–5390, 2006.
- [136] J. Wang, B. A. Wang, and S. P. Schwendeman, "Characterization of the initial burst release of a model peptide from poly(d,l-lactide-co-glycolide) microspheres," *Journal of Controlled Release*, vol. 82, no. 2-3, pp. 289–307, 2002.
- [137] S. Hwang and M. Davis, "Cationic polymers for gene delivery: Designs for overcoming barriers to systemic administration," *Current Opinion in Molecular Therapeutics*, vol. 3, pp. 183–191, APR 2001.
- [138] M. Davis, "Non-viral gene delivery systems," *Current Opinion in Biotechnology*, vol. 13, pp. 128–131, APR 2002.
- [139] K. Kodama, Y. Katayama, Y. Shoji, and H. Nakashima, "The features and shortcomings for gene delivery of current non-viral carriers," *Current Medicinal Chemistry*, vol. 13, no. 18, pp. 2155–2161, 2006.
- [140] M. Thomas, J. Lu, C. Zhang, J. Chen, and A. Klivanov, "Identification of novel superior polycationic vectors for gene delivery by high-throughput synthesis and screening of a combinatorial library," *Pharmaceutical Research*, vol. 24, pp. 1564–1571, AUG 2007.
- [141] U. Seker, B. Wilson, S. Dincer, I. Kim, E. Oren, J. Evans, C. Tamerler, and M. Sarikaya, "Adsorption behavior of linear and cyclic genetically engineered platinum binding peptides," *Langmuir*, vol. 23, pp. 7895–7900, JUL 17 2007.
- [142] H. Chen, X. Su, K. Neoh, and W. Choe, "Context-dependent adsorption behavior of cyclic and linear peptides on metal oxide surfaces," *Langmuir*, vol. 25, pp. 1588–1593, FEB 3 2009.
- [143] I. M. Verhamme and P. E. Bock, "Rapid-reaction kinetic characterization of the pathway of streptokinase-plasmin catalytic complex formation," *Journal of Biological Chemistry*, vol. 283, pp. 26137–26147, SEP 19 2008.
- [144] Z. Zhang and D. Smith, "Determination of amide hydrogen-exchange by mass-spectrometry - a new tool for protein-structure elucidation," *Protein Science*, vol. 2, pp. 522–531, APR 1993.

- [145] A. Hoofnagle, K. Resing, and N. Ahn, "Protein analysis by hydrogen exchange mass spectrometry," *Annual Review of Biophysics and Biomolecular Structure*, vol. 32, pp. 1–25, 2003.
- [146] J. Zhang and R. Stanforth, "Slow adsorption reaction between arsenic species and goethite ( $\alpha$ -FeOOH): Diffusion or heterogeneous surface reaction control," *Langmuir*, vol. 21, pp. 2895–2901, MAR 29 2005.
- [147] S. Chaudhuri, K. Basu, B. Sengupta, A. Banerjee, and P. Sengupta, "Ground- and excited-state proton transfer and antioxidant activity of 3-hydroxyflavone in egg yolk phosphatidylcholine liposomes: absorption and fluorescence spectroscopic studies," *Luminescence*, vol. 23, pp. 397–403, NOV-DEC 2008.
- [148] A. Stancik and E. Brauns, "Rearrangement of partially ordered stacked conformations contributes to the rugged energy landscape of a small RNA hairpin," *Biochemistry*, vol. 47, pp. 10834–10840, OCT 14 2008.
- [149] T. Costa and J. De Melo, "The effect of gamma-cyclodextrin addition in the self-assembly behavior of pyrene labeled poly(acrylic) acid with different chain sizes," *Journal of Polymer Science A- Polymer Chemistry*, vol. 46, pp. 1402–1415, FEB 15 2008.
- [150] C. Tamerler, E. E. Oren, M. Duman, E. Venkatasubramanian, and M. Sarikaya, "Adsorption kinetics of an engineered gold binding peptide by surface plasmon resonance spectroscopy and a quartz crystal microbalance," *Langmuir*, vol. 22, pp. 7712–7718, AUG 29 2006.
- [151] B. Yowler and C. Schengrund, "Botulinum neurotoxin a changes conformation upon binding to ganglioside GT1b," *Biochemistry*, vol. 43, pp. 9725–9731, AUG 3 2004.
- [152] R. Glaser, "Antigen-antibody binding and mass-transport by convection and diffusion to a surface - a 2-dimensional computer-model of binding and dissociation kinetics," *Analytical Biochemistry*, vol. 213, pp. 152–161, AUG 15 1993.
- [153] P. Schuck, "Kinetics of ligand binding to receptor immobilized in a polymer matrix, as detected with an evanescent wave biosensor .1. A computer simulation of the influence of mass transport," *Biophysical Journal*, vol. 70, pp. 1230–1249, MAR 1996.
- [154] J. Evans, R. Samudrala, T. Walsh, E. Oren, and C. Tamerler, "Molecular design of inorganic-binding polypeptides," *MRS Bulletin*, vol. 33, pp. 514–518, MAY 2008.
- [155] W. Norde and J. Favier, "Structure of adsorbed and desorbed proteins," *Colloids and Surfaces*, vol. 64, pp. 87–93, MAY 26 1992.
- [156] C. Haynes and W. Norde, "Structures and stabilities of adsorbed proteins," *Journal of Colloid and Interface Science*, vol. 169, pp. 313–328, FEB 1995.

- [157] P. Claesson, E. Blomberg, J. Froberg, T. Nylander, and T. Arnebrant, "Protein interactions at solid surfaces," *Advances in Colloid and Interface Science*, vol. 57, pp. 161–227, MAY 30 1995.
- [158] F. Hook, M. Rodahl, B. Kasemo, and P. Brzezinski, "Structural changes in hemoglobin during adsorption to solid surfaces: Effects of pH, ionic strength, and ligand binding," *Proceedings of the National Academy of Sciences of the United States of America*, vol. 95, pp. 12271–12276, OCT 13 1998.
- [159] R. York, O. Mermut, D. Phillips, K. McCrea, R. Ward, and G. Somorjai, "Influence of ionic strength on the adsorption of a model peptide on hydrophilic silica and hydrophobic polystyrene surfaces: Insight from SFG vibrational spectroscopy," *Journal of Physical Chemistry C*, vol. 111, pp. 8866–8871, JUN 28 2007.
- [160] P. Thanki, E. Dellacherie, and J. Six, "Surface characteristics of PLA and PLGA films," *Applied Surface Science*, vol. 253, pp. 2758–2764, DEC 30 2006.
- [161] D. OShannessy and D. Winzor, "Interpretation of deviations from pseudo-first-order kinetic behavior in the characterization of ligand binding by biosensor technology," *Analytical Biochemistry*, vol. 236, pp. 275–283, MAY 1 1996.
- [162] J. Kang and S. Schwendeman, "Determination of diffusion coefficient of a small hydrophobic probe in poly(lactide-co-glycolide) microparticles by laser scanning confocal microscopy," *Macromolecules*, vol. 36, pp. 1324–1330, FEB 25 2003.
- [163] B. Peelle, E. Krauland, K. Wittrup, and A. Belcher, "Design criteria for engineering inorganic material-specific peptides," *Langmuir*, vol. 21, pp. 6929–6933, JUL 19 2005.
- [164] K. Dill and S. Bromberg, *Molecular Driving Forces: Statistical Thermodynamics in Chemistry and Biology*. Garland Science, 2003.
- [165] K. Imamura, Y. Kawasaki, T. Awadzu, T. Sakiyama, and K. Nakanishi, "Contribution of acidic amino residues to the adsorption of peptides onto a stainless steel surface," *Journal of Colloid and Interface Science*, vol. 267, pp. 294–301, NOV 15 2003.
- [166] Y. Wei and R. Latour, "Determination of the adsorption free energy for peptide-surface interactions by SPR spectroscopy," *Langmuir*, vol. 24, pp. 6721–6729, JUL 1 2008.
- [167] T. Tsai, R. Mehta, and P. DeLuca, "Adsorption of peptides to poly(D,L-lactide-co-glycolide) .1. Effect of physical factors on the adsorption," *International Journal of Pharmaceutics*, vol. 127, pp. 31–42, JAN 15 1996.
- [168] T. Tsai, R. Mehta, and P. DeLuca, "Adsorption of peptides to poly(D,L-lactide-co-glycolide) .2. Effect of solution properties on the adsorption," *International Journal of Pharmaceutics*, vol. 127, pp. 43–52, JAN 15 1996.

- [169] L. A. Capriotti, T. P. Beebe, Jr., and J. P. Schneider, "Hydroxyapatite surface-induced peptide folding," *Journal of the American Chemical Society*, vol. 129, pp. 5281–5287, APR 25 2007.
- [170] J. Ramsden, "Puzzles and paradoxes in protein adsorption," *Chemical Society Reviews*, vol. 24, pp. 73–78, FEB 1995.
- [171] F. Macritchie, "Equilibrium between adsorbed and displaced segments of protein monolayers," *Journal of Colloid and Interface Science*, vol. 79, pp. 461–464, 1981.
- [172] D. Briggs and M. Seah, eds., *Practical Surface Analysis. Volume 1. Auger and X-ray Photoelectron Spectroscopy*. John Wiley and Sons, Chichester, UK, 1990.
- [173] V. Munk, S. Fakih, P. Murdoch, and P. Sadler, "Reactions of pt-ii diamine anticancer complexes with trypanothione and octreotide," *Journal of Inorganic Biochemistry*, vol. 100, pp. 1946–1954, DEC 2006.